

Aus dem Experimental and Clinical Research Center
der Medizinischen Fakultät Charité – Universitätsmedizin Berlin

DISSERTATION

Funktionelle und strukturelle Testverfahren des afferenten
visuellen Systems in neuroinflammatorischen Erkrankungen

zur Erlangung des akademischen Grades
Doctor medicinae (Dr. med.)

vorgelegt der Medizinischen Fakultät
Charité – Universitätsmedizin Berlin

von

Noah Ayadi

aus München

Datum der Promotion: 03.03.2023

Inhaltsverzeichnis

Zusammenfassung	3
Abstrakt	3
Abstract	4
1. Einführung	5
2. Methodik	6
2.1 Patienten.....	6
2.2. Untersuchungsmethoden	7
2.3 Statistik	10
3. Ergebnisse	11
3.1 Normative Daten der Netzhautschichten und halbautomatisiertes OCT-Segmentierungstool (SAMIRIX)	11
3.2 Eingeschränkte zeitliche visuelle Auflösung in Patient*innen mit MS	12
3.3 Eingeschränktes Bewegungssehen in Patient*innen mit MS und NMOSD	13
4. Diskussion	15
5. Literaturverzeichnis	20
Eidesstattliche Versicherung	25
Anteilerklärung an erfolgten Publikationen	27
Druckexemplare der ausgewählten Publikationen	29
Ayadi et al. Neurol Neuroimmunol Neuroinflamm 2018 (Kritische Flimmerfrequenz & Erkrankungsschwere)	30
Ayadi et al. Mult Scler. 2021 (Bewegungssehen & Sehbahnschaden)	40
Motamedi et al. Front Neurol 2019 (Normative Daten & Segmentierungspipeline)	54
Lebenslauf	67
Publikationsliste	69
Artikel in Fachzeitschriften	69
Kongressbeiträge	70
Danksagung	71

Zusammenfassung

Abstrakt

Multiple Sklerose (MS) und Neuromyelitis optica-Spektrum-Erkrankungen (NMOSD) sind beides inflammatorische Autoimmunerkrankungen des zentralen Nervensystems, welche mit Schaden des afferenten visuellen Systems durch neuro-axonalen Untergang und Demyelinisierung einhergehen.

Ziel dieser Arbeit war die Untersuchung der dynamischen Sehfunktion bei MS und NMOSD mittels zweier Testverfahren und deren Zusammenhang mit etablierten funktionellen und strukturellen Parametern des afferenten visuellen Systems: Die kritische Flimmerfrequenz (CFF), ein Testverfahren der zeitlichen visuellen Auflösung, und die Testung des Bewegungssehens mittels Numbers from Motion (NFM).

Zunächst wurde zur Bestimmung des strukturellen Schadens eine Segmentierungspipeline für retinale optische Kohärenztomographie (Optical coherence tomography, OCT) entwickelt und eine normative Datenbank der Netzhautschichten aufgebaut und analysiert.

In einer Querschnittsuntersuchung der CFF in Patient*innen mit MS wurde gezeigt, dass die CFF in MS-Patient*innen niedriger als in gesunden Kontrollproband*innen war. Es bestand kein Unterschied zwischen Augen mit vorheriger Optikusneuritis (ON) und Augen ohne ON (NON). Ein Zusammenhang mit dem Hochkontrastvisus (HCVA), dem Niedrigkontrastsehen (LCLA), den visuell evozierten Potenzialen (VEP) sowie der mittels OCT bestimmten Dicke der peripapillären retinalen Nervenfaserschicht (pRNFL) und der kombinierten Ganglienzell- und inneren plexiformen Schicht (GCIPL) wurde nicht beobachtet. Jedoch zeigte die CFF eine Assoziation mit der Expanded Disability Status Scale (EDSS) Skala und der tonischen Alertness, eine Komponente der Aufmerksamkeit, gemessen mit der Testbatterie für Aufmerksamkeitsprüfung (TAP) aber nicht mit dem Paced Auditory Serial Addition Tests (PASAT), einer Messung der Informationsverarbeitungsgeschwindigkeit.

Der NFM-Score zeigte sich in MS- und NMOSD Patient*innen niedriger als in gesunden Kontrollproband*innen. In NMOSD aber nicht MS kam es nach ON zu niedrigeren NFM-Scores. In beiden Krankheitsentitäten ging ein niedriger NFM-Score mit niedriger HCVA, LCLA, dünnerer pRNFL und GCIPL, jedoch nicht mit verlängerten VEP-Latenzen einher. In einer zweiten MS-Kohorte waren niedrige NFM-Scores mit dünnerer pRNFL und verlängerter multifokalen VEP (mfVEP)-Latenzen assoziiert.

Zusammenfassend ist die CFF ein Marker für allgemeinen Krankheitsprogress und möglicherweise auch kortikalen Schaden in MS. Neuro-axonaler Schaden der Sehbahn, gemessen mittels retinalem OCT, ist die treibende Kraft hinter eingeschränktem Bewegungssehen in MS und NMOSD.

Abstract

Multiple sclerosis (MS) and neuromyelitis optica spectrum disorders (NMOSD) are both inflammatory autoimmune diseases of the central nervous system associated with damage to the afferent visual system through neuro-axonal loss and demyelination.

The aim of this work was to investigate dynamic visual function in MS and NMOSD using two tests with regard to their relationship to established functional and structural parameters of the afferent visual system: critical flicker frequency (CFF), a test of temporal visual resolution, and Numbers from Motion (NFM) testing of motion vision.

First, a retinal optical coherence tomography (OCT) segmentation pipeline was developed to determine structural damage, and a normative database of retinal layers was assembled and analysed.

In a cross-sectional study of CFF in patients with MS, CFF was shown to be lower in MS patients than in healthy subjects. There was no difference between eyes with previous optic neuritis (ON) and eyes without ON (NON). No association was observed with high contrast visual acuity (HCVA), low contrast visual acuity (LCLA), visual evoked potentials (VEP), OCT thickness of the peripapillary retinal nerve fibre layer (pRNFL) and combined ganglion cell and inner plexiform layer (GCIPL). However, CFF showed an association with the Expanded Disability Status Scale (EDSS) and tonic alertness, a component of attention measured with the Test Battery for Attention Testing (TAP) but not with the Paced Auditory Serial Addition Tests (PASAT), a measure of information processing speed.

The NFM score was lower in MS and NMOSD patients than in healthy subjects. In NMOSD but not MS, NFM scores were lower after ON. In MS and NMOSD, a lower NFM scores were associated with lower HCVA, LCLA, thinner pRNFL and GCIPL, but not with prolonged VEP latencies. In a second MS cohort, low NFM scores were associated with thinner pRNFL and prolonged multifocal VEP (mfVEP) latencies.

In conclusion, CFF is a marker of overall disease progression and possibly cortical damage in MS. Neuro-axonal damage to the visual pathway, measured by retinal OCT, is the driving force behind impaired motion vision in MS and NMOSD.

1. Einführung

Die Multiple Sklerose (MS) und Neuromyelitis optica-Spektrum-Erkrankungen (NMOSD) sind beides inflammatorische Autoimmunerkrankungen des zentralen Nervensystems (ZNS). [1,2] Im Rahmen der MS kommt es zu variablen fokalneurologischen Defiziten und Symptomkonstellation. Bedingt zeigen sich diese durch entzündliche Entmarkungsherde an unterschiedlichen Stellen des ZNS.[1] Die häufigste Verlaufsform ist die schubförmig remittierenden MS (relapsing-remitting MS, RRMS).[3] Die wohlmöglich erste Beschreibung eines NMOSD suggestiven Falles erfolgte 1804 durch Antoine Portal, jedoch prägten erst Fernand Gault und dessen Doktorvater Eugène Devic nach Publikation einer Fallserie zu der Erkrankung mit dem Namen „*neuro-myélite optique aiguë*“ die Geschichte der NMOSD.[2] Bis zum Anfang des 21. Jahrhunderts und Entdeckung der Aquaporin-4-Antikörper galt die NMOSD aufgrund einer ähnlichen Symptomatik als Form der MS.[5] Heute stellt die NMOSD die wichtigste Differentialdiagnose der MS dar. Gemeinsam haben beide Erkrankungsentitäten häufig eine Schädigung des afferenten visuellen Systems, in MS einerseits durch akuten fokalen Schaden, z.B. im Rahmen einer Optikusneuritis (ON), andererseits durch chronischen diffusen Schaden [6], in NMOSD hauptsächlich ON-bedingt.[7] In beiden Fällen führt diese Schädigungen zu visueller Dysfunktion und relevanter Einschränkung der Lebensqualität.[8,9] Der klinische Verlauf der NMOSD zeigt sich jedoch im Vergleich zur MS meist schwerer und geht, falls unbehandelt, mit einer schlechteren Schubremission einher.[2] Die klinische Beurteilung der Sehbahn spielt daher eine wichtige Rolle in der Diagnose und Verlaufsbeurteilung der MS und NMOSD. Dank bildgebender Verfahren wie z.B. der optischen Kohärenztomographie (OCT) oder funktionellen Tests wie z.B. den visuell evozierten Potenzialen (VEP) dient die Sehbahn zudem als Modell für das bessere Krankheitsverständnis beider Erkrankungen.[6]

Die kritische Flimmerfrequenz (CFF) ist definiert als Frequenz einer pulsierender Lichtquelle, ab welcher ein Individuum das Signal als Flimmern wahrnimmt.[10] Ihre Messung spielt aktuell klinisch eine Rolle in der frühen Diagnose einer hepatischen Enzephalopathie, in welcher von einer retinalen Gliopathie, a.e. durch erhöhtes Ammoniak, ausgegangen wird.[10] Frühere Studien zwischen 1957 und 1981 zeigten in Abwesenheit moderner Bildgebungs- und funktioneller Testverfahren eine reduzierte CFF in MS-Patient*innen abhängig[11,12] als auch unabhängig[13,14] von

ON. Niedrige CFF-Messungen nach okzipitalem Schädelhirntrauma weisen zudem auf eine Verarbeitung der zeitlichen visuellen Auflösung durch den primär visuellen Kortex hin.[15]

Das Bewegungssehen ist eine weitere dynamische Funktion, welche der Beurteilung des visuellen Systems dient.[16] Die Wahrnehmung von Bewegung beginnt in der Retina, von wo aus das Signal über das magnozelluläre System am Corpus geniculatum laterale des Thalamus vorbei in das mediotemporale Areal zur weiteren kortikalen Verarbeitung geleitet wird.[17,18] Eine jüngste Serie an Studien zeigte einen Zusammenhang zwischen eingeschränktem Bewegungssehen und verlängerten VEP-Latenzen in Patient*innen mit MS oder ON [16,19,20], das Bewegungssehen stelle daher ein klinisches Korrelat verlängerter Übertragungsgeschwindigkeiten dar und könne als zukünftiger Biomarker für den Myelinisierungsgrad der Sehbahn dienen. Einschränkungen des Bewegungssehen in anderen Erkrankungen, wie des Morbus Alzheimer [21] oder des Offenwinkelglaukoms [22] weisen auch auf kognitive oder strukturelle Schäden als mögliche Ätiologie hin.

Die vorliegende Arbeit fokussierte sich auf a) die CFF bei MS-Patient*innen und mögliche Assoziationen mit klinischer Erkrankungsschwere und aktuellen strukturellen und funktionellen Parametern des visuellen Systems, b) die Validierung der Messung des Bewegungssehens als Biomarker für den Myelinisierungsgrad in MS und mögliche Assoziationen des Bewegungssehens mit strukturellem retinalen Schaden und kognitiver Einschränkung und c) der Untersuchung retinaler Schichtdicken in gesunden Kontrollproband*innen.

2. Methodik

2.1 Patienten

Alle Fragestellungen wurden im Rahmen longitudinaler Beobachtungsstudien von MS und NMOSD Patient*innen in der AG Klinische Neuroimmunologie am NeuroCure Clinical Research Center, Charité - Universitätsmedizin Berlin untersucht. Einschlusskriterien waren ein Alter zwischen 18 und 70 Jahren, in Kritische Flimmerfrequenz & Erkrankungsschwere[23] Vorliegen einer RRMS nach revidierten McDonald-Kriterien 2010[24], in Bewegungssehen & Sehbahnschaden[25] Vorliegen

einer RRMS nach revidierten McDonald-Kriterien 2017[26] oder Vorliegen einer NMOSD nach internationalen Konsensuskriterien 2015[27], Einwilligungsfähigkeit und schriftliche Einwilligung. Ausschlusskriterien waren relevante Augenerkrankungen mit Einschränkung für die Auswertung der klinisch visuellen und strukturellen Testung und neurologische Erkrankungen für die gesunden Kontrollproband*innen. Für die zweite Kohorte in Bewegungssehen & Sehbahnschaden[25] wurden zudem RRMS-Patient*innen aus einer Beobachtungsstudie der Macquarie Universität, Sydney rekrutiert.

Diese Studien wurde von den lokalen Ethikkommissionen in Berlin (EA1/216/11, EA1/182/10, EA1/163/12, EA1/041/14) und Sydney genehmigt und in Übereinstimmung mit der Deklaration von Helsinki in ihrer jeweils gültigen Fassung und den geltenden lokalen Gesetzen durchgeführt. Alle Teilnehmer*innen gaben eine schriftliche Einverständniserklärung ab.

2.2. Untersuchungsmethoden

Kritische Flimmerfrequenz

Die Analyse der kritischen Flimmerfrequenz (CFF) erfolgte monokular mittels Headsets von HEPATonorm-Analysator (nevoLAB GmbH, Maierhöfen, Deutschland), welches jegliches Außenlicht von den Augen der Teilnehmer*innen abschirmt. Durchgeführt wurde die Testung in einem ruhigen und halb abgedunkelten Raum.

Die CFF-Messung basiert auf einer intrafovealen visuellen Stimulation mittels einer roten Leuchtdiode, ein anfängliches Lichtsignal von 60 Hz wird in 0,1 Hz Schritten abgesenkt und initial als kontinuierliche Lichtquelle wahrgenommen. Sobald die Teilnehmer*innen ein flackerndes Signal wahrnahmen drückten sie eine Stopptaste. Die entsprechende Pulsfrequenz wird als CFF definiert und vom Handsteuergerät aufgezeichnet. Jedes Auge wurde 8 Mal getestet und der mittlere CFF (mCFF) Wert bestimmt. Vor Durchführung erfolgte eine Trainingseinheit mit 5 Messungen.[10,28]

Bewegungssehen

Das Bewegungssehen, gemessen als Zahlen aus Bewegung (numbers from motion, NFM) wurde monokular mit einer überarbeiteten Testsoftware getestet, welche von der Abteilung für funktionelle Magnetresonanztomographie (fMRI) der neurologischen Abteilung des Hadassah Medical Center, Hebrew University, Jerusalem, Israel,

entwickelt wurde.[16] Die Messung basiert auf einem von Regan et al.[29] entwickelten Bewegungswahrnehmungstest und ist programmiert, eine automatisch berechnete Punktzahl auszugeben. Die NFM-Testung besteht aus 80 dreistelligen Zahlen, die in 4 Blöcken zu je 20 Stimuli aufgeteilt sind um eine mehrfache Testung zwischen den Augen ohne Lerneffekt zu ermöglichen. Bei jedem Stimulus, basierend auf in sich in entgegengesetzte Richtung bewegende Punkte an einem Computerbildschirm, bildet sich eine dreistellige Zahl. Das Erkennen der Zahl durch die Teilnehmer*innen hängt direkt von dem Bewegungssehen ab.[16] Präsentiert wurden die Zahlen mit einer Geschwindigkeit von 4 bis 24,5 (4; 5,5; 7,5; 10; 13,5; 18; 24,5) Pixel/s, begonnen mit der langsamsten Geschwindigkeit, bei welcher die Wahrnehmung der NFM am schwierigsten ist. Nach 5 nicht erkannten Zahlen wurden diese in der nächsthöheren Geschwindigkeitsstufe erneut präsentiert bis 20 Zahlen richtig oder keine Zahl bei höchster Geschwindigkeit erkannt wurden. NFM, welche bei der niedrigsten Geschwindigkeit identifiziert wurden, erhielten eine Punktzahl von 7, während NFM bei schnellster Geschwindigkeit eine Punktzahl von 1 und nicht erkannte Zahlen eine Punktzahl von 0 erhielten. Somit reicht der NFM-Score von 0 bis 140, wobei 20 Zahlen oder keine Zahlen bei höchster Geschwindigkeit identifiziert werden mussten. [16] Vor der Testung absolvierten alle Teilnehmer*innen ein kurzes binokulares Training.

Optische Kohärenztomographie (OCT)

Alle Teilnehmer*innen erhielten OCT-Aufnahmen mit einem Spectralis SD-OCT von Heidelberg Engineering (Heidelberg, Deutschland) mit Eye Explorer 1.9.10.0 Software, automatisierter Mittelwertbildung (automatic real time (ART) avering) in Echtzeit und aktiver Augenverfolgung.[30] Die Dicke der peripapillären retinalen Nervenfaserschicht (pRNFL) wurde aus einem Standard-Ring-Scan um den Sehnervenkopf (12° , 1536 A-Scans, $16 \leq \text{ART} \leq 100$) durch Segmentierung mit der Software des Geräts mit dem Viewing Module 6.0.14.0 bestimmt und als durchschnittliche Dicke in μm angegeben. Die Volumen-Scans wurden in einem Bereich von $25^\circ \times 30^\circ$ um die Fovea aufgenommen (61 vertikale B-Scans, 768 A-Scans pro B-Scan, $16 \leq \text{ART} \leq 100$). Das totale Volumen der Makula (TMV), der kombinierten Ganglienzell- und inneren plexiformen Schicht (GCIPL) und inneren Körnerschicht (inner nuclear layer, INL) wurde in mm^3 in einem 6mm Durchmesser um die Fovea angegeben. Für Normative Daten & Segmentierungspipeline[31] wurde zudem die Dicke der Makula (MT), der

makulären retinalen Nervenfaserschicht (mRNFL), der GCIPL und INL auch in μm angegeben.

Die Segmentierung der makulären Volumen-Scans erfolgte mittels hausinterner entwickelter Segmentierungspipeline SAMIRIX [31] basierend auf der Johns Hopkins Hopkins OCT-Schichtsegmentierungsmethode (AURA Tools version 1.2).[32]

Visuelle Funktionsparameter

Der Hochkontrastvisus (HCVA) wurde in Kritische Flimmerfrequenz & Erkrankungsschwere [23] mit dem Functional Vision Analyzer Optec 6500P System (Stereo Optical Co, Chicago, IL) monokular unter habitueller Korrektur und photopischen Bedingungen (85 cd/m^2) mittels Early Treatment of Diabetic Retinopathy Study (ETDRS) Charts in einer simulierten Entfernung von 20 Fuß durchgeführt. [33] In Bewegungssehen & Sehbahnschaden [25] erfolgte die HCVA Testung monokular mit bester Refraktionskorrektur mit Hilfe von retro-illuminieren ETDRS-Tafeln in 4 m Entfernung gemessen und in logMAR-Einheiten (Logarithm of the Minimum Angle of Resolution) umgerechnet. In Flimmerfrequenz & Erkrankungsschwere [23] erfolgte die Bestimmung des Niedrigkontrastvisus (LCLA) binokular unter gewohnter Korrektur mit 2,5% Kontrast Sloan-Tafeln in 2 m Entfernung.[34] In Bewegungssehen & Sehbahnschaden [25] erfolgte diese monokulare unter bester Refraktionskorrektur mit derselben Methodik.

In Berlin wurden die visuell evozierten Potentiale (VEP) mit dem DantecTM Keypoint VEP-System (Natus Europe GmbH, Planegg, Deutschland) mit Nadelelektroden und mit dem RETI-port/scan 21-Gerät (Roland Consult GmbH, Brandenburg, Deutschland) mit Goldnapfelektroden gemessen. Die P100-Latenzzeit wurde mit einer Standard Schwarz-Weiß-Schachbrett-Stimulation (60', 1 m Entfernung) und von der Oz-Elektrode gegen eine Cz-Referenzelektrode nach dem internationalen 10-20 System aufgezeichnet. Die Messungen beider Geräte wurden getrennt analysiert.

In Sydney wurden multifokale VEP (mfVEP) unter bester Refraktionskorrektur mit dem VisionSearch 1 System (VisionSearch, Sydney, NSW, Australien) mit vier Goldnapfelektroden (Grass, West Warwick, RI, USA) getestet. [35] Für die statistische Analyse wurde die mittlere mfVEP-Latenz der 56 Segmente benutzt.

Klinische und kognitive Testung

Für alle Patient*innen erfolgte eine ausführliche Anamnese und eine vollständige neurologische Untersuchung einschließlich der Bestimmung der Erkrankungsschwere mittels der Expanded Disability Status Scale (EDSS) Skala.[36]

In Kritische Flimmerfrequenz & Erkrankungsschwere [23] erfolgte die Durchführung der 3-Sekunden-Version des Paced Auditory Serial Addition Tests (PASAT), eine Messung der Informationsverarbeitungsgeschwindigkeit und eine Aufgabe aus der Testbatterie für Aufmerksamkeitsprüfung (TAP) zur Testung der Alertness.[37,38] Die Alertness, auch Aufmerksamkeitsaktivierung genannt, beschreibt den allgemeinen Wachheitszustand eines Individuums und dient als Voraussetzung für die adäquate Reaktion auf Umweltreize.[37,39] Unterteilt wird die Alertness in tonische Alertness, einer anhaltenden Aktivierung, welche zirkadianen Schwankungen unterliegt und in phasische Alertness, die Fähigkeit, nach externen Stimuli, die Aktivierung und somit die Aufmerksamkeitsleistung passager zu steigern.[39] Die Aufgaben der TAP-Testung bestanden aus einer einfachen visuellen Reaktionszeit-Aufgabe (RT) ohne akustisches Warnsignal zur Quantifizierung der tonischen Alertness und aus einer visuellen RT-Aufgabe, mit vorangehendem Warnsignal, zur Quantifizierung der phasischen Alertness. Im Rahmen der Messung wurden die beiden Aufgaben mehrfachst alternierend durchgeführt und die Teilnehmer*innen geboten so schnell wie möglich mit Knopfdruck zu reagieren, sobald ein Kreuz angezeigt wurde.[37] Die mittlere RT ohne vorangehendes akustisches Warnsignal, als Maß für die tonische Alertness, wurde für die Beschreibung der allgemeinen Aufmerksamkeitsaktivierung benutzt.

In Bewegungssehen & Sehbahnschaden [25] wurde zur kognitiven Testung zudem der Symbol Digit Modalities Test (SDMT) durchgeführt. [40]

2.3 Statistik

Die Statistik und Abbildungen wurden mit Hilfe des Programms R (Versionen 3.1.2, 3.4.2, 3.4.4) mit u.a. den Paketen „psych“, „ggplot2“, „geepack“, „ICC“ durchgeführt.[41] Messwerte wurden, wenn nicht anders angegeben, als Mittelwert und Standardabweichung oder Median und Spannweite angegeben. Das Signifikanzlevel wurde für alle Tests bei $p < 0,05$ festgelegt. Für demographische Vergleiche zwischen Patient*innen und Kontrollproband*innen wurde der Pearson Chi-Quadrat-Test für das

Geschlecht und der nichtparametrische Mann-Whitney-U-Test für das Alter verwendet. Generalisierte Schätzgleichungen (Generalized estimating equations, GEEs) wurden für Gruppenvergleiche und Assoziationen mit augenbezogenen Messungen verwendet, um Abhängigkeiten zwischen beiden Augen einer Person zu berücksichtigen. Die GEE-Ergebnisse wurden mit Regressionskoeffizient (B) und Standardfehler (SE) angegeben. Alle Messungen wurden als kontinuierliche Variablen behandelt und die Gruppen wurden innerhalb der Patient*innen in ON- und Nicht-ON-Augen unterteilt. Für die Beurteilung der Test-Retest-Reliabilität bzw. der Intra- und Interrater-Reliabilität erfolgte die Bestimmung der Intraklassen-Korrelation (ICC) und seines 95%-Konfidenzintervalls. Ein ICC über 0,9 wurde als hoch, zwischen 0,8 und 0,9 als mäßig und unter 0,8 als niedrig betrachtet.[42] Für Normative Daten & Segmentierungspipeline [31] wurde zudem die minimal nachweisbare Veränderung nach Beckerman et al. bestimmt.[43]

In Kritische Flimmerfrequenz & Erkrankungsschwere [23] erfolgte eine Korrektur für Mehrfachvergleich mit der Bonferroni-Holm-Methode.[44]

3. Ergebnisse

3.1 Normative Daten der Netzhautschichten und halbautomatisiertes OCT-Segmentierungstool (SAMIRIX)

Normative Daten & Segmentierungspipeline[31]

In dieser Studie wurde eine halbautomatische intraretinale Segmentierungspipeline für OCT-Bilder der Makula entwickelt sowie normative Daten der Netzhautschichten als zukünftige Referenzwerte für weitere Studien erhoben.

SAMIRIX ist ein auf einem Segmentierungsalgorithmus eines Drittanbieters „OCTLayerSegmentation“ von Lang et al.[32] basierende halbautomatische intraretinale Segmentierungspipeline, welcher durch NeuroImaging Tools & Resources Collaboratory (NTRC) zur Verfügung gestellt wird und aufgrund seiner durchschnittlichen absoluten Fehler von unter $3,5\mu\text{m}$ ausgewählt wurde. SAMIRIX ermöglicht die Ansicht von OCT-Bildern, deren Segmentierung mit Überprüfung, manueller Korrektur und Export der Netzhautschichtdicken. Diese Pipeline diente unter anderem der OCT-Segmentierung für die Studien des Bewegungssehens in MS und NMOSD Patient*innen [23] und der zeitlichen visuellen Auflösung in MS-Patient*innen[25].

Für die Erhebung des normativen Datensatzes erfolgte eine Querschnittsanalyse von 218 gesunden Proband*innen (144 Frauen/74 Männer) mit einem Durchschnittsalter von $36,5 \pm 12,3$ Jahren (18-69). So ergaben sich Durchschnittswerte für die Makuladicke, die mRNFL, die GCIPL und die INL. Gezeigt werden konnte eine Abnahme der Schichtdicken mit zunehmendem Alter. In männlichen Probanden zeigte sich im Vergleich zu weiblichen Probandinnen eine dickere Makuladicke und GCIPL. Zudem zeigte sich eine positive Assoziation zwischen den verschiedenen Retinaschichten.

Die Reliabilitätsmessung für die manuelle Korrektur von automatisch segmentierten Retinaschichten erbrachte einen Intraklassen-Korrelationskoeffizient von $> 0,99$ für alle Schichten. Detaillierte Ergebnisse sind in den Tabellen 1-3 dieser Publikation dargestellt. [31] Zudem konnte gezeigt werden, dass ein Verlaufsmonitoring der retinalen Neurodegeneration von MS-Patient*innen mittels OCT aktuell nur unzureichend möglich ist, da die technisch minimal nachweisbaren Veränderungen höher als die typischen jährlichen MS-bedingten Schichtdickenabnahmen sind.

3.2 Eingeschränkte zeitliche visuelle Auflösung in Patient*innen mit MS

Kritische Flimmerfrequenz & Erkrankungsschwere [23]

Es handelt sich hier um eine Querschnittsstudie zur Untersuchung der zeitlichen visuellen Auflösung in MS-Patient*innen und gesunden Kontrollproband*innen sowie ihres Zusammenhanges mit Schädigungen des visuellen Systems, allgemeiner Behinderung und kognitiver Funktion. Die demographischen Daten der 39 Patient*innen und 31 alters- und geschlechts-gematchten Kontrollproband*innen sind in Tabelle 1 in der Publikation [23] zusammengefasst.

Die mCFF von Kontrollproband*innen lag bei $44,8 \pm 4,4$ Hz und zeigte sich nicht geschlechterabhängig. Jedoch ließ sich eine Abnahme der mCFF mit zunehmendem Alter beobachten. Es bestand kein Zusammenhang der mCFF mit der Hoch- und Niedrigkontrastvisusmessung sowie der Leitungsgeschwindigkeit des Sehnervs, gemessen mittels VEP. Nach Testung der tonischen Alertness mittels der Testbatterie zur Aufmerksamkeitsprüfung konnte kein Zusammenhang mit der mCFF gezeigt werden. Für CFF bestand eine hohe Test-Retest-Reliabilität bei einem ICC-Wert von 0,91 (95% Konfidenzintervall 0,87-0,94).

In MS-Patient*innen konnte eine im Vergleich zu Kontrollproband*innen erniedrigte mCFF von $40,9 \pm 4,72$ Hz nachgewiesen werden. Es bestand kein Unterschied zwischen Augen mit und ohne Optikusneuritis. Die mCFF zeigte nach Korrektur für multiple Vergleich keinen Zusammenhang mit erniedrigtem Hoch- und Niedrigkontrastvisus, der Demyelinisierung mittels VEP-Messung sowie retinalem Schaden, bestimmt durch die OCT-Untersuchung. Die Test-Retest-Reliabilität war bei einem ICC-Wert von 0,89 (0,85-0,92) moderat.

Im Rahmen der Untersuchung eines möglichen Zusammenhanges der mCFF mit der Gesamtbehinderung konnte gezeigt werden, dass höhere EDSS-Scores mit einer niedrigeren mCFF einhergingen. Die tonische Alertness der MS-Patient*innen zeigte einen Zusammenhang mit der mCFF. So ging eine reduzierte allgemeine Aufmerksamkeitsaktivierung mit einer schlechteren zeitlichen visuellen Auflösung einher. Bei fehlendem Zusammenhang zwischen der Standardabweichung der mCFF und der tonischen Alertness konnte ein Einfluss letzterer auf die korrekte Ausführung der mCFF Testung ausgeschlossen werden. Zusätzlich bestand kein Einfluss der Informationsverarbeitungsgeschwindigkeit, gemessen mittels PASAT Testung, auf die mCFF. Nach Korrektur für multiple Vergleiche blieben die Zusammenhänge zwischen mCFF und EDSS sowie mCFF und der tonischen Alertness signifikant.

3.3 Eingeschränktes Bewegungssehen in Patient*innen mit MS und NMOSD

Bewegungssehen & Sehbahnschaden[25]

Es handelt sich hier um eine Querschnittsstudie zur Untersuchung des Bewegungssehens in MS und NMOSD Patient*innen und dessen zugrundeliegender Schädigung der Sehbahn. Hierzu wurden 38 MS-, 13 NMOSD-Patient*innen, 33 gesunde Kontrollproband*innen in Berlin und 43 MS-Patient*innen in Sydney eingeschlossen, die demographischen Daten sind in der Tabelle 1 der Publikation zusammengefasst.[25]

Bei Patient*innen und Kontrollproband*innen in Berlin erfolgte eine Testung des Bewegungssehens, eine OCT-Untersuchung mit Bestimmung von pRNFL, GCIP und INL, eine Hoch- und Niedrigkontrastvisusmessung, eine VEP-Messung, eine Erhebung des EDSS-Scores und eine kognitive Testung mittels SDMT. Bei den Patient*innen in Sydney erfolgte zusätzlich zu der OCT- und Bewegungssehensmessung eine mfVEP-Untersuchung.

MS-Patient*innen in der Berlin Kohorte hatten ein im Vergleich zu Kontrollproband*innen eingeschränktes Bewegungssehen, gemessen mittels NFM-Score, welches sich nicht zwischen Augen mit und ohne Optikusneuritis unterschied. Es bestand ein Zusammenhang mit dem Hoch- und Niedrigkontrastsehen, der pRNFL sowie der GCIPL. Ein Einfluss der Demyelinisierung, objektiviert durch die VEP P100 Latenz, auf das Bewegungssehen wurde nicht beobachtet. Zudem bestand kein Zusammenhang mit der INL.

In einer Subgruppenanalyse von ausschließlich Augen mit Optikusneuritis ließen sich diese Ergebnisse reproduzieren. In Patient*innen mit einseitiger Optikusneuritis erbrachte eine Asymmetrieanalyse einen signifikanten Zusammenhang zwischen eingeschränktem Bewegungssehen und retinalem Schaden. Es zeigte sich kein Zusammenhang zwischen NFM- und EDSS-Score, jedoch ein Zusammenhang zwischen eingeschränktem Bewegungssehen und erniedrigtem SDMT-Score. Nach Ausschluss von Ausreißern, definiert als NFM-Score < 50 zeigten sich die Ergebnisse reproduzierbar.

Auch in einer separaten Analyse von VEP-Messungen an einem zweiten Gerät wurde kein Einfluss der Demyelinisierung auf das Bewegungssehen beobachtet.

In der Sydney MS-Kohorte wurde der Zusammenhang zwischen eingeschränktem Bewegungssehen und retinalem Schaden bestätigt, jedoch zeigte sich hier ein deutlich reduzierter NFM-Score in Augen mit Optikusneuritis im Vergleich zu Augen ohne Optikusneuritis. Anders als in der Berlin Kohorte ging ein eingeschränktes Bewegungssehen mit verlängerten mfVEP Latenzen einher und schien auch die stattgefundene Demyelinisierung widerzuspiegeln. Eine multivariate Analyse belegte jedoch einen höheren Einfluss der pRNFL auf den NFM-Score als die mfVEP, ähnliches ließ sich auch in einer Subgruppenanalyse von ausschließlich Augen mit Optikusneuritis beobachten. Die Asymmetrieanalyse in Patient*innen mit unilateraler Optikusneuritis erbrachte ein vergleichbares Ergebnis wie in der Berlin Kohorte. Auch nach Ausschluss nach Ausreißern, definiert als NFM-Score < 20, zeigten sich die Ergebnisse reproduzierbar.

Eine erstmalige Untersuchung des Bewegungssehens in Patient*innen mit NMOSD erbrachte ein im Vergleich zu Kontrollproband*innen eingeschränktes Bewegungssehen, welches in Augen mit Optikusneuritis schlechter als in Augen ohne

Optikusneuritis war. Verglichen mit den Ergebnissen in Patient*innen mit MS wurde ein Zusammenhang mit retinalem Schaden (pRNFL, GCIP) und Hoch- und Niedrigkontrastvisus beobachtet. Auch hier bestand kein Anhalt für einen Zusammenhang des Bewegungssehen mit der INL, der VEP-Messung und der EDSS-Skala. Niedrige SDMT-Scores gingen nicht mit eingeschränktem Bewegungssehen einher. Auch nach Ausschluss von Ausreißern zeigten sich weiterhin Trends in dieselbe Richtung.

4. Diskussion

In dieser Arbeit wurden Testverfahren der zeitlichen visuellen Auflösung und des Bewegungssehens in neuroinflammatorischen Erkrankungen auf mögliche Zusammenhänge mit etablierten klinischen, funktionellen und strukturellen Messungen der Sehbahn, der Krankheitsschwere und Kognition sowie auf deren Bedeutung für das Krankheitsmonitoring untersucht. Beigetragen wurde hierbei auch zu der Optimierung der Bildanalyse von makulären OCT-Bildern mit Erstellung einer Segmentierungspipeline, Erhebung minimal nachweisbarer Änderungen und Zusammenstellung eines normativen Datensatzes zu retinalen Schichtdicken für zukünftige Studien.

Die Arbeit zeigt, dass a) die CFF bei MS-Patient*innen im Vergleich zu Kontrollproband*innen reduziert ist, jedoch nicht mit strukturellem oder funktionellem Schaden des afferenten visuellen Systems, dafür aber mit eingeschränkter allgemeiner Aufmerksamkeitsaktivierung und Krankheitsschwere in MS einhergeht [23], b) neuro-axonaler Schadens des visuellen Systems einen größeren Einfluss auf das Bewegungssehen in MS hat als Demyelinisierung [25], c) das Bewegungssehen in NMO-SD-Patient*innen eingeschränkt ist [25], d) ein Zusammenhang zwischen eingeschränktem Bewegungssehen und kognitiven Defiziten in MS-, aber nicht NMO-SD-Patient*innen besteht.

Eine eingeschränkte CFF in MS-Patient*innen konnte schon in früheren Studien beobachtet werden.[11–13] Als Ätiologie in Betracht gezogen wurde einerseits bei eingeschränkter CFF in Patient*innen mit als auch ohne ON eine Beeinträchtigung der Wahrnehmung auf zentraler Ebene durch kortikalen Schaden [11], andererseits durch die neuro-axonale Degeneration der Retina und der Sehbahn. [12] Insbesondere Zellen des magnozellulären Systems, wie die retinalen Ganglienzellen, seien

mitverantwortlich für die Wahrnehmung von hochfrequenten Stimuli. [45] In unserer Studie konnte jedoch kein Zusammenhang zwischen eingeschränkter CFF und neuroaxonalem retinalen Schaden oder Demyelinisierung nachgewiesen werden. Ein Zusammenhang zwischen eingeschränkter CFF und verlängerter RT im TAP-Test weist auf einen Einfluss der tonischen Alertness auf die Wahrnehmung hochfrequenter Stimuli hin. Bei fehlendem Zusammenhang zwischen RT und CFF SD konnte ein Einfluss der tonischen Alertness auf die adäquate Durchführung der Testung ausgeschlossen werden.

Die tonische Alertness ist Voraussetzung für die Aufmerksamkeitsleistung und basiert vor allem auf der Aktivierung rechtshemisphärischer frontoparietaler und thalamischer Regionen.[39] Die CFF spiegelt daher möglicherweise Schaden kognitiv assoziierter Areale wieder. Einen Zusammenhang der CFF mit der Informationsverarbeitungsgeschwindigkeit, getestet durch den PASAT konnte in unserer Studie jedoch nicht gezeigt werden. Frühere Studien aus den Jahren 1950/1960 suggerierten einen Zusammenhang zwischen CFF und allgemeiner Erkrankungsschwere der MS [11,46], welchen wir mit dem Nachweis eines Zusammenhangs zwischen CFF und EDSS verifizieren konnten.

Unsere CFF-Messungen in gesunden Kontrollproband*innen und deren Abnahme mit zunehmendem Alter ist vereinbar mit vorherigen Ergebnissen [47], bei hohem ICC-Wert zeigt sich die CFF-Testung in Kontrollproband*innen und MS-Patient*innen als gut reproduzierbar.

Limitiert war unsere Studie zur kritischen Flimmerfrequenz durch mehrere Faktoren. Eine insgesamt kleine Fallzahl sowie noch kleinere Fallzahlen in Subgruppenanalyse können dazu beigetragen haben, kleine Effekte zu übersehen. Bei binokular getestetem Niedrigkontrastvisus sind unsere Ergebnisse möglicherweise nicht vergleichbar mit monokular getesteter CFF. Da es sich hierbei um eine Querschnittsstudie handelt konnte die zeitliche Dynamik evtl. CFF-Änderungen in MS-Patient*innen nicht untersucht werden. Viele vorherige Studien stammen aus den Fünfziger- und Sechzigerjahren, sodass die Vergleichbarkeit bei unterschiedlichen Testmethoden eingeschränkt sein könnte.[11,46] Zudem erfolgte in unserer Studie keine MR-tomographische Bildgebung, ein Zusammenhang mit radiologischer Krankheitsaktivität konnte daher nicht untersucht werden.

Raz et al. [16] zeigten zuletzt einen Zusammenhang der CFF mit dem Bewegungssehen. Das Bewegungssehen wurde in früheren Studien mit MS-Patient*innen im Frühstadium oder akuten ON-Fällen als dynamische visuelle Funktion dargestellt, welche aufgrund eines Zusammenhanges mit verlängerten VEP-Latenzen auf eine schnelle Übertragung visueller Stimuli basiere und den Myelinisierungsgrad der Sehbahn widerspiegele.[16,20] In unserer Studie zum Bewegungssehen zeigten sich in beiden Kohorten ein starker Zusammenhang zwischen reduziertem NFM-Score und Abnahme der pRNFL und GCIPL. Neuro-axonaler Schaden der Retina und des Sehnervs präsentierten sich damit als wesentliche Ätiologie eingeschränkten Bewegungssehen in MS und NMOSD.

Unsere Studie ergab keinen Zusammenhang zwischen Bewegungssehen, gemessen als NFM-Score, und VEP-Latenz in der Berliner Kohorte an zwei unterschiedlichen VEP-Geräten. In der zweiten MS-Kohorte aus Sydney konnte jedoch ein Zusammenhang zwischen reduziertem NFM-Score und verlängerter mfVEP-Latenz beobachtet werden. Dieser Effekt zeigte sich in Augen mit ON am größten. Dies kann gut mit der größeren Fallzahl, die für die Demyelinisierung sensitiverer mfVEP-Messungen (im Vergleich zu Vollfeld-VEP) [48] und eine im Durchschnitt dünnere pRNFL in ON-Augen in Sydney erklärt werden. Die Ergebnisse der Asymmetrieanalyse in Patient*innen mit unilateraler ON und der multivariaten Analyse zeigten, dass eine verlängerte Übertragungsgeschwindigkeit nicht, wie bisher postuliert, der einzige Grund eines eingeschränkten Bewegungssehens ist.

Die Rolle des neuroaxonalen Schadens für das Bewegungssehen lässt sich möglicherweise dadurch erklären, dass die Wahrnehmung von Bewegung in der Retina beginnt. [49] Studien zeigten, dass ein Schaltkreis richtungsselektiver Zellen, bestehend aus bipolaren, amakrinen Zellen und v.a. bewegungssensitiven Parasol-Ganglienzellen, für die retinale Bewegungskodierung zuständig ist.[50–52] Da ein statistischer Zusammenhang zwischen reduziertem NFM-Score und Abnahme der Dicke von pRNFL und GCIPL, welche in MS und NMOSD Patient*innen unabhängig einer ON auftritt [7,53,54], besteht, postulieren wir, dass das Bewegungssehen auf der strukturellen Integrität der Retina basiert. Das Bewegungssehen stellt somit ein klinisches Korrelat des neuro-axonalen Schadens dar.

Unsere Studie ist die erste, die das Bewegungssehen in Patient*innen mit NMOSD untersucht. Der Unterschied in der Schwere des eingeschränkten Bewegungssehen zwischen NMOSD-Augen lässt sich damit erklären, dass ON in NMOSD primär durch

axonalen Schaden gekennzeichnet ist, während ON in MS v.a. zu Demyelinisierung führt.[35] Eingeschränktes Bewegungssehen in NMOSD-Augen ohne ON könnte auf mikrostrukturelle Veränderungen vermittelt durch eine Astrozythopathie im afferenten visuellen System hinweisen [55], während diese in MS-Augen ohne ON vermutlich chronische Neurodegeneration repräsentiert.

Aufgrund des Zusammenhanges zwischen Bewegungssehen und Hoch- und Niedrigkontrastvisus erfolgte eine Subgruppenanalyse von Patient*innen mit HCVA \leq 0.1 logMAR, welche vergleichbare Ergebnisse zeigte. Ein wesentlicher Einfluss der Sehkraft auf das Bewegungssehen ist somit unwahrscheinlich.

In MS-Patient*innen zeigte sich ein Einfluss der eingeschränkten Informationsverarbeitungsgeschwindigkeit und Kognition, gemessen mittels SDMT, auf das Bewegungssehen. Dieses Ergebnis ließ sich in NMOSD-Patient*innen nicht reproduzieren und ist bei limitierter Fallzahl nur bedingt aussagekräftig.

Limitiert ist auch diese Studie durch eine kleine Fallzahl, v.a. in der NMOSD Subgruppe, welche bedingen könnte, dass kleine Effekte übersehen oder signifikante Effekte überinterpretiert werden können. So führte der Ausschluss von NFM-Ausreißern dazu, dass manche Ergebnisse nicht mehr signifikant waren. In Vergleich zu den vorherigen Studien zum Bewegungssehen in MS-Patient*innen bestand unsere Kohorte aus einer heterogenen Gruppe in einer stabilen Krankheitsphase mit nur milder Demyelinisierung, sodass ein möglicherweise bestehender, subtiler Zusammenhang der NFM mit der VEP-Latenz nicht nachgewiesen werden konnte. Die NFM-Testung erfolgte zudem unter gewohnter Korrektur, so dass nicht korrigierte Refraktionsfehler die Ergebnisse beeinflusst haben könnten. Die von Raz et al.[16] berichtete Assoziation zwischen NFM und CFF deutet möglicherweise auf eine zentrale Komponente des Bewegungssehen hin. Eingeschränktes Bewegungssehen unabhängig von Optikusneuropathie, z.B. im Rahmen einer Alzheimer-Erkrankung [21] bestätigen diese Vermutung. Das Querschnittstudiendesign ermöglichte uns zudem keine dynamische Beobachtung des Bewegungssehen.

Unsere beiden Studien zu CFF und Bewegungssehen basierten maßgeblich auf der strukturellen Untersuchung der Retinaschichten, sodass ein schnelle und verlässliche Segmentierungspipeline notwendig war. Im Rahmen von Normative Daten & Segmentierungspipeline [31] wurden nicht nur eine hausinterne Segmentierungspipeline „SAMIRIX“ entworfen sondern auch normative Daten zu den verschiedenen Netzhautschichten in gesunden Proband*innen gesammelt. So zeigte

sich ein Zusammenhang zwischen MT, mRNFL, GCIPL und INL mit dem Alter. Dieses Ergebnis war im Einklang mit vorherigen Beobachtungen, welche auch berichteten, dass Frauen dünnere Retinaschichten aufwiesen. [56,57] Dies war in unserer Normkohorte nur für die MT und GCIPL der Fall. Von klinischer Relevanz zeigte sich auch die positive Assoziation zwischen GCIPL und INL in gesunden Proband*innen, da in neuroinflammatorischen Prozessen ein gegensätzliches Verhalten beider Schichten, mit Abnahme der GCIPL bei Neurodegeneration und Zunahme der INL durch inflammatorische Prozesse, zu beobachten ist. [58] Wir zeigten zudem eine sehr gute Interrater-Reliabilität bei einem ICC-Wert $> 0,99$ für alle retinalen Schichten. Zusätzlich konnten wir zeigen, dass typische jährliche Änderungen im Rahmen neurodegenerativer Prozesse unter Berücksichtigung minimal nachweisbarer Veränderungen nur unzureichend nachgewiesen werden können.

Limitiert ist diese Studie vor allem dadurch, dass nur OCT-Gerät mit nur einem Scan-Protokoll berücksichtigt wurde. So ist zu berücksichtigen, dass ein Vergleich zwischen verschiedenen Geräten nur eingeschränkt möglich ist.[59] Die normativen Daten basieren auf einer kaukasischen Kohorte, eine Studie berichtete ethnische Unterschiede.[56]

Mit der vorliegenden Arbeit konnten die kritische Flimmerfrequenz, ein über 100 Jahre altes Testverfahren, sowie das Bewegungssehen hinsichtlich potenzieller Zusammenhänge mit neuen funktionellen und strukturellen Parametern des afferenten visuellen Systems in neuroinflammatorischen Erkrankungen untersucht werden. Die kritische Flimmerfrequenz spiegelt globalen Krankheitsprogress und kortikalen Schaden in MS-Patient*innen wider. Die Beeinträchtigung des Bewegungssehens in MS und NMOSD Patient*innen ist eine Folge sowohl der neuro-axonalen Schädigung der Sehbahn als auch der Demyelinisierung. Um beide Testverfahren als Verlaufsbiomarker zu etablieren sind weitere großangelegte longitudinale Studien notwendig. Kortikaler Schaden, mittels MR-tomographischen Verfahren, sollte auf einen Zusammenhang mit der kritischen Flimmerfrequenz und des Bewegungssehen in MS und NMOSD untersucht werden.

5. Literaturverzeichnis

1. Reich DS, Lucchinetti CF, Calabresi PA. Multiple Sclerosis. *N Engl J Med*. 11. Januar 2018;378(2):169–80.
2. Jarius S, Wildemann B, Paul F. Neuromyelitis optica: clinical features, immunopathogenesis and treatment. *Clin Exp Immunol*. Mai 2014;176(2):149–64.
3. Weinshenker BG. Natural history of multiple sclerosis. *Ann Neurol*. 1994;36 Suppl:S6-11.
4. Jarius S, Wildemann B. The case of the Marquis de Causan (1804): an early account of visual loss associated with spinal cord inflammation. *J Neurol*. 1. Juli 2012;259(7):1354–7.
5. Zekeridou A, Lennon VA. Aquaporin-4 autoimmunity. *Neurology - Neuroimmunology Neuroinflammation*. 1. August 2015;2(4).
6. Martínez-Lapiscina EH, Sanchez-Dalmau B, Fraga-Pumar E, Ortiz-Perez S, Tercero-Urbe AI, Torres-Torres R, Villoslada P. The visual pathway as a model to understand brain damage in multiple sclerosis. *Mult Scler*. November 2014;20(13):1678–85.
7. Oertel FC, Specovius S, Zimmermann HG, Chien C, Motamedi S, Bereuter C, Cook L, Lana Peixoto MA, Fontanelle MA, Kim HJ, Hyun J-W, Palace J, Roca-Fernandez A, Leite MI, Sharma S, Ashtari F, Kafieh R, Dehghani A, Pourazizi M, Pandit L, D’Cunha A, Aktas O, Ringelstein M, Albrecht P, May E, Tongco C, Leocani L, Pisa M, Radaelli M, Martinez-Lapiscina EH, Stiebel-Kalish H, Siritho S, de Seze J, Senger T, Havla J, Marignier R, Calvo AC, Bichuetti D, Tavares IM, Asgari N, Soelberg K, Altintas A, Yildirim R, Tanriverdi U, Jacob A, Huda S, Rimler Z, Reid A, Mao-Draayer Y, Soto de Castillo I, Petzold A, Green AJ, Yeaman MR, Smith T, Brandt AU, Paul F. Retinal Optical Coherence Tomography in Neuromyelitis Optica. *Neurol Neuroimmunol Neuroinflamm*. November 2021;8(6):e1068.
8. Schinzel J, Zimmermann H, Paul F, Ruprecht K, Hahn K, Brandt AU, Dörr J. Relations of low contrast visual acuity, quality of life and multiple sclerosis functional composite: a cross-sectional analysis. *BMC Neurol*. 20. Februar 2014;14:31.
9. Schmidt F, Zimmermann H, Mikolajczak J, Oertel FC, Pache F, Weinhold M, Schinzel J, Bellmann-Strobl J, Ruprecht K, Paul F, Brandt AU. Severe structural and functional visual system damage leads to profound loss of vision-related quality of life in patients with neuromyelitis optica spectrum disorders. *Mult Scler Relat Disord*. Januar 2017;11:45–50.
10. Sharma P, Sharma BC, Puri V, Sarin SK. Critical flicker frequency: diagnostic tool for minimal hepatic encephalopathy. *J Hepatol*. Juli 2007;47(1):67–73.
11. Parsons OA, Miller PN. Flicker Fusion Thresholds in Multiple Sclerosis. *AMA Arch NeurPsych*. 1. Februar 1957;77(2):134–9.

12. Titcombe AF, Willison RG. Flicker fusion in multiple sclerosis. *J Neurol Neurosurg Psychiatry*. August 1961;24(3):260–5.
13. Daley ML, Swank RL, Ellison CM. Flicker fusion thresholds in multiple sclerosis. A functional measure of neurological damage. *Arch Neurol*. Mai 1979;36(5):292–5.
14. Patterson VH, Foster DH, Heron J, Mason RJ. Multiple sclerosis. Luminance threshold and measurements of temporal characteristics of vision. *Arch Neurol*. November 1981;38(11):687–9.
15. Bender MB, Teuber H-L. Disturbances in Visual Perception Following Cerebral Lesions. *The Journal of Psychology*. 1. Juli 1949;28(1):223–33.
16. Raz N, Shear-Yashuv G, Backner Y, Bick AS, Levin N. Temporal aspects of visual perception in demyelinating diseases. *J Neurol Sci*. 15. Oktober 2015;357(1–2):235–9.
17. Chapman C, Hoag R, Giaschi D. The effect of disrupting the human magnocellular pathway on global motion perception. *Vision Research*. 1. Oktober 2004;44(22):2551–7.
18. Born RT, Bradley DC. Structure and function of visual area MT. *Annu Rev Neurosci*. 2005;28:157–89.
19. Raz N, Dotan S, Benoliel T, Chokron S, Ben-Hur T, Levin N. Sustained motion perception deficit following optic neuritis: Behavioral and cortical evidence. *Neurology*. 14. Juni 2011;76(24):2103–11.
20. Raz N, Dotan S, Chokron S, Ben-Hur T, Levin N. Demyelination affects temporal aspects of perception: an optic neuritis study. *Ann Neurol*. April 2012;71(4):531–8.
21. Gilmore GC, Wenk HE, Naylor LA, Koss E. Motion Perception and Alzheimer's Disease. *J Gerontol*. 1. März 1994;49(2):P52–7.
22. Silverman SE, Trick GL, Hart WM. Motion perception is abnormal in primary open-angle glaucoma and ocular hypertension. *Invest Ophthalmol Vis Sci*. 1. April 1990;31(4):722–9.
23. Ayadi N, Dörr J, Motamedi S, Gawlik K, Bellmann-Strobl J, Mikolajczak J, Brandt AU, Zimmermann H, Paul F. Temporal visual resolution and disease severity in MS. *Neurol Neuroimmunol Neuroinflamm*. 1. September 2018;5(5).
24. Polman CH, Reingold SC, Banwell B, Clanet M, Cohen JA, Filippi M, Fujihara K, Havrdova E, Hutchinson M, Kappos L, Lublin FD, Montalban X, O'Connor P, Sandberg-Wollheim M, Thompson AJ, Waubant E, Weinshenker B, Wolinsky JS. Diagnostic criteria for multiple sclerosis: 2010 revisions to the McDonald criteria. *Ann Neurol*. Februar 2011;69(2):292–302.
25. Ayadi N, Oertel FC, Assemer S, Rust R, Duchow A, Kuchling J, Bellmann-Strobl J, Ruprecht K, Klistorner A, Brandt AU, Paul F, Zimmermann HG. Impaired motion perception is associated with functional and structural visual pathway damage in

multiple sclerosis and neuromyelitis optica spectrum disorders. *Mult Scler.* 11. August 2021;13524585211032800.

26. Thompson AJ, Banwell BL, Barkhof F, Carroll WM, Coetzee T, Comi G, Correale J, Fazekas F, Filippi M, Freedman MS, Fujihara K, Galetta SL, Hartung HP, Kappos L, Lublin FD, Marrie RA, Miller AE, Miller DH, Montalban X, Mowry EM, Sorensen PS, Tintoré M, Traboulsee AL, Trojano M, Uitdehaag BMJ, Vukusic S, Waubant E, Weinshenker BG, Reingold SC, Cohen JA. Diagnosis of multiple sclerosis: 2017 revisions of the McDonald criteria. *Lancet Neurol.* 2018;17(2):162–73.
27. Wingerchuk DM, Banwell B, Bennett JL, Cabre P, Carroll W, Chitnis T, de Seze J, Fujihara K, Greenberg B, Jacob A, Jarius S, Lana-Peixoto M, Levy M, Simon JH, Tenenbaum S, Traboulsee AL, Waters P, Wellik KE, Weinshenker BG, International Panel for NMO Diagnosis. International consensus diagnostic criteria for neuromyelitis optica spectrum disorders. *Neurology.* 14. Juli 2015;85(2):177–89.
28. Romero-Gómez M, Córdoba J, Jover R, del Olmo JA, Ramírez M, Rey R, de Madaria E, Montoliu C, Nuñez D, Flavia M, Compañy L, Rodrigo JM, Felipe V. Value of the critical flicker frequency in patients with minimal hepatic encephalopathy. *Hepatology.* April 2007;45(4):879–85.
29. Regan D, Kothe AC, Sharpe JA. Recognition of motion-defined shapes in patients with multiple sclerosis and optic neuritis. *Brain.* 1. Juni 1991;114(3):1129–55.
30. Cruz-Herranz A, Balk LJ, Oberwahrenbrock T, Saidha S, Martinez-Lapiscina EH, Lagreze WA, Schuman JS, Villoslada P, Calabresi P, Balcer L, Petzold A, Green AJ, Paul F, Brandt AU, Albrecht P. The APOSTEL recommendations for reporting quantitative optical coherence tomography studies. *Neurology.* 14. Juni 2016;86(24):2303–9.
31. Motamedi S, Gawlik K, Ayadi N, Zimmermann HG, Asseyer S, Bereuter C, Mikolajczak J, Paul F, Kadas EM, Brandt AU. Normative Data and Minimally Detectable Change for Inner Retinal Layer Thicknesses Using a Semi-automated OCT Image Segmentation Pipeline. *Front Neurol.* 2019;10.
32. Lang A, Carass A, Hauser M, Sotirchos ES, Calabresi PA, Ying HS, Prince JL. Retinal layer segmentation of macular OCT images using boundary classification. *Biomed Opt Express.* 14. Juni 2013;4(7):1133–52.
33. Bock M, Brandt AU, Kuchenbecker J, Dörr J, Pfueller CF, Weinges-Evers N, Gaede G, Zimmermann H, Bellmann-Strobl J, Ohlraun S, Zipp F, Paul F. Impairment of contrast visual acuity as a functional correlate of retinal nerve fibre layer thinning and total macular volume reduction in multiple sclerosis. *Br J Ophthalmol.* Januar 2012;96(1):62–7.
34. Baier ML, Cutter GR, Rudick RA, Miller D, Cohen JA, Weinstock-Guttman B, Mass M, Balcer LJ. Low-contrast letter acuity testing captures visual dysfunction in patients with multiple sclerosis. *Neurology.* 22. März 2005;64(6):992–5.

35. Shen T, You Y, Arunachalam S, Fontes A, Liu S, Gupta V, Parratt J, Wang C, Barnett M, Barton J, Chitranshi N, Zhu L, Fraser CL, Graham SL, Klistorner A, Yiannikas C. Differing Structural and Functional Patterns of Optic Nerve Damage in Multiple Sclerosis and Neuromyelitis Optica Spectrum Disorder. *Ophthalmology*. März 2019;126(3):445–53.
36. Kurtzke JF. Rating neurologic impairment in multiple sclerosis An expanded disability status scale (EDSS). *Neurology*. 11. Januar 1983;33(11):1444–1444.
37. Zimmermann P, Fimm B. Test for Attentional Performance (TAP)-Version 1.02, Manual. Würselen, Germany: Psytest; 1994.
38. Cutter GR, Baier ML, Rudick RA, Cookfair DL, Fischer JS, Petkau J, Syndulko K, Weinstock-BG, Antel JP, Confavreux C, Ellison GW, Lublin F, Miller AE, Rao SM, Reingold S, Thompson A, Willoughby E. Development of a multiple sclerosis functional composite as a clinical trial outcome measure. *Brain*. Mai 1999;122 (Pt 5):871–82.
39. Sturm W, Willmes K. On the functional neuroanatomy of intrinsic and phasic alertness. *Neuroimage*. Juli 2001;14(1 Pt 2):S76-84.
40. Parmenter BA, Weinstock-Guttman B, Garg N, Munschauer F, Benedict RHB. Screening for cognitive impairment in multiple sclerosis using the Symbol digit Modalities Test. *Mult Scler*. Januar 2007;13(1):52–7.
41. R Core Team. R: A Language and Environment for Statistical Computing. R Core Team; 2017.
42. Wolak ME, Fairbairn DJ, Paulsen YR. Guidelines for estimating repeatability. *Methods in Ecology and Evolution*. 3(1):129–37.
43. Beckerman H, Roebroek ME, Lankhorst GJ, Becher JG, Bezemer PD, Verbeek AL. Smallest real difference, a link between reproducibility and responsiveness. *Qual Life Res*. 2001;10(7):571–8.
44. Holm S. A Simple Sequentially Rejective Multiple Test Procedure. *Scandinavian Journal of Statistics*. 1979;6(2):65–70.
45. Jacobson DM, Olson KA. Impaired critical flicker frequency in recovered optic neuritis. *Ann Neurol*. August 1991;30(2):213–5.
46. Sandry M. Critical Flicker Frequency in Multiple Sclerosis. *Percept Mot Skills*. 1. Februar 1963;16(1):103–8.
47. Misiak H. Age and sex differences in critical flicker frequency. *J Exp Psychol*. August 1947;37(4):318–32.
48. Graham SL, Klistorner A. Afferent visual pathways in multiple sclerosis: a review. *Clin Experiment Ophthalmol*. Januar 2017;45(1):62–72.
49. Barlow HB, Hill RM, Levick WR. Retinal ganglion cells responding selectively to direction and speed of image motion in the rabbit. *J Physiol (Lond)*. Oktober 1964;173:377–407.

50. Euler T, Detwiler PB, Denk W. Directionally selective calcium signals in dendrites of starburst amacrine cells. *Nature*. 22. August 2002;418(6900):845–52.
51. Kim JS, Greene MJ, Zlateski A, Lee K, Richardson M, Turaga SC, Purcaro M, Balkam M, Robinson A, Behabadi BF, Campos M, Denk W, Seung HS. Space–time wiring specificity supports direction selectivity in the retina. *Nature*. Mai 2014;509(7500):331–6.
52. Manookin MB, Patterson SS, Linehan CM. Neural Mechanisms Mediating Motion Sensitivity in Parasol Ganglion Cells of the Primate Retina. *Neuron*. 21. März 2018;97(6):1327-1340.e4.
53. Brandt AU, Martinez-Lapiscina EH, Nolan R, Saidha S. Monitoring the Course of MS With Optical Coherence Tomography. *Curr Treat Options Neurol*. April 2017;19(4):15.
54. Oertel FC, Zimmermann H, Paul F, Brandt AU. Optical coherence tomography in neuromyelitis optica spectrum disorders: potential advantages for individualized monitoring of progression and therapy. *EPMA J*. März 2018;9(1):21–33.
55. Oertel FC, Kuchling J, Zimmermann H, Chien C, Schmidt F, Knier B, Bellmann-Strobl J, Korn T, Scheel M, Klistorner A, Ruprecht K, Paul F, Brandt AU. Microstructural visual system changes in AQP4-antibody–seropositive NMOSD. *Neurol Neuroimmunol Neuroinflamm*. 22. Februar 2017;4(3).
56. Girkin CA, McGwin G, Sinai MJ, Sekhar GC, Fingeret M, Wollstein G, Varma R, Greenfield D, Liebmann J, Araie M, Tomita G, Maeda N, Garway-Heath DF. Variation in Optic Nerve and Macular Structure with Age and Race with Spectral-Domain Optical Coherence Tomography. *Ophthalmology*. 1. Dezember 2011;118(12):2403–8.
57. Song WK, Lee SC, Lee ES, Kim CY, Kim SS. Macular Thickness Variations with Sex, Age, and Axial Length in Healthy Subjects: A Spectral Domain–Optical Coherence Tomography Study. *Investigative Ophthalmology & Visual Science*. 1. August 2010;51(8):3913–8.
58. Knier B, Schmidt P, Aly L, Buck D, Berthele A, Mühlau M, Zimmer C, Hemmer B, Korn T. Retinal inner nuclear layer volume reflects response to immunotherapy in multiple sclerosis. *Brain*. 1. November 2016;139(11):2855–63.
59. Pierro L, Giatsidis SM, Mantovani E, Gagliardi M. Macular Thickness Interoperator and Intraoperator Reproducibility in Healthy Eyes Using 7 Optical Coherence Tomography Instruments. *American Journal of Ophthalmology*. 1. August 2010;150(2):199-204.e1.

Eidesstattliche Versicherung

„Ich, Noah Ayadi, versichere an Eides statt durch meine eigenhändige Unterschrift, dass ich die vorgelegte Dissertation mit dem Thema: „Funktionelle und strukturelle Testverfahren des afferenten visuellen Systems in neuroinflammatorischen Erkrankungen“ / “Functional and structural testing of the afferent visual system in neuroinflammatory diseases” selbstständig und ohne nicht offengelegte Hilfe Dritter verfasst und keine anderen als die angegebenen Quellen und Hilfsmittel genutzt habe.

Alle Stellen, die wörtlich oder dem Sinne nach auf Publikationen oder Vorträgen anderer Autoren/innen beruhen, sind als solche in korrekter Zitierung kenntlich gemacht. Die Abschnitte zu Methodik (insbesondere praktische Arbeiten, Laborbestimmungen, statistische Aufarbeitung) und Resultaten (insbesondere Abbildungen, Graphiken und Tabellen) werden von mir verantwortet.

Ich versichere ferner, dass ich die in Zusammenarbeit mit anderen Personen generierten Daten, Datenauswertungen und Schlussfolgerungen korrekt gekennzeichnet und meinen eigenen Beitrag sowie die Beiträge anderer Personen korrekt kenntlich gemacht habe (siehe Anteilserklärung). Texte oder Textteile, die gemeinsam mit anderen erstellt oder verwendet wurden, habe ich korrekt kenntlich gemacht.

Meine Anteile an etwaigen Publikationen zu dieser Dissertation entsprechen denen, die in der untenstehenden gemeinsamen Erklärung mit dem/der Erstbetreuer/in, angegeben sind. Für sämtliche im Rahmen der Dissertation entstandenen Publikationen wurden die Richtlinien des ICMJE (International Committee of Medical Journal Editors; www.icmje.org) zur Autorenschaft eingehalten. Ich erkläre ferner, dass ich mich zur Einhaltung der Satzung der Charité – Universitätsmedizin Berlin zur Sicherung Guter Wissenschaftlicher Praxis verpflichte.

Weiterhin versichere ich, dass ich diese Dissertation weder in gleicher noch in ähnlicher Form bereits an einer anderen Fakultät eingereicht habe.

Die Bedeutung dieser eidesstattlichen Versicherung und die strafrechtlichen Folgen

einer unwahren eidesstattlichen Versicherung (§§156, 161 des Strafgesetzbuches)
sind mir bekannt und bewusst.“

Datum

Unterschrift

Anteilserklärung an erfolgten Publikationen

Noah Ayadi hatte folgenden Anteil an den folgenden Publikationen:

Kritische Flimmerfrequenz & Erkrankungsschwere [23]

Noah Ayadi, Jan Dörr, Seyedamirhosein Motamedi, Kay Gawlik, Judith Bellmann-Strobl, Janine Mikolajczak, Alexander U. Brandt, Hanna Zimmermann, Friedemann Paul, **Temporal visual resolution and disease severity in MS**, Neurol Neuroimmunol Neuroinflamm, 2018.

Beitrag im Einzelnen: Erhebung und Zusammenstellung der CFF- und VEP-Daten, Segmentierung der OCT-Daten, statistische Analyse unter Supervision von Hanna G. Zimmermann, Interpretation der Ergebnisse, Erstellung des Manuskripts inklusive der Graphen 1-4 und Tabelle 1 anhand der Datenanalyse

Bewegungssehen & Sehbahnschaden[25]

Noah Ayadi, Frederike C Oertel, Susanna Asseyer, Rebecca Rust, Ankelien Duchow, Joseph Kuchling, Judith Bellmann-Strobl, Klemens Ruprecht, Alexander Klistorner, Alexander U Brandt, Friedemann Paul, Hanna G Zimmermann, **Impaired motion perception is associated with functional and structural visual pathway damage in multiple sclerosis and neuromyelitis optica spectrum disorders**, Mult Scler., 2021.

Beitrag im Einzelnen: Erhebung der NFM-Daten, Segmentierung der OCT-Daten, statistische Analyse unter Supervision von Hanna G. Zimmermann, Interpretation der Ergebnisse, Erstellung des Manuskripts inklusive der Graphen 1-4 und Tabellen 1-2 anhand der Datenanalyse

Normative Daten & Segmentierungspipeline[31]

Seyedamirhosein Motamedi, Kay Gawlik, **Noah Ayadi**, Hanna G. Zimmermann, Susanna Asseyer, Charlotte Bereuter, Janine Mikolajczak, Friedemann Paul, Ella Maria Kadas, Alexander Ulrich Brandt, **Normative Data and Minimally Detectable Change for Inner Retinal Layer Thicknesses Using a Semi-automated OCT Image Segmentation Pipeline**, Front Neurol, 2019.

Beitrag im Einzelnen: Rekrutierung gesunder Proband*innen, Erhebung der OCT-

Daten, Segmentierung der OCT-Daten, diese Daten trugen zu den Tabellen 1, 3 & 4 sowie zu den Graphen 2 & 3 bei, Überarbeitung des Manuskripts

Unterschrift, Datum und Stempel des erstbetreuenden Hochschullehrers

Unterschrift des Doktoranden

Druckexemplare der ausgewählten Publikationen

Noah Ayadi, Jan Dörr, Seyedamirhosein Motamedi, Kay Gawlik, Judith Bellmann-Strobl, Janine Mikolajczak, Alexander U. Brandt, Hanna Zimmermann, Friedemann Paul, Temporal visual resolution and disease severity in MS, *Neurol Neuroimmunol Neuroinflamm*, 2018.

Journal Impact Factor 2018: 7.353 (war 2017 noch nicht in der Journal Summary List aufgeführt)

Noah Ayadi, Frederike C Oertel, Susanna Asseyer, Rebecca Rust, Ankelien Duchow, Joseph Kuchling, Judith Bellmann-Strobl, Klemens Ruprecht, Alexander Klistorner, Alexander U Brandt, Friedemann Paul, Hanna G Zimmermann, Impaired motion perception is associated with functional and structural visual pathway damage in multiple sclerosis and neuromyelitis optica spectrum disorders, *Mult Scler.*, 2021.

Journal Impact Factor 2019: 5.412

Seyedamirhosein Motamedi, Kay Gawlik, Noah Ayadi, Hanna G. Zimmermann, Susanna Asseyer, Charlotte Bereuter, Janine Mikolajczak, Friedemann Paul, Ella Maria Kadas, Alexander Ulrich Brandt, Normative Data and Minimally Detectable Change for Inner Retinal Layer Thicknesses Using a Semi-automated OCT Image Segmentation Pipeline, *Front Neurol*, 2019.

Journal Impact Factor 2017: 3.508

Ayadi et al. Neurol Neuroimmunol Neuroinflamm 2018
(Kritische Flimmerfrequenz & Erkrankungsschwere)

Journal Data Filtered By: **Selected JCR Year: 2018** Selected Editions: SCIE,SSCI
 Selected Categories: **"CLINICAL NEUROLOGY"** Selected Category
 Scheme: WoS

Gesamtanzahl: 199 Journale

Rank	Full Journal Title	Total Cites	Journal Impact Factor	Eigenfactor Score
1	LANCET NEUROLOGY	30,748	28.755	0.069460
2	Nature Reviews Neurology	9,548	21.155	0.031060
3	ACTA NEUROPATHOLOGICA	20,206	18.174	0.041660
4	Alzheimers & Dementia	13,341	14.423	0.036340
5	JAMA Neurology	8,683	12.321	0.042040
6	BRAIN	52,970	11.814	0.074030
7	SLEEP MEDICINE REVIEWS	6,920	10.517	0.010920
8	NEURO-ONCOLOGY	11,858	10.091	0.029150
9	ANNALS OF NEUROLOGY	37,336	9.496	0.048630
10	NEUROLOGY	89,258	8.689	0.115200
11	JOURNAL OF NEUROLOGY NEUROSURGERY AND PSYCHIATRY	29,660	8.272	0.030730
12	MOVEMENT DISORDERS	26,964	8.061	0.037650
13	Neurology-Neuroimmunology & Neuroinflammation	1,996	7.353	0.008220
14	Brain Stimulation	5,457	6.919	0.014470
15	Epilepsy Currents	799	6.909	0.001560
16	NEUROPATHOLOGY AND APPLIED NEUROBIOLOGY	3,876	6.878	0.006420
17	NEUROSCIENTIST	4,986	6.791	0.008520
18	BRAIN PATHOLOGY	5,263	6.155	0.007880
19	Alzheimers Research & Therapy	3,160	6.142	0.010700
20	STROKE	64,814	6.046	0.082630

1

Selected JCR Year: 2018; Selected Categories: "CLINICAL NEUROLOGY"

Das Journal „Neurology – Neuroimmunology & Neuroinflammation“ erschien im Jahr 2014 und wurde erstmals im Jahr 2018 gelistet.

Temporal visual resolution and disease severity in MS

Noah Ayadi, Jan Dörr, MD, Seyedamirhosein Motamedi, MSc, Kay Gawlik, MSc, Judith Bellmann-Strobl, MD, Janine Mikolajczak, PhD, Alexander U. Brandt, MD, Hanna Zimmermann, PhD,* and Friedemann Paul, MD*

Correspondence

Dr. Dörr
jan-markus.doerr@charite.de

Neurol Neuroimmunol Neuroinflamm 2018;5:e492. doi:10.1212/NXI.0000000000000492

Abstract

Objective

To examine temporal visual resolution assessed as critical flicker frequency (CFF) in patients with MS and to investigate associations with visual system damage and general disability and cognitive function.

Methods

Thirty-nine patients with MS and 31 healthy controls (HCs) were enrolled in this cross-sectional study and underwent CFF testing, high- and low-contrast visual acuity, alertness and information processing speed using the paced auditory serial addition task (PASAT), and retinal optical coherence tomography (OCT). In patients with MS, visual evoked potentials (VEPs) and Expanded Disability Status Scale (EDSS) scores were assessed.

Results

CFF in patients with MS (mean \pm SD: 40.9 \pm 4.4 Hz) was lower than in HCs (44.8 \pm 4.4 Hz, $p < 0.001$). There was no significant CFF difference between eyes with and without previous optic neuritis (ON). CFF was not associated with visual acuity, VEP latency, the peripapillary retinal nerve fiber layer thickness, and the combined ganglion cell and inner plexiform layer volume. Instead, reduced CFF was associated with worse EDSS scores ($r^2 = 0.26$, $p < 0.001$) and alertness ($r^2 = 0.42$, $p = 0.00042$) but not with PASAT ($p = 0.33$).

Conclusion

CFF reduction in MS occurs independently of ON and structural visual system damage. Its association with the EDSS score and alertness suggests that CFF reflects global disease processes and higher cortical processing rather than focal optic nerve or retinal damage.

*Equally contributing senior authors.

From the Charité—Universitätsmedizin Berlin (N.A., J.D., S.M., K.G., J.B.-S., J.M., A.U.B., H.Z., F.P.), Corporate Member of Freie Universität Berlin, Humboldt-Universität zu Berlin, and Berlin Institute of Health, NeuroCure Clinical Research Center; Neurology Department (J.D.), Multiple Sclerosis Center, Oberhavel Clinic, Henningsdorf; Experimental and Clinical Research Center (J.B.-S., F.P.), Max Delbrueck Center for Molecular Medicine and Charité—Universitätsmedizin Berlin, Corporate Member of Freie Universität Berlin, Humboldt-Universität zu Berlin, and Berlin Institute of Health; and Department of Neurology (F.P.), Charité—Universitätsmedizin Berlin, Corporate Member of Freie Universität Berlin, Humboldt-Universität zu Berlin, and Berlin Institute of Health, Germany.

Funding information and disclosures are provided at the end of the article. Full disclosure form information provided by the authors is available with the full text of this article at Neurology.org/NN.

The Article Processing Charge was funded by *Neurology: Neuroimmunology & Neuroinflammation*.

This is an open access article distributed under the terms of the Creative Commons Attribution-NonCommercial-NoDerivatives License 4.0 (CC BY-NC-ND), which permits downloading and sharing the work provided it is properly cited. The work cannot be changed in any way or used commercially without permission from the journal.

Glossary

ART = automatic real-time; **CFF** = critical flicker frequency; **EDSS** = Expanded Disability Status Scale; **GCIP** = ganglion cell and inner plexiform layer; **GEE** = Generalized estimating equation; **HC** = healthy control; **HCVA** = high-contrast visual acuity; **ICC** = intraclass correlation coefficient; **INL** = inner nuclear layer; **LCLA** = Low-contrast letter acuity; **OCT** = optical coherence tomography; **ON** = optic neuritis; **PASAT** = paced auditory serial addition task; **pRNFL** = Peripapillary retinal nerve fiber layer thickness; **RRMS** = relapsing-remitting MS; **RT** = reaction time; **SE** = standard error; **TAP** = Test of Attentional Performance; **TMV** = total macular volume; **VEP** = visual evoked potential.

Afferent visual pathway damage in MS results from acute focal damage, i.e., by optic neuritis (ON) or chronic diffuse damage,^{1–3} which leads to visual dysfunction and has a relevant impact on the quality of life of patients.⁴ Thus, clinical assessment of the visual pathway by means of high-contrast visual acuity (HCVA), functional assessment by means of visual evoked potentials (VEP),⁵ and more recently also structural assessment by optical coherence tomography (OCT) have become integral in diagnosing and monitoring patients with MS.⁶

An intriguing aspect of visual function is the visual temporal resolution, commonly assessed as the critical flicker frequency (CFF).⁷ CFF represents the frequency of a pulsed light source, from which an individual perceives the signal as flickering. Braunstein already reported in 1903 that CFF was decreased in optic atrophy and other ophthalmologic conditions.^{7,8} From the 1950s onward, CFF was investigated in MS,⁹ and decreased CFF was found to relate to ON,^{9–11} but independence from ON was also reported.^{12,13} Furthermore, higher cortical processes had an impact on CFF in patients with cerebral injuries¹⁴ and hepatic encephalopathy.¹⁵

Despite these early studies suggesting CFF as a potentially important marker for visual function, it remains unclear how CFF could serve as a marker for monitoring disease severity in MS. Our study is thus aimed at evaluating the potential of CFF measurements by investigating its association with clinical and cognitive assessments and structural visual system damage assessed by OCT.

Methods

Patients and controls

Forty-two patients with relapsing-remitting MS (RRMS) and 31 healthy controls (HCs) were enrolled in this prospective, cross-sectional pilot study. Inclusion criteria were diagnosis of RRMS according to the 2010 revised McDonald criteria¹⁶ (or HC) and age between 18 and 70 years. Exclusion criteria were any comorbidity (e.g., glaucoma, retinal disease, diabetes mellitus, ophthalmologic surgery), which could influence vision or the retina. Patients with MS were recruited consecutively over 5 years (2012–2017) from the NeuroCure Clinical Research Center, Berlin. HCs were recruited from volunteers.

To match the groups for sex and age, the 3 oldest female patients with MS were excluded before analysis, leading to a final number of 39 patients included in the analysis.

All patients with MS underwent clinical assessment and were scored using the Expanded Disability Status Scale (EDSS).¹⁷ A demographic and clinical overview is given in table 1.

Standard protocol approvals, registrations, and patient consents

This study was conducted in line with the strengthening the reporting of observational studies in epidemiology statement¹⁸ and was approved by the local ethics committee (EA1/216/11). It was conducted in accordance with the Declaration of Helsinki in its applicable version and applicable German laws. All participants provided written informed consent.

Table 1 Cohort description

	MS	HC	<i>p</i> Value
Participants, N	39	31	
Sex, male/female (N)	13/26	12/19	0.6 (χ^2)
Age/years, mean \pm SD (range)	45.9 \pm 8.4 (27–66)	45.0 \pm 16.1 (20–70)	0.6 (MWU)
Eyes with previous ON, yes/no (N)	28/50		
Time since diagnosis, mo, mean \pm SD (range)	156.8 \pm 92.3 (24–446)		
EDSS, median (range)	2.5 (0–6)		

Abbreviations: EDSS = Expanded Disability Status Scale; HC = healthy control; MWU = Mann-Whitney *U* test; ON = optic neuritis.

Critical flicker frequency

CFF measurement was performed monocularly using a HEPAtonorm analyzer (nevoLAB GmbH, Maierhöfen, Germany) in a quiet and semidarkened room. The device includes a headset that shields any external light from the participant's eyes and that features intrafoveal visual stimulation with a red luminous diode. The initial light signal of 60 Hz is perceived as continuous by the participant. Participants were instructed to press a stop button as soon as they perceive a flickering signal. When the operator starts the measurement on a hand-held controller, the pulse frequency decreases until it is perceived as flickering. The corresponding pulse frequency is defined as CFF and recorded by the hand-held controlling unit. CFF thresholds were determined monocularly, where each eye was tested 8 times, and the mean CFF (mCFF) value was calculated. All participants underwent a training session with 5 measurements before each initial measurement session.^{15,19}

Visual function parameters

HCVA was assessed with the Functional Vision Analyzer Optec 6500P system (Stereo Optical Co, Chicago, IL), as described previously.²⁰ Testing was performed monocularly under habitual correction and photopic conditions (85 cd/m²) with Early Treatment of Diabetic Retinopathy Study charts in a simulated distance of 20 ft.²⁰ Low-contrast letter acuity (LCLA) was assessed binocularly with 2.5% contrast Sloan charts in 2 m distance.²¹

Visual evoked potentials (VEP) were tested using the Dantec Keypoint VEP system (Natus Europe GmbH, Planegg, Germany). The P100 latency was measured using a standard black-and-white checkerboard stimulation (15'/50–60', at 1 m) and were recorded from the Oz electrode against a Cz reference electrode according to the 10–20 International System. The P100 amplitude was not analyzed.

Alertness and cognitive parameters

Because of time constraints, denial by participants and technical issues, only a subset of 17 patients with MS and 20 HCs underwent a selected task from the computerized test of attentional performance (TAP) battery for alertness testing.²² The tasks consist of a simple visual reaction time (RT) task without an acoustic warning signal, called tonic alertness task (part A) and a visual RT task preceded by an acoustic warning signal, phasic alertness (part B). To measure alertness, several trials were undertaken by alternating part A and part B. The participant was then asked to respond as fast as possible by pushing a button whenever a cross is displayed.²² Mean RTs from tests without acoustic warning signal were considered a measure of alertness.

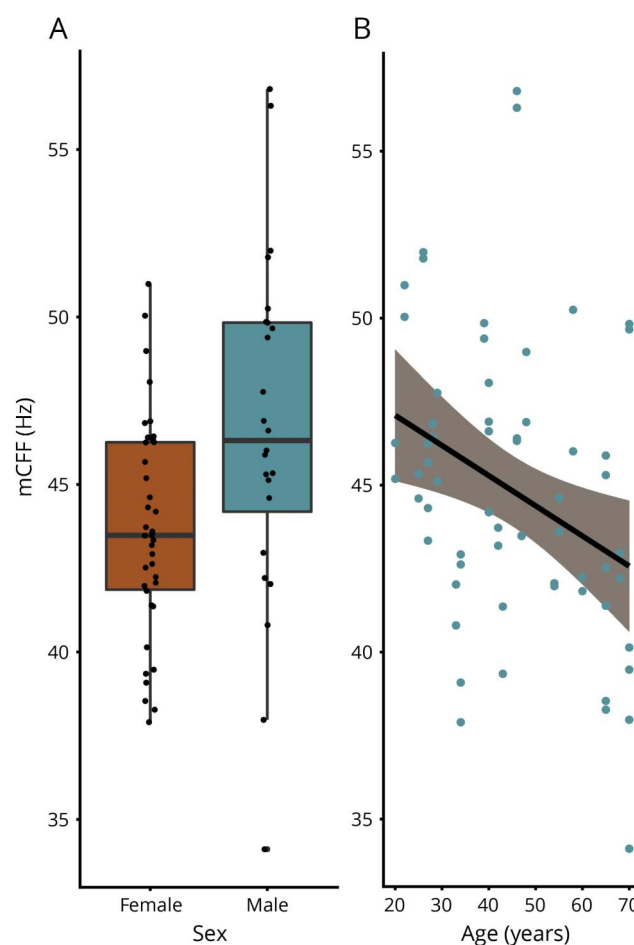
Also because of time constraints, only a subset of 29 patients with MS were tested with the 3-second version of the paced auditory serial addition task (PASAT), a measure of information processing speed.²³ For 14 patients, both alertness and PASAT testing were available.

OCT and intraretinal segmentation

All participants underwent retinal examination using a spectral domain OCT (Spectralis SD-OCT; Heidelberg Engineering, Heidelberg, Germany) using Eye Explorer 1.9.10.0 and automatic real-time (ART) image averaging.²⁴ Peripapillary retinal nerve fiber layer thickness (pRNFL) was derived from a standard ring scan around the optic nerve head (12°, 1536 A-scans, 16 ≤ ART ≤ 100) using segmentation by the device's software with viewing module 6.0.14.0. A macular volume scan (25° × 30°, 61 B-scans, 768 A-scans per B-scan, 12 ≤ ART ≤ 15) was acquired for total macular volume (TMV) including all retinal layers from the inner limiting membrane and Bruch membrane, as determined by the device's segmentation software within a 6-mm diameter cylinder around the fovea.

Intraretinal segmentation of combined ganglion cell and inner plexiform layer (GCIP) volume and inner nuclear layer (INL) volume was performed on macular scans with the Johns Hopkins OCT layer segmentation method (AURA Tools

Figure 1 Critical flicker frequency measurements in healthy controls



Comparison of CFF measurements between female and male HCs (A) and association of CFF measurements with age (B). HC = healthy control; mCFF = mean critical flicker frequency.

version 1.2)²⁵ combined with in-house pre-processing (cropping of volume scans to 6 × 6 mm) and postprocessing tools (graphical user interface for manual correction of segmentation results). All OCT scans were carefully checked for retinal changes unrelated to MS, sufficient quality,^{26,27} segmentation errors, and were manually corrected by a blinded experienced grader if necessary.

Statistical analysis

Statistical analyses were performed with R version 3.1.2 including geepack package 1.2-0. For demographic comparisons between patients and HCs, the Pearson χ^2 test for sex and nonparametric Mann-Whitney *U* test for age were used. Generalized estimating equation (GEE) models with working correlation matrix “exchangeable” and corrected for age and sex were used for group comparisons and associations involving eye-related measurements to account for within-subject intereye effects. GEE results are given with regression coefficient (B) and standard error (SE). All measurements were treated as continuous variables, and groups were stratified within patients with MS in ON and non-ON eyes. For the assessment of the test-retest reliability, the intraclass correlation coefficient (ICC) and its 95% confidence intervals were estimated using the R ICC package.²⁸ As suggested in a previous study, we considered an ICC greater than 0.9 as high and as moderate if between 0.8 and 0.9.²⁹ Statistical significance was established at $p < 0.05$. A correction for multiple comparisons with the Bonferroni-Holm method was performed for all correlation analyses.³⁰

Data availability

All data of this study will be shared by request from any qualified investigator.

Results

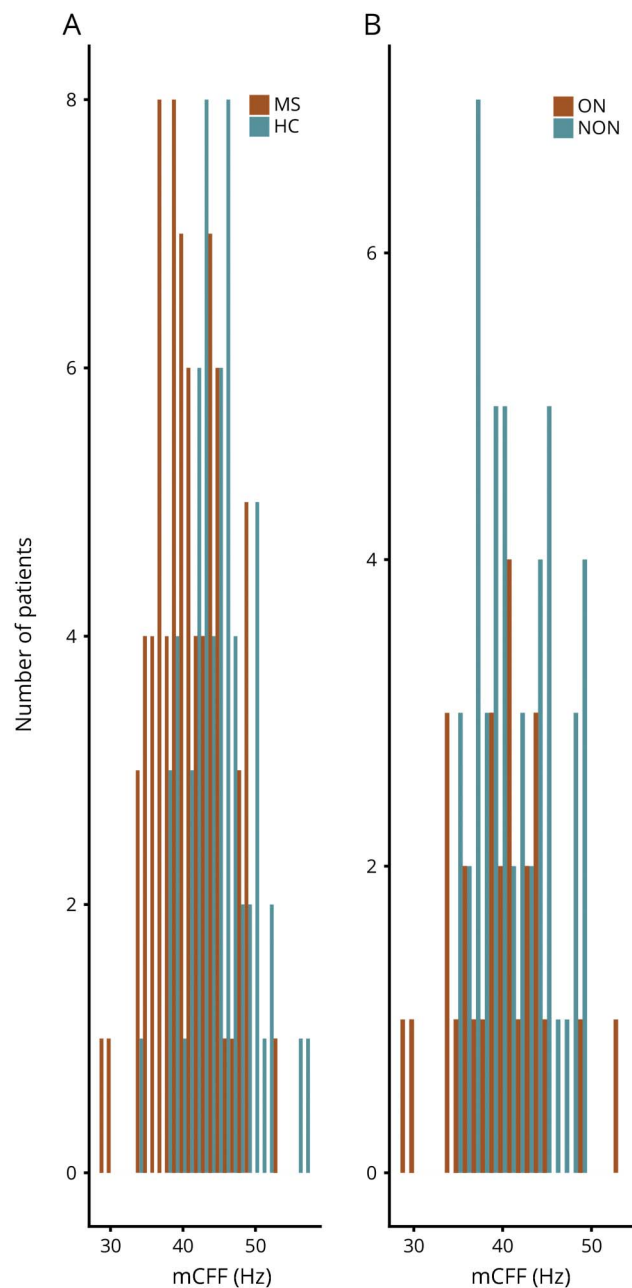
CFF in HC

HC had an mCFF of 44.8 ± 4.4 Hz. There was no mCFF difference between female and male HCs (43.70 ± 3.24 vs 46.6 ± 5.3 Hz, $B = 1.7188$, $SE = 4.06$, $p = 0.67$) (figure 1A), but lower mCFF was associated with higher age ($B = -0.090$, $SE = 0.043$, $p = 0.036$) (figure 1B) in HC. Also, in HC, there was no association between mCFF and HCVA ($B = 2.30$, $SE = 1.99$, $p = 0.34$), mCFF and LCLA ($B = 0.029$, $SE = 0.078$, $p = 0.71$), or VEP P100 latency ($B = 0.044$, $SE = 0.042$, $p = 0.29$). Likewise, alertness did not correlate with mCFF ($B = -0.011$, $SE = 0.0093$, $p = 0.25$). Mean results are presented in a supplemental file (table e-1, links.lww.com/NXI/A65). The test-retest reliability in HC was high, with an ICC value of 0.91 (0.87–0.94).

CFF in MS

mCFF in patients with MS was lower than in HC (40.9 ± 4.72 Hz, $p < 0.001$). There was no difference between ON and non-ON eyes (39.7 ± 5.22 vs 41.5 ± 4.33 Hz, $p = 0.094$) (figure 2). mCFF was also not associated with visual function as determined by HCVA, LCLA, VEP latencies, and retinal OCT parameters pRNFL (global and papillomacular bundle),

Figure 2 Critical flicker frequency measurements



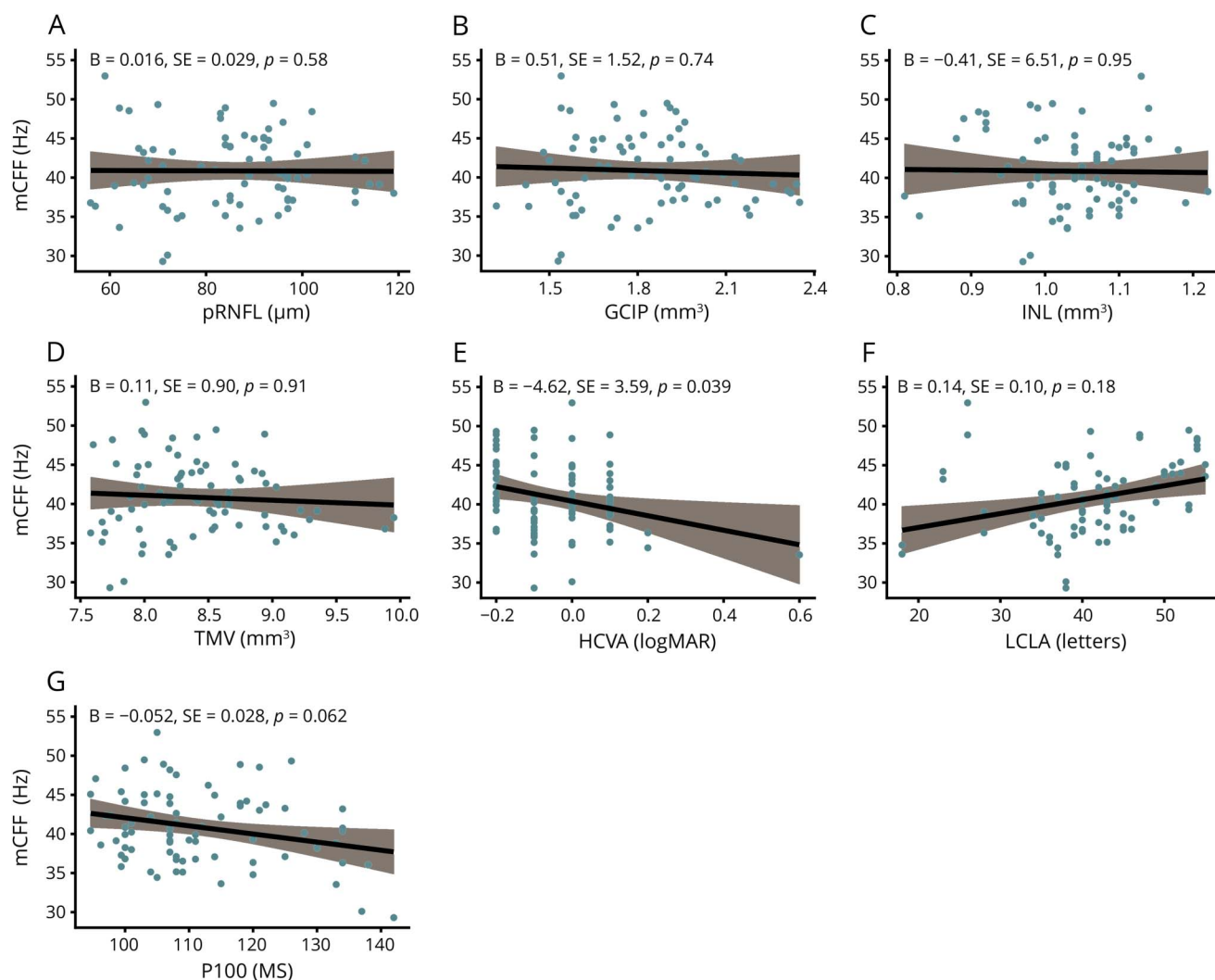
Comparison of CFF measurements between HCs and patients with MS (A) and comparison of CFF measurements between eyes with optic neuritis (ON) and eyes without ON (NON) in patients with MS (B). HC = healthy control; mCFF = mean critical flicker frequency.

GCIP, INL, and TMV (figure 3). Mean results are presented in a supplemental file (table e-1, links.lww.com/NXI/A65). The test-retest reliability was moderate, with an ICC value of 0.89 (0.85–0.92).

CFF and disability

We then investigated whether CFF was associated with overall disability, alertness, and information processing speed in MS patients. Here, overall disability was found as higher EDSS scores, which was inversely correlated with lower

Figure 3 Critical flicker frequency measurements and visual function in MS



Association of CFF measurements with structural and visual functional parameters: pRNFL (A), GCIP (B), INL (C), TMV (D), HCVA (E), LCLA (F), P100 (G). After Bonferroni-Holm correction, no p value remained significant. GCIP = ganglion cell/inner plexiform layer; HCVA = high-contrast visual acuity; INL = inner nuclear layer; LCLA = low-contrast letter acuity; mCFF = mean critical flicker frequency; pRNFL = peripheral retinal nerve fiber layer; TMV = total macular volume; VEP = visual evoked potential.

mCFF ($r^2 = 0.26$, $B = -1.77$, $SE = 0.50$, $p = 0.00036$) (figure 4A). Moreover, lower mCFF was associated with worse alertness ($r^2 = 0.42$, $B = -0.048$, $SE = 0.014$, $p = 0.00042$) (figure 4B), but not with information processing speed, assessed by PASAT ($B = 0.063$, $SE = 0.065$, $p = 0.33$). After Bonferroni-Holm correction, the associations between mCFF and alertness and between mCFF and EDSS remained significant. The SD of the CFF measurements was not associated with alertness ($B = 0.0015$, $SE = 0.0035$, $p = 0.68$).

Discussion

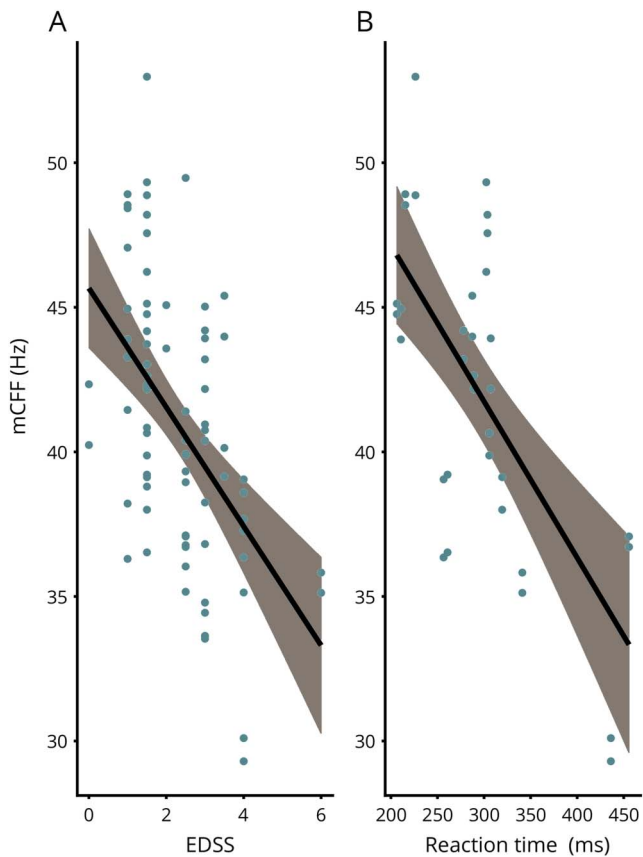
In this study, we investigated the visual temporal resolution by means of CFF assessment in patients with MS. Key findings are as follows: (1) CFF is reduced in MS compared with HC; (2) CFF is not or only weakly associated with structural and functional measures of afferent visual system damage in MS;

and (3) by contrast, CFF is associated with alertness and clinical disability.

Previous studies consistently reported impaired CFF in MS and ON.^{9,10,12} Some investigators interpreted these results as support for cortical damage causing impairment at the central perceptual-discriminative level.^{9,31} Thus, they recommended CFF as a general measure of cortical processing capacity.³² On the other hand, neuroaxonal degeneration in the retina and the visual pathway of patients with MS could affect CFF as well.⁹

Perception of high-frequency stimuli has been suggested to be influenced by retinal ganglion cells.³² Furthermore, cells of the magnocellular system are confirmed to be more sensitive to higher temporal frequency stimulation than cells of the parvocellular system.³³ Thus, we postulated that CFF could

Figure 4 Critical flicker frequency measurements in patients with MS



Association of CFF measurements with the EDSS (A) and with reaction time in MS (B). EDSS = Expanded Disability Status Scale; mCFF = mean critical flicker frequency.

reflect integrity of the magnocellular retinal cells' ability to detect higher frequency stimuli,³⁴ and damage of magnocellular retinal ganglion cells might specifically cause decreased CFF. However, our results show no significant association of CFF with any afferent visual system marker, indicating that retinal neuroaxonal retinal damage had no or only negligible influence to CFF in patients with MS.^{34,35} These findings could be explained by effects being small and masked by other associations. However, neuroaxonal retinal damage and demyelination of our MS cohort seem to be comparable to other MS cohorts regarding OCT and VEP measurements.^{36,37}

By contrast, our results showed that lower CFF values are associated with longer RTs in a test of alertness, whereas there is no association with CFF SD. This suggests that the association of CFF with alertness is not caused by impaired alertness reducing the ability to comply with the CFF assessment. Tonic alertness refers to a cognitive control of wakefulness and arousal in the absence of a warning and is part of the domain of attention.³⁸ It is based on the activation of frontoparietal and partly thalamic regions of the right hemisphere.³⁸ Alertness was shown to be impaired after

appearance of right hemispheric lesions,³⁸ and we could report an association with MS-related fatigue in an earlier study.³⁹ This suggests that impaired CFF reflects damage to higher cognitive areas involved in alertness and cognition. Contrarily, the PASAT, which focuses on information processing speed, the cognitive domain most commonly affected in MS, showed no association with CFF in our study.

CFF also correlated with overall disability as represented by the EDSS score. Studies from the 1950/1960s already suggested an association of CFF with general disease disability, but did not investigate this systematically.^{9,40}

CFF measurements from our HC are in line with previous studies regarding the mean CFF and an increase of CFF with age.⁴¹ However, although 1 study found sex differences in CFF, this difference was not significant in our study.⁴² The ICC values for CFF measurements in HC and MS showed that this method produces reliable results.

Our study has several limitations. Sample sizes of <40 in both MS and control groups might have been insufficient to detect small effects. This is particularly important for a potential effect of a previous ON on the CFF, which was not significant in our study, but gave a low *p* value indicative of a potential power issue. Moreover, the subsets with available TAP and PASAT tests were even smaller, and differences in sample size due to some technical problems and time restrictions in the assessment of the measurements may have resulted in a selection bias potentially weakening our conclusions. We therefore might have missed an association of CFF to information processing as assessed by PASAT. It should also be noted that exclusion of the 3 oldest patients has to be regarded critically because higher age is associated with decreased CFF and impaired visual parameters potentially influencing our findings in regard of the absence of associations between CFF and visual parameters. All visual parameters were measured monocularly except the LCLA because of unavailability at the beginning of the study, potentially reducing the validity of its comparison to monocularly measured CFF values. We did not perform MRI in our study, so we have no information on the association of radiologic disease activity and CFF. Likewise, we have only cross-sectional measurements, so the dynamics of CFF in context of the disease course and any causal inferences remain unclear. It is important to note that most previous studies on CFF in ON and MS were published in the 1950–1970s.^{11–13} Thus, test procedures regarding CFF and other parameters might differ, making comparison of our results to these previous ones difficult. The interpretation of the findings of this study is mostly based on the absence of association with functional and visual parameters. Therefore, we believe that adding MRI and conducting longitudinal observations would be the next step in validating CFF measurements in MS.

Our study showed that visual temporal resolution as assessed by CFF is impaired in patients with MS independent of visual and structural visual system damage. Whether CFF

can serve as a marker for overall disease activity warrants further investigation.

Author contributions

N. Ayadi: assessed CFF data, performed statistical analysis, and drafted the manuscript. J. Dörr: conceived the study and critically revised the manuscript. S. Motamedi and K. Gawlik: analyzed OCT data and critically revised the manuscript. J. Bellmann-Strobl, J. Mikolajczak, and A.U. Brandt: contributed to data interpretation and critically revised the manuscript. H. Zimmermann: contributed to the design of the study and data interpretation and drafted the manuscript. F. Paul: contributed to the design of the study and data interpretation and critically revised the manuscript.

Acknowledgment

The authors thank Cynthia Kraut and Katharina Stößlein for excellent technical support. They also thank Claudia Chien for English proofreading.

Study funding

This study was supported by a research grant by Novartis Pharma GmbH (Germany). F. Paul is supported by Deutsche Forschungsgemeinschaft (DFG Exc 257).

Disclosure

N. Ayadi reports no disclosures. J. Dörr served on the advisory boards of Bayer, Novartis, Sanofi Genzyme, and Merck Serono; received travel funding from Novartis, Sanofi Genzyme, Biogen, and Bayer and speaker honoraria from Novartis, Merck Serono, Sanofi Genzyme, Biogen, and Roche; and received research support from Novartis and Bayer. S. Motamedi has a patent pending for method for estimating shape parameters of the fovea by optical coherence tomography. K. Gawlik has a patent pending for retinal image analysis. J. Bellmann-Strobl received travel funding and speaker honoraria from Bayer, Sanofi-Aventis/Genzyme, Merck, and Teva. J. Mikolajczak received travel funding and/or speaker honoraria from Teva, Biogen, Bayer, and Novartis. A.U. Brandt has a patent pending for perceptive visual computing based motor function analysis, MS biomarker, and retinal image analysis; serves on the executive board of IMSVISUAL; received research support from Novartis, Biogen, BMWi, BMBF, University of California, Irvine, and The Guthy Jackson Charitable Foundation; and holds stock or stock options held in Motognosis and Nocturne. H. Zimmermann received speaker honoraria from Teva and Bayer and received research support from Novartis. F. Paul served on the scientific advisory boards of Novartis and MedImmune; received travel funding and/or speaker honoraria from Bayer, Novartis, Biogen, Teva, Sanofi-Aventis/Genzyme, Merck Serono, Alexion, Chugai, MedImmune, and Shire; is an academic editor of *PLoS One* and an associate editor of *Neurology: Neuroimmunology & Neuroinflammation*; consulted for Sanofi Genzyme, Biogen, MedImmune, Shire, and Alexion; and received research support from Bayer, Novartis, Biogen, Teva, Sanofi-Aventis/Genzyme, Alexion,

Merck Serono, German Research Council, Werth Stiftung of the City of Cologne, German Ministry of Education and Research, Arthur Arnstein Stiftung Berlin, Arthur Arnstein Foundation Berlin, Guthy Jackson Charitable Foundation, and NMMS. Full disclosure form information provided by the authors is available with the full text of this article at Neurology.org/NN.

Received March 14, 2018. Accepted in final form June 25, 2018.

References

1. Martínez-Lapiscina EH, Sanchez-Dalmau B, Fraga-Pumar E, et al. The visual pathway as a model to understand brain damage in multiple sclerosis. *Mult Scler* 2014;20:1678–1685.
2. Kuchling J, Brandt AU, Paul F, Scheel M. Diffusion tensor imaging for multilevel assessment of the visual pathway: possibilities for personalized outcome prediction in autoimmune disorders of the central nervous system. *EPMA J* 2017;8:279–294.
3. Backner Y, Kuchling J, Massarwa S, et al. Anatomical wiring and functional networking changes in the visual system following optic neuritis. *JAMA Neurol* 2018;75:287–295.
4. Schinzel J, Zimmermann H, Paul F, et al. Relations of low contrast visual acuity, quality of life and multiple sclerosis functional composite: a cross-sectional analysis. *BMC Neurol* 2014;14:31.
5. Halliday AM, McDonald WI, Mushin J. Visual evoked response in diagnosis of multiple sclerosis. *Br Med J* 1973;4:661–664.
6. Brandt AU, Martínez-Lapiscina EH, Nolan R, Saidha S. Monitoring the course of MS with optical coherence tomography. *Curr Treat Options Neurol* 2017;19:15.
7. Brenton RS, Thompson HS, Maxner C. Critical flicker frequency: a new look at an old test [internet]. In: *New Methods of Sensory Visual Testing*. New York: Springer; 1989:29–52. Available at: link.springer.com/chapter/10.1007/978-1-4613-8835-7_3.
8. Braunstein EP. Beitrag zur Lehre des intermittierenden Lichtreizes der gesunden und kranken Retina. *Z Psychol Physiol Sinnesorgan* 1903;33:171–206, 241–288.
9. Parsons OA, Miller PN. Flicker fusion thresholds in multiple sclerosis. *AMA Arch Neurol Psychiatry* 1957;77:134–139.
10. Titcombe AF, Willison RG. Flicker fusion in multiple sclerosis. *J Neurol Neurosurg Psychiatry* 1961;24:260–265.
11. Galvin RJ, Regan D, Heron JR. Impaired temporal resolution of vision after acute retrobulbar neuritis. *Brain* 1976;99:255–268.
12. Daley ML, Swank RL, Ellison CM. Flicker fusion thresholds in multiple sclerosis: a functional measure of neurological damage. *Arch Neurol* 1979;36:292–295.
13. Patterson VH, Foster DH, Heron J, Mason RJ. Multiple sclerosis: luminance threshold and measurements of temporal characteristics of vision. *Arch Neurol* 1981;38:687–689.
14. Bender MB, Teuber HL. Disturbances in visual perception following cerebral lesions. *J Psychol* 1949;28:223–233.
15. Sharma P, Sharma BC, Puri V, Sarin SK. Critical flicker frequency: diagnostic tool for minimal hepatic encephalopathy. *J Hepatol* 2007;47:67–73.
16. Polman CH, Reingold SC, Banwell B, et al. Diagnostic criteria for multiple sclerosis: 2010 revisions to the McDonald criteria. *Ann Neurol* 2011;69:292–302.
17. Kurtzke JF. Rating neurologic impairment in multiple sclerosis: an expanded disability status scale (EDSS). *Neurology* 1983;33:1444.
18. von Elm E, Altman DG, Egger M, et al. Strengthening the reporting of observational studies in epidemiology (STROBE) statement: guidelines for reporting observational studies. *BMJ* 2007;335:806–808.
19. Romero-Gómez M, Córdoba J, Jover R, et al. Value of the critical flicker frequency in patients with minimal hepatic encephalopathy. *Hepatology* 2007;45:879–885.
20. Bock M, Brandt AU, Kuchenbecker J, et al. Impairment of contrast visual acuity as a functional correlate of retinal nerve fibre layer thinning and total macular volume reduction in multiple sclerosis. *Br J Ophthalmol* 2012;96:62–67.
21. Baier ML, Cutter GR, Rudick RA, et al. Low-contrast letter acuity testing captures visual dysfunction in patients with multiple sclerosis. *Neurology* 2005;64:992–995.
22. Zimmermann P, Fimm B. Test for Attentional Performance (TAP)-Version 1.02. Manual. Würselen: Psytest; 1994.
23. Cutter GR, Baier ML, Rudick RA, et al. Development of a multiple sclerosis functional composite as a clinical trial outcome measure. *Brain J Neurol* 1999;122:871–882.
24. Cruz-Herranz A, Balk LJ, Oberwahrenbrock T, et al. The APOSTEL recommendations for reporting quantitative optical coherence tomography studies. *Neurology* 2016;86:2303–2309.
25. Lang A, Carass A, Hauser M, et al. Retinal layer segmentation of macular OCT images using boundary classification. *Biomed Opt Express* 2013;4:1133–1152.
26. Tewarie P, Balk L, Costello F, et al. The OSCAR-IB consensus criteria for retinal OCT quality assessment. *PLoS One* 2012;7:e34823.
27. Schippling S, Balk LJ, Costello F, et al. Quality control for retinal OCT in multiple sclerosis: validation of the OSCAR-IB criteria. *Mult Scler* 2015;21:163–170.
28. Wolak ME, Fairbairn DJ, Paulsen YR. Guidelines for estimating repeatability. *Methods Ecol Evol* 2012;3:129–137.
29. Vaz S, Falkmer T, Passmore AE, et al. The case for using the repeatability coefficient when calculating test–retest reliability. *PLoS One* 2013;8:e73990.
30. Holm SA. Simple sequentially rejective multiple test procedure. *Scand J Stat* 1979;6:65–70.

31. Ross AT, Reitan Intellectual RM, Functions affective: in multiple sclerosis: a quantitative study. *AMA Arch Neurol Psychiatry* 1955;73:663–677.
32. Seitz AR, Sr JEN, Holloway SR, Watanabe T. Perceptual learning of motion leads to faster flicker perception. *PLoS One* 2006;1:e28.
33. Derrington AM, Lennie P. Spatial and temporal contrast sensitivities of neurones in lateral geniculate nucleus of macaque. *J Physiol* 1984;357:219–240.
34. Jacobson DM, Olson KA. Impaired critical flicker frequency in recovered optic neuritis. *Ann Neurol* 1991;30:213–215.
35. Raz N, Shear-Yashuv G, Backner Y, et al. Temporal aspects of visual perception in demyelinating diseases. *J Neurol Sci* 2015;357:235–239.
36. Petzold A, de Boer JF, Schipling S, et al. Optical coherence tomography in multiple sclerosis: a systematic review and meta-analysis. *Lancet Neurol* 2010;9:921–932.
37. Trip SA, Schlottmann PG, Jones SJ, et al. Retinal nerve fiber layer axonal loss and visual dysfunction in optic neuritis. *Ann Neurol* 2005;58:383–391.
38. Sturm W, Willmes K. On the functional neuroanatomy of intrinsic and phasic alertness. *NeuroImage* 2001;14(1 pt 2):S76–S84.
39. Weinges-Evers N, Brandt AU, Bock M, et al. Correlation of self-assessed fatigue and alertness in multiple sclerosis. *Mult Scler J* 2010;16:1134–1140.
40. Sandry M. Critical flicker frequency in multiple sclerosis. *Percept Mot Skills* 1963;16:103–108.
41. Misiak H. Age and sex differences in critical flicker frequency. *J Exp Psychol* 1947;37:318–332.
42. Ginsburg N, Jurenovskis M, Jamieson J. Sex differences in critical flicker frequency. *Percept Mot Skills* 1982;54(3 suppl):1079–1082.

Ayadi et al. Mult Scler. 2021 (Bewegungssehen &
Sehbahnschaden)

Journal Data Filtered By: **Selected JCR Year: 2019** Selected Editions: SCIE,SSCI
 Selected Categories: **"CLINICAL NEUROLOGY"** Selected Category
 Scheme: WoS

Gesamtanzahl: 204 Journale

Rank	Full Journal Title	Total Cites	Journal Impact Factor	Eigenfactor Score
1	LANCET NEUROLOGY	33,050	30.039	0.062420
2	Nature Reviews Neurology	11,029	27.000	0.028770
3	Alzheimers & Dementia	16,289	17.127	0.042180
4	ACTA NEUROPATHOLOGICA	21,908	14.251	0.040740
5	JAMA Neurology	10,471	13.608	0.043110
6	BRAIN	53,282	11.337	0.067050
7	NEURO-ONCOLOGY	12,950	10.247	0.029050
8	SLEEP MEDICINE REVIEWS	8,077	9.613	0.013000
9	ANNALS OF NEUROLOGY	37,304	9.037	0.044120
10	NEUROLOGY	90,213	8.770	0.103530
11	MOVEMENT DISORDERS	27,638	8.679	0.031140
12	JOURNAL OF NEUROLOGY NEUROSURGERY AND PSYCHIATRY	30,621	8.234	0.028510
13	Neurology-Neuroimmunology & Neuroinflammation	2,232	7.724	0.008400
14	NEUROPATHOLOGY AND APPLIED NEUROBIOLOGY	3,992	7.500	0.005960
15	Journal of Stroke	1,247	7.470	0.004240
16	STROKE	66,466	7.190	0.078010
17	Brain Stimulation	6,537	6.565	0.015580
18	NEUROSCIENTIST	5,188	6.500	0.007220
19	Alzheimers Research & Therapy	3,876	6.116	0.011650
20	EPILEPSIA	26,560	6.040	0.029790




Selected JCR Year: 2019; Selected Categories: "CLINICAL NEUROLOGY"

1

Rank	Full Journal Title	Total Cites	Journal Impact Factor	Eigenfactor Score
21	Neurotherapeutics	4,998	6.035	0.009520
22	Translational Stroke Research	2,274	5.780	0.004520
23	BRAIN PATHOLOGY	5,308	5.568	0.007020
24	Pain and Therapy	354	5.526	0.001230
25	PAIN	37,753	5.483	0.035730
26	Multiple Sclerosis Journal	11,792	5.412	0.019460
27	BIPOLAR DISORDERS	4,838	5.410	0.006610
28	Therapeutic Advances in Neurological Disorders	1,421	5.000	0.002960
29	International Journal of Stroke	4,853	4.882	0.015560
30	CEPHALALGIA	11,053	4.868	0.011970
31	NEUROSURGERY	29,977	4.853	0.021690
32	SLEEP	22,296	4.805	0.024610
33	JOURNAL OF HEADACHE AND PAIN	3,898	4.797	0.007600
34	CNS DRUGS	4,768	4.786	0.007670
35	Stroke and Vascular Neurology	496	4.765	0.002000
36	JOURNAL OF PAIN	10,887	4.621	0.015040
37	EUROPEAN JOURNAL OF NEUROLOGY	11,015	4.516	0.017330
38	DEVELOPMENTAL MEDICINE AND CHILD NEUROLOGY	13,007	4.406	0.012730
39	Current Neurology and Neuroscience Reports	3,429	4.376	0.006810
40	Nature and Science of Sleep	728	4.375	0.001970
41	PROGRESS IN NEURO-PSYCHOPHARMACOLOGY & BIOLOGICAL PSYCHIATRY	11,179	4.361	0.013670
42	INTERNATIONAL JOURNAL OF NEUROPSYCHOPHARMACOLOGY	6,749	4.333	0.011150

Selected JCR Year: 2019; Selected Categories: "CLINICAL NEUROLOGY"

Impaired motion perception is associated with functional and structural visual pathway damage in multiple sclerosis and neuromyelitis optica spectrum disorders

Noah Ayadi , Frederike C Oertel, Susanna Asseyer , Rebekka Rust, Ankelien Duchow, Joseph Kuchling, Judith Bellmann-Strobl, Klemens Ruprecht, Alexander Klistorner, Alexander U Brandt , Friedemann Paul and Hanna G Zimmermann

Abstract

Background: Decreased motion perception has been suggested as a marker for visual pathway demyelination in optic neuritis (ON) and/or multiple sclerosis (MS).

Objectives: To examine the influence of neuro-axonal damage on motion perception in MS and neuromyelitis optica spectrum disorders (NMOSD).

Methods: We analysed motion perception with numbers-from-motion (NFM), visual acuity, (multifocal (mf)) VEP, optical coherence tomography in patients with MS ($n = 38$, confirmatory cohort $n = 43$), NMOSD ($n = 13$) and healthy controls ($n = 33$).

Results: NFM was lower compared with controls in MS ($B = -12.37$, $p < 0.001$) and NMOSD ($B = -34.5$, $p < 0.001$). NFM was lower in ON than in non-ON eyes ($B = -30.95$, $p = 0.041$) in NMOSD, but not MS. In MS and NMOSD, lower NFM was associated with worse visual acuity ($B = -139.4$, $p < 0.001/B = -77.2$, $p < 0.001$) and low contrast letter acuity ($B = 0.99$, $p = 0.002/B = 1.6$, $p < 0.001$), thinner peripapillary retinal nerve fibre layer ($B = 1.0$, $p < 0.001/B = 0.92$, $p = 0.016$) and ganglion cell/inner plexiform layer ($B = 64.8$, $p < 0.001/B = 79.5$, $p = 0.006$), but not with VEP P100 latencies. In the confirmatory MS cohort, lower NFM was associated with thinner retinal nerve fibre layer ($B = 1.351$, $p < 0.001$) and increased mfVEP P100 latencies ($B = -1.159$, $p < 0.001$).

Conclusions: Structural neuro-axonal visual pathway damage is an important driver of motion perception impairment in MS and NMOSD.

Keywords: Multiple sclerosis, neuromyelitis optica spectrum disorders, motion perception, retina, vision disorders, optical coherence tomography, visual evoked potentials

Date received: 21 March 2021; revised: 8 June 2021; accepted: 28 June 2021

Introduction

Visual system damage is common in multiple sclerosis (MS) and neuromyelitis optica spectrum disorders (NMOSD).¹⁻³ The resulting visual function loss is assessed by visual acuity, contrast sensitivity, and visual fields.⁴ Structural neuro-axonal visual system damage can be quantified by retinal optical coherence tomography (OCT) and demyelination of the afferent visual pathway by visual evoked potentials (VEP).^{5,6}

An alternative and intriguing concept for assessing visual system damage is the measurement of dynamic

functions, such as motion perception.^{7,8} Motion perception begins in the retina where the signal is transferred through the magnocellular cells past the lateral geniculate nucleus to the middle temporal visual area to be cortically processed.^{9,10} Deficits in motion perception were previously described in patients with MS and optic neuritis (ON).¹¹ These could be relevant for visual difficulties in executing everyday tasks.¹²

There are competing concepts regarding the cause of motion perception deficits in MS and ON. Worse motion perception was associated with increased VEP latencies,



Correspondence to:

HG Zimmermann
Experimental and
Clinical Research Center,
Lindenberger Weg 80, 13125
Berlin, Germany.
[hanna.zimmermann@
charite.de](mailto:hanna.zimmermann@charite.de)

Noah Ayadi
Susanna Asseyer
Rebekka Rust
Ankelien Duchow
Judith Bellmann-Strobl
Hanna G Zimmermann
Experimental and Clinical
Research Center, Max
Delbrück Center for
Molecular Medicine and
Charité – Universitätsmedizin
Berlin, corporate member
of Freie Universität Berlin
and Humboldt-Universität
zu Berlin, Berlin, Germany/
NeuroCure Clinical
Research Center, Charité
– Universitätsmedizin
Berlin, corporate member of
Freie Universität Berlin and
Humboldt-Universität zu
Berlin, Berlin, Germany

Frederike C Oertel
Experimental and Clinical
Research Center, Max
Delbrück Center for
Molecular Medicine and
Charité – Universitätsmedizin
Berlin, corporate member
of Freie Universität Berlin
and Humboldt-Universität
zu Berlin, Berlin, Germany/
NeuroCure Clinical
Research Center, Charité
– Universitätsmedizin
Berlin, corporate member
of Freie Universität Berlin
and Humboldt-Universität
zu Berlin, Berlin, Germany/
Department of Neurology,
University of California, San
Francisco, San Francisco,
CA, USA

Joseph Kuchling
Friedemann Paul
Experimental and Clinical
Research Center, Max
Delbrück Center for
Molecular Medicine and

Charité – Universitätsmedizin Berlin, corporate member of Freie Universität Berlin and Humboldt-Universität zu Berlin, Berlin, Germany/ NeuroCure Clinical Research Center, Charité – Universitätsmedizin Berlin, corporate member of Freie Universität Berlin and Humboldt-Universität zu Berlin, Berlin, Germany/ Department of Neurology, Charité – Universitätsmedizin Berlin, corporate member of Freie Universität Berlin and Humboldt-Universität zu Berlin, Berlin, Germany

Klemens Ruprecht
Department of Neurology, Charité – Universitätsmedizin Berlin, corporate member of Freie Universität Berlin and Humboldt-Universität zu Berlin, Berlin, Germany

Alexander Klistorner
Faculty of Medicine, Health and Human Sciences, Macquarie University, Sydney, NSW, Australia/ Save Sight Institute, The University of Sydney, Sydney, NSW, Australia

Alexander U Brandt
Experimental and Clinical Research Center, Max Delbrück Center for Molecular Medicine and Charité – Universitätsmedizin Berlin, corporate member of Freie Universität Berlin and Humboldt-Universität zu Berlin, Berlin, Germany/ NeuroCure Clinical Research Center, Charité – Universitätsmedizin Berlin, corporate member of Freie Universität Berlin and Humboldt-Universität zu Berlin, Germany/ Department of Neurology, University of California, Irvine, Irvine, CA, USA

and both persisted after recovery of static visual function following acute ON.¹³ Impaired motion perception might thus be the clinical correlate to prolonged VEP or side-discrepant latencies reflecting optic nerve demyelination.¹³ Based on these findings, studies in MS suggested motion perception as a marker for visual dysfunction and demyelination.^{13,14} However, motion perception changes are not specific for ON and are also altered in primary open-angle glaucoma,¹⁵ Alzheimer's disease¹⁶ and in autism.¹⁷ This suggests that motion perception deficits could originate from different levels of the visual system and involve higher cortical function. Especially cognitive deficits could be relevant confounders in MS, since patients regularly present with cognitive dysfunction and motion perception testing requires a certain ability of information processing.¹⁸

Thus, the aim of our study was (a) to confirm the association of motion perception with VEP-assessed visual pathway myelination status in MS, (b) to explore associations with structural retinal damage and cognition and (c) to first-time investigate motion perception in patients with NMOSD.

Materials and methods

Patient and controls

Inclusion criteria for this prospective, cross-sectional study were an age between 18 and 70 years and a diagnosis of relapsing-remitting multiple sclerosis (RRMS) according to the 2017 revised McDonald criteria,¹ clinically isolated syndrome (CIS), NMOSD according to the 2015 International Consensus Diagnostic Criteria² or – for healthy controls (HC) – being free of neurological diseases. Exclusion criteria were any comorbidities influencing vision or the retina. Patients and HC were recruited from ongoing prospective observational cohort studies at Charité – Universitätsmedizin Berlin and at Macquarie University, Sydney. Berlin patients were clinically assessed and scored using the Expanded Disability Status Scale (EDSS)¹⁹ and underwent the Symbol Digit Modalities Test (SDMT), a test for information processing speed and concentration.²⁰

This study was approved by the local ethics committees in Berlin and Sydney and conducted in accordance with the Declaration of Helsinki in its applicable version and applicable local laws. All participants gave written informed consent.

Motion perception

Motion perception, specifically numbers from motion (NFM), was tested monocularly under habitual visual

acuity (personal eye wear, if applicable) on a computer screen at a distance of 50 cm, using a revised testing software developed by the Functional Magnetic Resonance Imaging (fMRI) Unit, Neurology Department, Hadassah.⁷ The test presents moving pixels revealing camouflaged three-digit numbers, based on the motion perception test assessed by Regan et al.¹¹ and is programmed to output an automatically calculated score ranging from 0 (worst) to 140 (best).⁷ Prior to the test, all subjects underwent a short binocular training session. In two ON eyes of two MS patients and one NMOSD eye, NFM assessment was not possible due to low visual function. Those eyes were excluded from all analyses.

Visual function

In Berlin, high contrast VA (HCVA) and low contrast letter acuity (LCLA) were acquired monocularly with best refraction correction. HCVA was assessed by the use of retro-illuminated ETDRS charts in 4 m distance and converted into logMAR units. LCLA was tested with 2.5% contrast retro-illuminated Sloan charts in 2 m distance. As reported by a recent study, the use of the motion tool might be limited in patients with low VA, therefore a supplementary analysis of a subgroup including only patients with HCVA \leq 0.1 logMAR was performed.²¹ For this analysis, one eye with lower HCVA from the main MS cohort and three eyes from the NMOSD cohort were excluded.

In Berlin, full-field VEP was measured under best refraction correction using the RETI-port/scan 21 device (Roland Consult GmbH, Brandenburg, Germany) with gold-cup electrodes and the Dantec™ Keypoint VEP system (Natus Europe GmbH, Planegg, Germany).⁸ We analysed measurements of the different VEP devices separately and had to exclude MS and NMOSD patients' VEP measurements from 5 eyes due to insufficient VEP signal. We therefore analysed a subset of 47 eyes of 24 MS patients and 23 eyes of 12 NMOSD patients measured on the first device and a subset of 23 eyes of 12 MS (ON/NON eyes: 4/19) patients measured on the second device.

In Sydney, multifocal VEP (mfVEP) were tested under best corrected conditions using the VisionSearch 1 system (VisionSearch, Sydney, NSW, Australia) with four gold-disc electrodes (Grass, West Warwick, RI, US).²² The mean mfVEP latency of the 56 segments was used for statistical analysis.

Optical coherence tomography

All participants underwent retinal examination using a spectral domain OCT (Spectralis SD-OCT; Heidelberg

Table 1. Demographic and clinical cohort description.

		Berlin Cohort			Sydney Cohort
		MS	NMOSD	HC	MS
Participants	N_{patients}	38	13	33	43
Sex	Male/female (N_{patients})	11/27	1/12	9/24	16/27
Age/years	Mean \pm SD (range)	36.56 \pm 9.95 (20–61)	47.86 \pm 15.36** (21–66)	37.37 \pm 15.85 (21–70)	42.72 \pm 10.02 (19–65)
None/Unilateral/ Bilateral ON	N_{patients}	16/18/4	6/1/6		19/24/0
Eyes with previous ON	yes/no (N_{eyes})	22/54	13/12		31/55
Time from last ON/years	Mean \pm SD (range)	5.56 \pm 8.51 (0.08–28.75)	5.88 \pm 3.64 (1.17–12.92)		
Disease duration/years	Mean \pm SD (range)	3.46 \pm 3.61 (0.08–17.67)	5.67 \pm 3.33 (0.33–12.75)		
EDSS	Median (range)	1.5 (0–4.5)	3.5 (1.5–6.0)		
SDMT	Mean \pm SD (range)	63.42 \pm 13.65 (34–94)	51.15 \pm 4.12 (45–57) ($n =$ 13)		

MS: multiple sclerosis; NMOSD: neuromyelitis optica spectrum disorders; HC: healthy controls; SD: standard deviation; ON: optic neuritis; EDSS: expanded disability status scale; SDMT: symbol digit modalities test. Significant difference to HC marked by asterisks: * $p = 0.05$, ** $p \leq 0.01$, *** $p \leq 0.001$.

Engineering, Heidelberg, Germany). We acquired a ring scan for peripapillary retinal nerve fibre layer thickness (pRNFL) and a 6 mm diameter macular volume scan for combined ganglion cell and inner plexiform layer (GCIP) and inner nuclear layer (INL) volume. Detailed OCT methods—in line with the APOSTEL recommendations²³ and including segmentation^{8,24} and quality control²⁵ can be found elsewhere. Eight scans from seven subjects had to be excluded due to insufficient quality.

Statistical analysis

Statistical analyses were performed with R version 3.4.2 including geepack package 1.2-1 and ggplot2 version 3.1.0.²⁶ All results are given as mean \pm standard deviation (SD), unless indicated differently. Generalized estimating equation (GEE) models with working correlation matrix ‘exchangeable’ and corrected for age were used for associations involving eye-related measurements accounting for within-subject inter-eye effects and for group comparisons. GEE results are given with regression coefficient (B) and standard error (SE). Linear regression models including each eye as an individual case were applied when including only one eye per subject. Statistical significance was established at $p < 0.05$. Due to the exploratory nature of the study, no correction for multiple testing was performed.

Data availability

The datasets for this manuscript will be shared by request from any qualified investigator.

Results

In Berlin, 33 patients with RRMS, 5 patients with CIS (of those, 2 with unilateral ON and 3 with other symptoms), 13 patients with NMOSD (Anti-Aquaporin 4 antibody +/-: 11/2), and 33 HC were included. Patients with RRMS and CIS were pooled and referred to as ‘MS’. One eye of a MS patient was excluded due to amblyopia, and one eye of a NMOSD patient was excluded due to a branch retinal artery occlusion. A demographic and clinical overview is given in Table 1, exclusions are shown in Figure 1. From Sydney, 43 RRMS patients (male/female ($n = 16/27$, mean age (years) \pm SD = 42.36 \pm 9.03, 24 with a unilateral ON history) were included. Main results from both centres are shown in Table 2.

Motion perception in healthy controls

The mean NFM score in HC was 126.6 \pm 12.3 and did not differ between female and male HCs (126.5 \pm 12.4 vs 127.1 \pm 12.4, $B = -2.75$, SE = 4.32, $p = 0.524$) (Figure 2(a)). Lower NFM scores were associated with older age ($B = -0.698$, SE = 0.171, $p < 0.001$; Figure 2(b)) in HC.

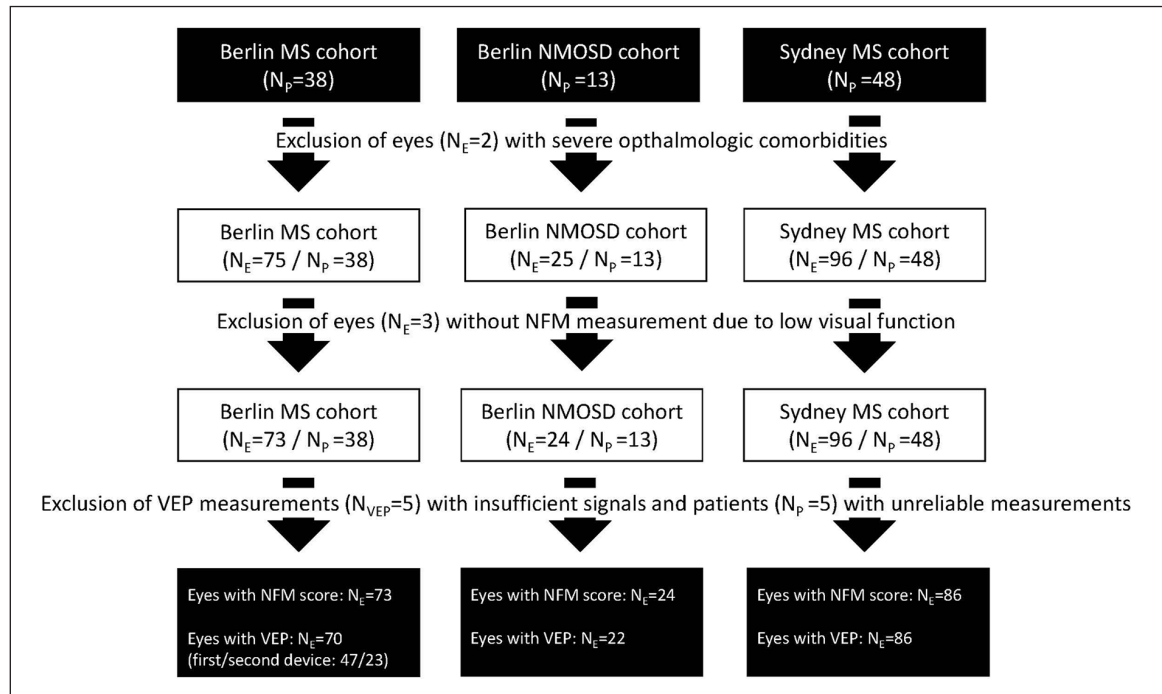


Figure 1. Exclusion flow chart for the Berlin MS/NMOSD and the Sydney MS cohorts.

Flow chart showing the exclusions in the three main cohorts in this study.

MS: multiple sclerosis; NMOSD: neuromyelitis optica spectrum disorders; N_p: number of patients; N_E: number of eyes; N_{VEP}: number of VEP measurements.

Motion perception in multiple sclerosis

MS patients in the Berlin cohort had an NFM score of 114.8 ± 23.2 , which was lower than in HC ($B = -12.374$, $SE = 3.285$, $p < 0.001$). NFM scores did not differ between ON and non-ON eyes ($B = -7.965$, $SE = 5.823$, $p = 0.171$). Further, NFM was associated with HCVA ($B = -139.4$, $SE = 29.7$, $p < 0.001$), LCLA ($B = 0.99$, $SE = 0.32$, $p = 0.002$), pRNFL ($B = 1.0$, $SE = 0.2$, $p < 0.001$) and GCIP ($B = 64.8$, $SE = 14.3$, $p < 0.001$) (Figure 3(a)–(d)). In contrast, INL ($B = -64.4$, $SE = 43.0$, $p = 0.152$, Figure 3(e)) and P100 latency ($B = -0.4$, $SE = 0.5$, $p = 0.400$, Figure 3(f)) were not associated with NFM score. In a subset with no missing VEP measurements of the first device, associations of pRNFL and GCIP with NFM were still significant. Similar results were obtained when excluding the eye with HCVA > 0.1 logMAR.

In an analysis including only ON eyes (in case of ON in both eyes, only the eye with worse NFM was included), NFM score was associated with pRNFL ($B = 1.464$, $SE = 0.349$, $r^2 = 0.545$, $p < 0.001$, $n = 18$ eyes) and GCIP ($B = 139.739$, $SE = 34.554$, $r^2 = 0.544$, $p = 0.001$, $n = 17$ eyes) but not with P100 latency ($B = -0.846$, $SE = 0.803$, $r^2 = 0.114$, $p = 0.317$, $n = 13$ eyes). When performing asymmetry analysis in patients with unilateral ON, inter-eye NFM score was associated with inter-eye pRNFL

($B = -1.149$, $SE = 0.260$, $r^2 = 0.610$, $p < 0.001$, $n = 16$), inter-eye GCIP ($B = -77.588$, $SE = 15.362$, $r^2 = 0.688$, $p < 0.001$, $n = 15$) but not with inter-eye P100 latency ($B = -0.227$, $SE = 0.706$, $r^2 = 0.027$, $p = 0.756$, $n = 11$). NFM was not associated with EDSS ($B = 2.147$, $SE = 2.488$, $p = 0.390$), but with SDMT score ($B = 0.396$, $SE = 0.188$, $p = 0.035$). After the exclusion of one eye with a recent ON episode (27 days before the visit) similar results were obtained, except for the association of NFM with SDMT ($B = 0.221$, $SE = 0.197$, $p = 0.260$). Similar results were also obtained after excluding the outliers with a NFM below 50 (Supplemental Figure 1). In a separate analysis of the VEP measurements from the second device, we found no association between NFM and P100 latency ($B = 0.497$, $SE = 0.894$, $p = 0.580$), excluding one eye with HCVA > 0.1 logMAR (Supplemental Figure 2).

In the Sydney cohort, a lower NFM score was likewise associated with thinner pRNFL ($B = 1.351$, $SE = 0.276$, $p < 0.001$). In contrast to the Berlin MS cohort, NFM score in the Sydney cohort was significantly lower in ON (92.92 ± 41.21) than in non-ON eyes (113.74 ± 20.77 , $B = -24.955$, $SE = 6.911$, $p < 0.001$) and was inversely associated with mfVEP latencies ($B = -1.159$, $SE = 0.296$, $p < 0.001$). In a multivariable analysis (NFM~pRNFL + P100) the

Table 2. Mean results of Numbers from motion score and all functional and structural visual parameters for eyes with optic neuritis and without optic neuritis in MS, NMOSD patients and for healthy controls.

	Berlin Cohort		Sydney cohort			
	MS ONeyes	MS NONeyes	NMOSD NONeyes	MS ONeyes		
NFM	Score	110.45 ± 29.58* (n = 20)	116.49 ± 20.42*** (n = 53)	110.50 ± 18.23* (n = 12)	92.92 ± 41.21*** (n = 24)	113.74 ± 20.77** (n = 62)
HCVA	LogMAR units (Mean ± SD)	-0.03 ± 0.35 (n = 20)	-0.15 ± 0.08 (n = 52)	0.22 ± 0.56 (n = 12)	-0.10 ± 0.11 (n = 12)	
LCLA	Letters (out of 70) (Mean ± SD)	34.85 ± 14.78 (n = 20)	45.38 ± 5.69 (n = 52)	30.33 ± 12.29 (n = 9)	38.58 ± 9.72 (n = 12)	
VEP	P100 latency (Mean ± SD)	116.75 ± 13.25 (n = 15)	109.19 ± 8.06 (n = 32)	119.14 ± 12.75 (n = 10)	114.33 ± 9.13 (n = 12)	
mfVEP	Latency (Mean ± SD)				162.58 ± 15.43 (n = 24)	153.56 ± 12.36 (n = 62)
pRNFL	Thickness in µm (Mean ± SD)	83.80 ± 15.10 (n = 20)	97.20 ± 9.47 (n = 53)	67.50 ± 23.55 (n = 12)	96.83 ± 13.62 (n = 12)	76.33 ± 11.77 (n = 24)
GCIP	Volume in mm ³ (Mean ± SD)	1.67 ± 0.16 (n = 19)	1.93 ± 0.15 (n = 52)	1.54 ± 0.29 (n = 12)	1.95 ± 0.19 (n = 12)	90.21 ± 11.25 (n = 62)
INL	Volume in mm ³ (Mean ± SD)	1.04 ± 0.07 (n = 19)	1.02 ± 0.06 (n = 52)	0.98 ± 0.10 (n = 12)	0.98 ± 0.08 (n = 12)	

MS: multiple sclerosis; NMOSD: neuromyelitis optica spectrum disorders; (N)ON: (non-) optic neuritis; n: number of eyes; HC: healthy control; HCVA: high contrast visual acuity; LCLA: low contrast letter acuity; VEP: full field visual evoked potentials; mfVEP: multifocal visual evoked potentials; pRNFL: peripapillary retinal nerve fibre layer; GCIP: ganglion cell/inner plexiform layer; INL: inner nuclear layer.
Significant difference to HC marked by asterisks: **p* ≤ 0.05, ***p* ≤ 0.01, ****p* ≤ 0.001 (only analysed for NFM).

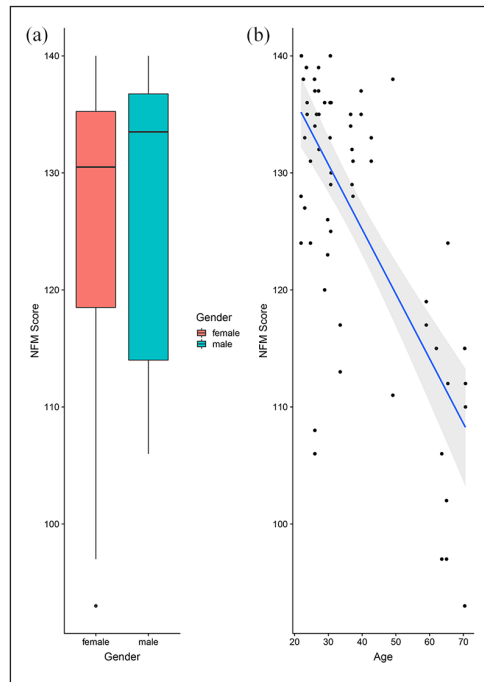


Figure 2. Numbers from motion score in healthy controls (a) boxplots comparing the numbers from motion (NFM) scores between female and male, healthy controls and (b) scatterplot showing the association of NFM scores measurements with age in healthy controls.

influence of pRNFL on NFM ($B = 0.987$, $SE = 0.293$, $p < 0.001$) was more pronounced than of mfVEP latencies ($B = -0.533$, $SE = 0.309$, $p = 0.085$). When only ON eyes were analysed, the association between NFM and pRNFL ($B = 2.120$, $SE = 0.594$, $r^2 = 0.367$, $p = 0.002$) was found to be stronger than between NFM and mfVEP latencies ($B = -1.097$, $SE = 0.531$, $r^2 = 0.187$, $p = 0.051$). Asymmetry analysis in unilateral ON patients demonstrated a significant association of decreased NFM in ON eyes with thinner pRNFL ($B = -1.409$, $SE = 0.532$, $r^2 = 0.242$, $p = 0.015$), but only a trend towards an association with longer mfVEP latency ($B = -1.128$, $SE = 0.572$, $r^2 = 0.150$, $p = 0.062$). Similar results were obtained after excluding the outliers with a NFM below 20 (Supplemental Figure 3).

Motion perception in neuromyelitis optica spectrum disorders

NFM score in patients with NMOSD was 91.1 ± 39.6 and lower than in HC ($B = -34.5$, $SE = 10.4$, $p < 0.001$). NFM score was lower in ON eyes than in non-ON eyes (Table 2, $B = -30.9$, $SE = 15.1$, $p = 0.041$) and NFM score in non-ON eyes was still lower than in HC ($B = -21.04$, $SE = 5.9$, $p < 0.001$). There was an association between NFM score and HCVA ($B = -77.2$,

$SE = 5.2$, $p < 0.001$), LCLA ($B = 1.6$, $SE = 0.3$, $p < 0.001$), pRNFL ($B = 0.92$, $SE = 0.38$, $p = 0.016$) and GCIP ($B = 79.5$, $SE = 28.7$, $p = 0.006$) (Figure 4(a)–(d)). INL ($B = -55.4$, $SE = 63.5$, $p = 0.383$) and P100 latency ($B = -0.786$, $SE = 0.713$, $p = 0.270$) were not associated with NFM score (Figure 4(e) and (f)). NFM was neither associated with EDSS ($B = 0.819$, $SE = 3.502$, $p = 0.815$) nor with SDMT score ($B = 0.355$, $SE = 0.593$, $p = 0.550$). When excluding the eyes with HCVA > 0.1 logMAR (3 eyes from 2 patients) similar results were obtained but for the association between NFM and pRNFL ($B = 0.360$, $SE = 0.284$, $p = 0.205$). When excluding the outliers with a NFM score of 0 the influence of pRNFL ($B = 0.293$, $SE = 0.157$, $p = 0.062$) on NFM was, though not significantly, still more pronounced than of P100 latencies ($B = 0.008$, $SE = 0.286$, $p = 0.977$). Trends towards the previous associations remained (Supplemental Figure 4).

Discussion

The results of this study (a) support an association of motion perception with VEP-assessed visual pathway myelination status in MS, (b) reveal impaired motion perception in NMOSD, (c) demonstrate association of motion perception with neuro-axonal visual system damage and reduced HCVA, and (d) suggests that motion perception is associated with cognitive deficits in MS but not NMOSD.

In earlier studies on early-stage MS and acute cases of ON, impaired motion perception was associated with longer VEP latencies in ON eyes.^{7,13} Therefore motion perception, as a dynamic visual function, was hypothesized to rely on a rapid transmission of visual information reflecting myelination levels of the visual pathway.¹³

In our study both cohorts demonstrated a strong association between NFM score and pRNFL and GCIP loss, suggesting that neuro-axonal damage of the retina and optic nerve is one of the main drivers behind reduced motion perception in autoimmune inflammatory optic neuropathies.

While our study demonstrated no association between motion perception and VEP latencies from the main and second device in the Berlin cohort, the Sydney cohort found correlations of lower NFM score with mfVEP latency delay in its entire cohort and in ON eyes specifically. This may be explained by the larger sample size and multifocal mfVEP used in Sydney, which is more sensitive to demyelination damage than typical full-field VEP,³ as well as by more pronounced neuro-axonal damage in terms of pRNFL thickness in

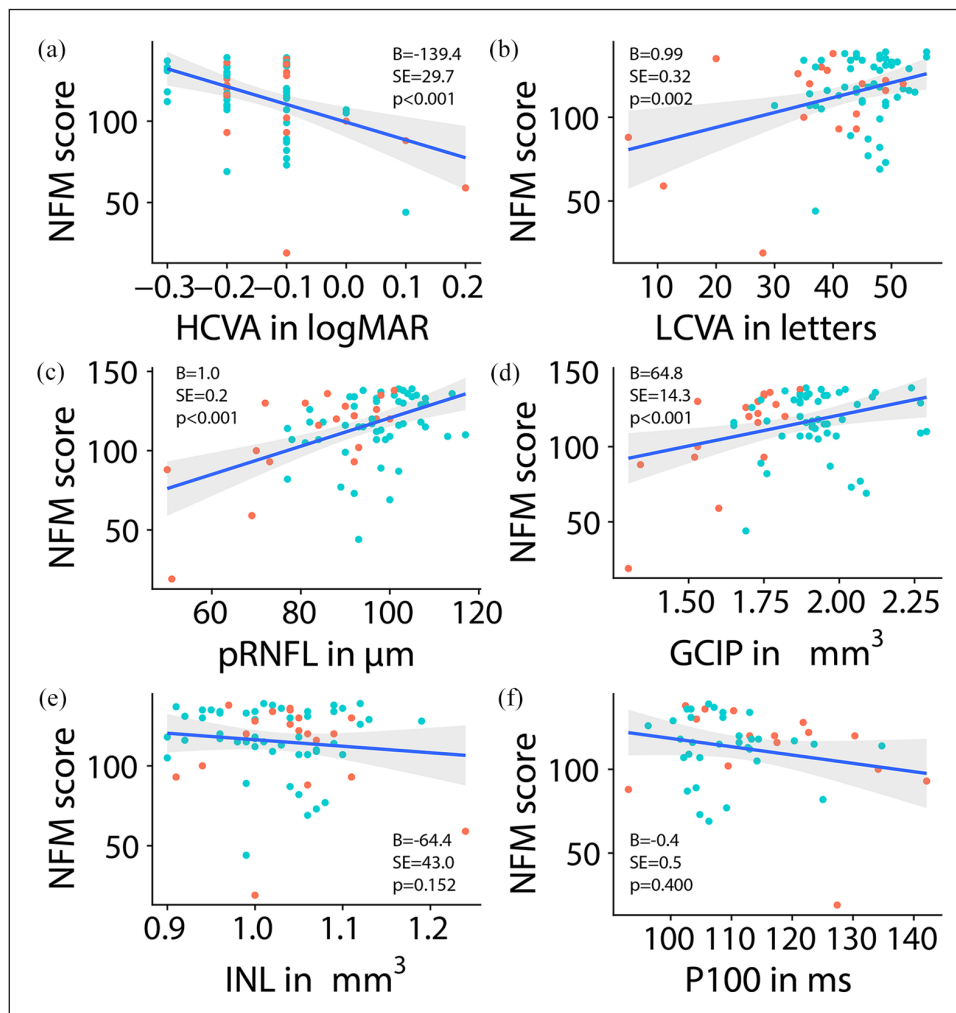


Figure 3. Association of numbers from motion (NFM) scores with functional and structural visual parameters in the main multiple sclerosis cohort (a) high contrast visual acuity (HCVA), (b) low contrast letter acuity (LCLA), (c) peripapillary retinal nerve fibre layer (pRNFL) thickness, (d) ganglion cell/inner plexiform layer (GCIP) volume; (e) INL: inner nuclear layer (INL) volume and (f) P100 latency; Red points represent optic neuritis eyes, turquoise points non-optic neuritis eyes.

ON eyes of the Sydney cohort compared to the Berlin cohort. Furthermore, the mean P100 latency being only slightly delayed in the Berlin cohort, one could hypothesize whether motion perception is only affected by severely delayed latencies. A future analysis of binocular motion perception testing in unilateral ON patients might yield clarification.

Weaker correlation between NFM score and VEP latencies (in comparison to pRNFL) is also apparent in the asymmetry analysis of patients with unilateral ON history, which is less susceptible to high inter-individual range of measurements. Thus, while ON-related neuro-axonal damage, as represented by inter-eye pRNFL and GCIP thinning, is associated with inter-eye motion perception impairment, it does

not correlate with full-field VEP latency of the main cohort and only shows trend in the confirmatory cohort. These findings indicate that prolonged visual input transmission is not the only driver of impaired motion perception in our cohorts. Thus, we suggest an additional underlying pathophysiological process:

The processing of motion perception is considered to begin in the retina.²⁷ Previous studies found that a retinal circuit based on direction selective cells is at the origin of retinal motion encoding.^{28–30} This circuit is focused around the interaction of various subtypes of bipolar, amacrine and ganglion cells, especially motion sensitive parasol ganglion cells.³¹ The neurites of these cells stratify in the inner plexiform layer.²⁹ Our study showed that impaired motion perception

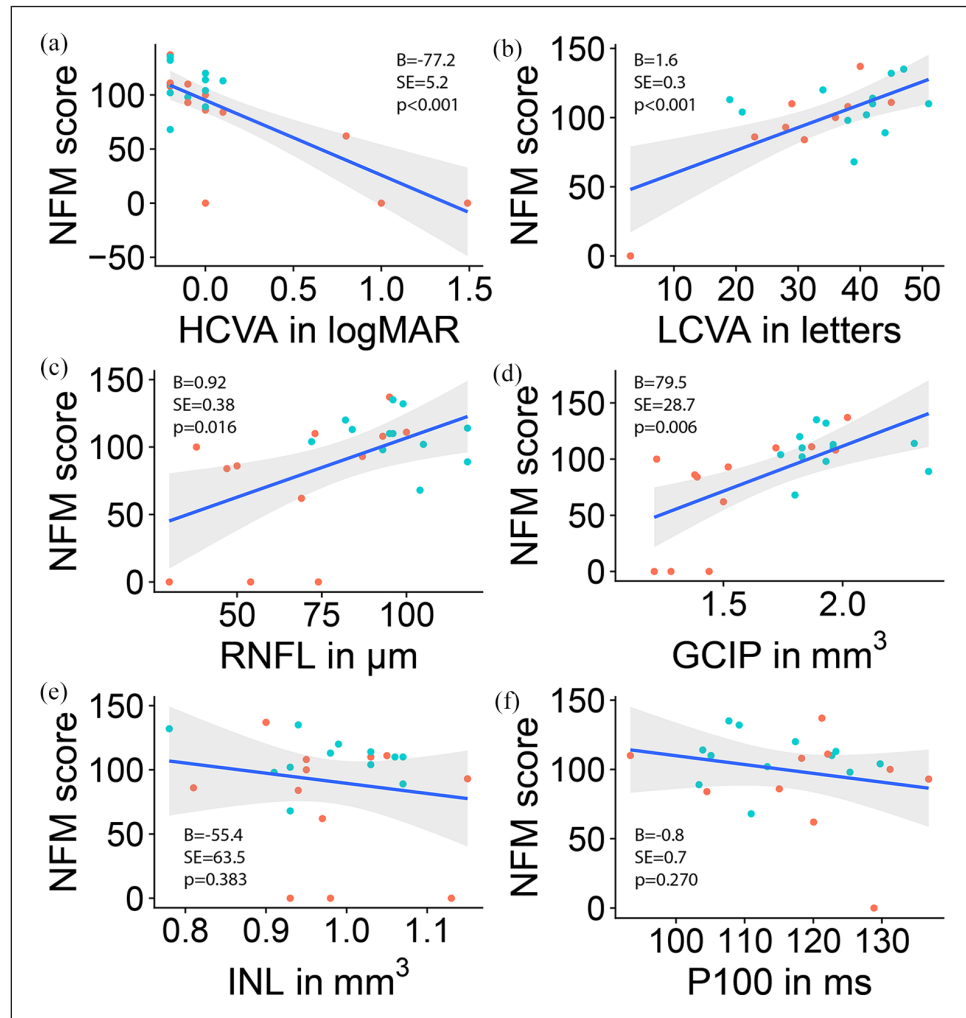


Figure 4. Association of NFM scores with functional and structural visual parameters in the neuromyelitis optica spectrum disorders cohort (a) high contrast visual acuity (HCVA), (b) low contrast letter acuity (LCLA), (c) peripapillary retinal nerve fibre layer (pRNFL) thickness, (d) ganglion cell/inner plexiform layer (GCIP) volume; (e) INL: inner nuclear layer (INL) volume (f) P100 latency; Red points represent optic neuritis eyes, turquoise points non-optic neuritis eyes.

was associated with pRNFL and GCIP thinning. GCIP and pRNFL thinning was shown to occur in MS and NMO/D patients with and without prior ON.^{5,6,32} Therefore, we suggest that motion perception relies on the structural integrity of the retina and represents a clinical correlate of neuro-axonal damage. The fact that we reproduced the association of motion perception impairment with pRNFL and GCIP thinning in NMO/D supports this idea, as the effect of axonal loss was shown to be stronger in NMO/D than in MS.^{6,22} This concept would also explain motion perception impairment in non-demyelinating diseases such as glaucoma, which features RNFL and GCIP damage as a consequence of increased intraocular pressure.^{15,33} Motion perception impairment in Alzheimer's disease, however, might be caused by

magnocellular pathway damage in the primary visual cortex.¹⁶ In this context, it would be interesting to investigate an association of cortical damage with worsened motion perception in MS and NMO/D.

Our study is – to the best of our knowledge – the first describing motion perception in NMO/D. A recent study demonstrated different patterns of ON damage in MS and NMO/D, showing that ON damage in MS, while being less severe, might primarily be caused by demyelination, whereas in NMO/D, ON damage was more severe and axonal loss presented itself as the main pathological factor.²² Motion perception in NMO/D was markedly reduced in comparison to controls, and more severely impaired in ON than in non-ON eyes, which could be explained by the strong ON-related

neuro-axonal damage in NMOSD. Notably, even in NMOSD non-ON eyes, motion perception was worse compared with controls, even in a similar range as MS ON eyes. This suggests a role of microstructural visual system changes for motion perception.³⁴ However, also the higher age in the NMOSD cohort might account for the lower NFM scores.

As also MS non-ON eyes showed decreased NFM in comparison to controls, motion perception impairment might occur attack-independent, reflecting chronic neurodegeneration in MS.

Motion perception in our study was also associated with HCVA and LCLA. Visual loss is associated with pRNFL and GCIP thinning.⁵ It can therefore be questioned whether visual loss directly impairs motion perception. Motion perception testing was suggested to rely on normal VA. We therefore performed a subgroup analysis on patients with best-corrected HCVA ≤ 0.1 logMAR. The results did not differ from the initial results in our Berlin MS cohort.

However, the cohort differences between our study and the previous studies of motion perception in MS must also be taken into consideration. While our cohorts represented a heterogeneous group of MS patients in a stable phase of the disease, previous studies of motion perception in MS focused on patients with either early-stage MS, acute ON or progressive MS. In early-stage MS and acute ON, acute inflammation plays a crucial role, therefore results could be influenced by stronger effects of acute demyelination. Of note, VEP/mfVEP latencies of ON eyes in both our MS cohorts were only to a small degree prolonged in comparison to non-ON eyes (Table 2), indicating only subtle ON-related visual pathway demyelination and/or subclinical demyelination in the non-ON eyes.

Furthermore, most studies on motion perception in MS used OCT measurements only for cohort characterization, therefore missing the opportunity to study whether motion perception was affected by neuro-axonal damage.¹⁴ One recent study featuring progressive MS patients showed no association between motion perception and OCT measurements,²¹ although motion perception impairment in non-ON eyes of progressive MS was thought to possibly rely on axonal loss.²¹ This finding could be explained with a different statistical approach.

We also show that motion perception was associated with SDMT, a commonly used test for measuring information processing speed and cognition in MS.²⁰

The motion tool used in our study relied on numbers being recognized, the task being directly associated with cognitive capacities is possible. Alternatively, SDMT score may be directly influenced by demyelination and thus reduced information processing speed in the afferent visual system.³⁵ This finding is however limited by a small sample size. Nevertheless, cognitive impairment does not seem to be a driver for motion perception impairment in our NMOSD cohort.

In MS, eye movement disorders, especially delayed saccadic latency, due to damage along the pathways of the visual system are observed and shown to be associated with impaired visual functioning in daily life.³⁶ Our motion perception test being based on fast moving pixels, delayed saccades might contribute to its impairment.

In healthy controls we found motion perception to be associated with age. This is in accordance with a study that reported motion perception to be impaired in older people due to a deficit in contrast sensitivity.³⁷

This study is subject to limitations. The small sample size, especially for our NMOSD subgroup, might lead to subtle effects being overlooked, or significant effects could be overinterpreted. In fact, we were not able to reproduce all results when we excluded outliers. Due to the small sample size in our NMOSD subgroup, we chose not to exclude two patients with negative anti-aquaporin 4 antibodies. In our main cohort, VEP measurements of the main device were only available for a smaller subset of patients, and the subset of patients with VEP measurements of the second device had mostly no history of ON, which could explain why the association of motion perception to P100 latencies missed significance in these groups. Motion perception testing was performed under habitual VA and uncorrected refraction errors might have influenced the results. As we performed a cross-sectional study, we cannot report on the development of motion perception over time. Furthermore, the heterogeneity of our main cohort regarding disease stages, especially with regards to the time since ON, might complicate the comparison to previous studies.

To conclude, our study suggests that motion perception impairment is likely to be a result of both visual pathway neuro-axonal damage and demyelination in MS and NMOSD. In the light of the past and current effort to study the neural circuits of motion processing, early motion encoding in the retina was found to play an important role. Motion perception impairment in MS and NMOSD might therefore present itself as a suitable human model for further investigations.

Acknowledgements

We thank Charlotte Bereuter and Jana Schließeit for excellent technical assistance, and Netta Levin and Yael Backner for providing the motion perception test software.

Declaration of Conflicting Interests

The author(s) declared the following potential conflicts of interest with respect to the research, authorship, and/or publication of this article: FCO was employee of Nocturne GmbH, unrelated to this work. SA received a travel grant from Celgene and speaker's honorary from Alexion, Bayer and Roche. JBS has received travel grants and speaking honoraria from Bayer Healthcare, Biogen Idec, Merck Serono, Sanofi Genzyme, Teva Pharmaceuticals, Roche, and Novartis, none of them related to preparing this manuscript. KR received research support from Novartis, Merck Serono, German Ministry of Education and Research, European Union (821283-2), Stiftung Charité (BIH Clinical Fellow Programme) and Arthur Arnstein Foundation; received speaker honoraria and travel grants from Bayer, Biogen Idec, Merck Serono, sanofi-aventis/Genzyme, Teva, Roche, Novartis, and Guthy Jackson Charitable Foundation. FP serves as an Associate Editor for *Neurology: Neuroimmunology & Neuroinflammation*, reports research grants and speaker honoraria from Bayer, Teva, Genzyme, Merck, Novartis, MedImmune and is member of the steering committee of the OCTIMS study (Novartis). AUB is cofounder and shareholder of motognosis and nocturne. He is named as inventor on several patent applications regarding MS serum biomarkers, OCT image analysis and perceive visual computing. HGZ received research grants from Novartis and speaking honoraria from Bayer Healthcare. All other authors declare that they have no conflicts of interest.

Funding

The author(s) received no financial support for the research, authorship, and/or publication of this article.

ORCID iDs

Noah Ayadi  <https://orcid.org/0000-0002-3495-3825>
Susanna Asseyer  <https://orcid.org/0000-0001-6289-1791>
Alexander U Brandt  <https://orcid.org/0000-0002-9768-014X>

Supplemental material

Supplemental material for this article is available online.

References

1. Thompson AJ, Banwell BL, Barkhof F, et al. Diagnosis of multiple sclerosis: 2017 revisions of the McDonald criteria. *Lancet Neurol* 2018; 17: 162–173.
2. Wingerchuk DM, Banwell BL, Bennett JL, et al. International consensus diagnostic criteria for neuromyelitis optica spectrum disorders. *Neurology* 2015; 85: 177–189.
3. Graham SL and Klistorner A. Afferent visual pathways in multiple sclerosis: A review. *Clin Exp Ophthalmol* 2017; 45(1): 62–72.
4. Petzold A, Wattjes MP, Costello F, et al. The investigation of acute optic neuritis: A review and proposed protocol. *Nat Rev Neurol* 2014; 10(8): 447–458.
5. Brandt AU, Martinez-Lapiscina EH, Nolan R, et al. Monitoring the course of MS with optical coherence tomography. *Curr Treat Options Neurol* 2017; 19(4): 15.
6. Oertel FC, Zimmermann H, Paul F, et al. Optical coherence tomography in neuromyelitis optica spectrum disorders: Potential advantages for individualized monitoring of progression and therapy. *EPMA J* 2018; 9(1): 21–33.
7. Raz N, Shear-Yashuv G, Backner Y, et al. Temporal aspects of visual perception in demyelinating diseases. *J Neurol Sci* 2015; 357: 235–239.
8. Ayadi N, Dörr J, Motamedi S, et al. Temporal visual resolution and disease severity in MS. *Neurol Neuroimmunol Neuroinflamm* 2018; 5: e492.
9. Born RT and Bradley DC. Structure and function of visual area MT. *Annu Rev Neurosci* 2005; 28: 157–189.
10. Chapman C, Hoag R and Giaschi D. The effect of disrupting the human magnocellular pathway on global motion perception. *Vision Res* 2004; 44(22): 2551–2557.
11. Regan D, Kothe AC and Sharpe JA. Recognition of motion-defined shapes in patients with multiple sclerosis and optic neuritis. *Brain* 1991; 114(pt 3): 1129–1155.
12. Frisen L, Hoyt WF, Bird AC, et al. Diagnostic uses of the Pulfrich phenomenon. *Lancet* 1973; 2: 385–386.
13. Raz N, Dotan S, Chokron S, et al. Demyelination affects temporal aspects of perception: An optic neuritis study. *Ann Neurol* 2012; 71(4): 531–538.
14. Raz N, Dotan S, Benoliel T, et al. Sustained motion perception deficit following optic neuritis: Behavioral and cortical evidence. *Neurology* 2011; 76: 2103–2111.
15. Silverman SE, Trick GL and Hart WM Jr. Motion perception is abnormal in primary open-angle

- glaucoma and ocular hypertension. *Invest Ophthalmol Vis Sci* 1990; 31(4): 722–729.
16. Gilmore GC, Wenk HE, Naylor LA, et al. Motion perception and Alzheimer's disease. *J Gerontol* 1994; 49: P52–P57.
 17. Bertone A, Mottron L, Jelenic P, et al. Motion perception in autism: A 'complex' issue. *J Cogn Neurosci* 2003; 15: 218–225.
 18. Paul F. Pathology and MRI: Exploring cognitive impairment in MS. *Acta Neurol Scand* 2016; 134(suppl. 200): 24–33.
 19. Kurtzke JF. Rating neurologic impairment in multiple sclerosis: An expanded disability status scale (EDSS). *Neurology* 1983; 33(11): 1444–1452.
 20. Parmenter BA, Weinstock-Guttman B, Garg N, et al. Screening for cognitive impairment in multiple sclerosis using the Symbol digit Modalities Test. *Mult Scler* 2007; 13(1): 52–57.
 21. Backner Y, Petrou P, Glick-Shames H, et al. Vision and vision-related measures in progressive multiple sclerosis. *Front Neurol* 2019; 10: 455.
 22. Shen T, You Y, Arunachalam S, et al. Differing structural and functional patterns of optic nerve damage in multiple sclerosis and neuromyelitis optica spectrum disorder. *Ophthalmology* 2019; 126(3): 445–453.
 23. Cruz-Herranz A, Balk LJ, Oberwahrenbrock T, et al. The APOSTEL recommendations for reporting quantitative optical coherence tomography studies. *Neurology* 2016; 86: 2303–2309.
 24. Motamedi S, Gawlik K, Ayadi N, et al. Normative data and minimally detectable change for inner retinal layer thicknesses using a semi-automated OCT image segmentation pipeline. *Front Neurol* 2019; 10: 1117.
 25. Tewarie P, Balk L, Costello F, et al. The OSCAR-IB consensus criteria for retinal OCT quality assessment. *PLoS One* 2012; 7(4): e34823.
 26. R Core Team. R: A language and environment for statistical computing, 2017, <https://www.R-project.org/>
 27. Barlow HB, Hill RM and Levick WR. Retinal ganglion cells responding selectively to direction and speed of image motion in the rabbit. *J Physiol* 1964; 173: 377–407.
 28. Euler T, Detwiler PB and Denk W. Directionally selective calcium signals in dendrites of starburst amacrine cells. *Nature* 2002; 418: 845–852.
 29. Kim JS, Greene MJ, Zlateski A, et al. Space–time wiring specificity supports direction selectivity in the retina. *Nature* 2014; 509: 331–336.
 30. Matsumoto A, Briggman KL and Yonehara K. Spatiotemporally asymmetric excitation supports mammalian retinal motion sensitivity. *Curr Biol* 2019; 29: 3277.e5–3288.e5.
 31. Manookin MB, Patterson SS and Linehan CM. Neural mechanisms mediating motion sensitivity in parasol ganglion cells of the primate retina. *Neuron* 2018; 97: 1327.e4–1340.e4.
 32. Oertel FC, Specovius S, Zimmermann HG, et al. Retinal optical coherence tomography in neuromyelitis optica. *Neurol Neuroimmunol Neuroinflamm*, 8: e1068.
 33. Weinreb RN, Aung T and Medeiros FA. The pathophysiology and treatment of glaucoma: A review. *JAMA* 2014; 311: 1901–1911.
 34. Oertel FC, Kuchling J, Zimmermann HG, et al. Microstructural visual system changes in AQP4-antibody–Seropositive NMOSD. *Neurol Neuroimmunol Neuroinflamm* 2017; 4: e334.
 35. Gabilondo I, Rilo O, Ojeda N, et al. The influence of posterior visual pathway damage on visual information processing speed in multiple sclerosis. *Mult Scler* 2017; 23(9): 1276–1288.
 36. Nij Bijvank JA, Petzold A, Coric D, et al. Saccadic delay in multiple sclerosis: A quantitative description. *Vision Res* 2020; 168: 33–41.
 37. Allen HA, Hutchinson CV, Ledgeway T, et al. The role of contrast sensitivity in global motion processing deficits in the elderly. *J Vis* 2010; 10: 15.

Visit SAGE journals online
[journals.sagepub.com/
 home/msj](https://journals.sagepub.com/home/msj)

 SAGE journals

Motamedi et al. Front Neurol 2019 (Normative Daten &
Segmentierungspipeline)

Journal Data Filtered By: **Selected JCR Year: 2017** Selected Editions: SCIE,SSCI
 Selected Categories: **"CLINICAL NEUROLOGY"** Selected Category
 Scheme: WoS

Gesamtanzahl: 197 Journale

Rank	Full Journal Title	Total Cites	Journal Impact Factor	Eigenfactor Score
1	LANCET NEUROLOGY	28,671	27.138	0.069040
2	Nature Reviews Neurology	8,095	19.819	0.028090
3	ACTA NEUROPATHOLOGICA	18,783	15.872	0.041490
4	Alzheimers & Dementia	10,423	12.740	0.030040
5	JAMA Neurology	6,885	11.460	0.035270
6	BRAIN	52,061	10.840	0.075170
7	SLEEP MEDICINE REVIEWS	6,080	10.602	0.010720
8	ANNALS OF NEUROLOGY	37,251	10.244	0.053390
9	NEURO-ONCOLOGY	10,930	9.384	0.030350
10	Epilepsy Currents	790	9.333	0.001600
11	MOVEMENT DISORDERS	26,511	8.324	0.037980
12	Translational Stroke Research	2,202	8.266	0.005260
13	NEUROLOGY	88,493	7.609	0.115530
14	NEUROSCIENTIST	4,738	7.461	0.008730
15	JOURNAL OF NEUROLOGY NEUROSURGERY AND PSYCHIATRY	29,695	7.144	0.032980
16	STROKE	65,854	6.239	0.088520
17	BRAIN PATHOLOGY	4,952	6.187	0.007750
18	Brain Stimulation	4,263	6.120	0.014510
19	NEUROPATHOLOGY AND APPLIED NEUROBIOLOGY	3,654	6.059	0.006350
20	Neurotherapeutics	3,973	5.719	0.008980
21	PAIN	36,132	5.559	0.038000
22	Multiple Sclerosis Journal	10,675	5.280	0.021890
23	SLEEP	20,547	5.135	0.025870
24	EPILEPSIA	26,301	5.067	0.032490
25	Alzheimers Research & Therapy	2,192	5.015	0.008470
26	JOURNAL OF NEUROTRAUMA	14,508	5.002	0.021130
27	JOURNAL OF PAIN	9,264	4.859	0.016890
28	Journal of Stroke	694	4.750	0.002880
28	Therapeutic Advances in Neurological Disorders	1,004	4.750	0.002800
30	JOURNAL OF PSYCHOPHARMACOLOGY	5,808	4.738	0.010900
31	PARKINSONISM & RELATED DISORDERS	8,967	4.721	0.019910
32	NEUROREHABILITATION AND NEURAL REPAIR	5,032	4.711	0.009850
33	Annals of Clinical and Translational Neurology	1,377	4.649	0.006450
34	EUROPEAN JOURNAL OF NEUROLOGY	10,206	4.621	0.019350
35	BIPOLAR DISORDERS	5,070	4.490	0.007870

1

Selected JCR Year: 2017; Selected Categories: "CLINICAL NEUROLOGY"

Rank	Full Journal Title	Total Cites	Journal Impact Factor	Eigenfactor Score
36	NEUROSURGERY	28,592	4.475	0.025930
37	JOURNAL OF NEUROSURGERY	34,561	4.318	0.030750
38	CNS DRUGS	4,364	4.206	0.007540
39	PROGRESS IN NEURO- PSYCHOPHARMACOLOGY & BIOLOGICAL PSYCHIATRY	9,823	4.185	0.013170
40	EUROPEAN NEUROPSYCHOPHARMACOLOGY	6,920	4.129	0.015110
41	CURRENT OPINION IN NEUROLOGY	5,344	4.010	0.010200
42	INTERNATIONAL JOURNAL OF NEUROPSYCHOPHARMACOLOGY	6,259	3.981	0.014550
43	CEPHALALGIA	8,721	3.882	0.013940
44	International Journal of Stroke	3,825	3.859	0.014880
45	NEUROGASTROENTEROLOGY AND MOTILITY	7,401	3.842	0.014960
46	JOURNAL OF AFFECTIVE DISORDERS	26,957	3.786	0.053380
47	JOURNAL OF NEUROLOGY	14,359	3.783	0.025160
48	NEUROEPIDEMIOLOGY	3,261	3.697	0.005640
49	Expert Review of Neurotherapeutics	3,888	3.692	0.006910
50	AMERICAN JOURNAL OF NEURORADIOLOGY	22,667	3.653	0.029840
51	Journal of Neurologic Physical Therapy	964	3.633	0.001530
52	EUROPEAN ARCHIVES OF PSYCHIATRY AND CLINICAL NEUROSCIENCE	3,837	3.617	0.005400
53	CLINICAL NEUROPHYSIOLOGY	18,399	3.614	0.023070
54	Frontiers in Neurology	4,272	3.508	0.015580
55	CNS SPECTRUMS	2,200	3.504	0.003180
56	Journal of Neurodevelopmental Disorders	1,106	3.500	0.003410
57	JOURNAL OF NEUROPATHOLOGY AND EXPERIMENTAL NEUROLOGY	9,252	3.490	0.008680
58	Current Neurology and Neuroscience Reports	2,770	3.478	0.007410
59	Journal of Neurogastroenterology and Motility	1,207	3.438	0.002930
60	JOURNAL OF SLEEP RESEARCH	5,092	3.433	0.007460
61	JOURNAL OF HEAD TRAUMA REHABILITATION	4,282	3.406	0.005540
62	JOURNAL OF HEADACHE AND PAIN	2,624	3.403	0.005510
63	Journal of Clinical Sleep Medicine	5,329	3.396	0.011800
64	SLEEP MEDICINE	9,130	3.395	0.016270
65	Current Alzheimer Research	3,740	3.289	0.007910
65	DEVELOPMENTAL MEDICINE AND CHILD NEUROLOGY	11,671	3.289	0.013680
67	JOURNAL OF PAIN AND SYMPTOM MANAGEMENT	9,734	3.249	0.013980



Normative Data and Minimally Detectable Change for Inner Retinal Layer Thicknesses Using a Semi-automated OCT Image Segmentation Pipeline

Seyedamirhosein Motamedi¹, Kay Gawlik¹, Noah Ayadi¹, Hanna G. Zimmermann¹, Susanna Asseyer¹, Charlotte Bereuter¹, Janine Mikolajczak¹, Friedemann Paul^{1,2,3}, Ella Maria Kadas¹ and Alexander Ulrich Brandt^{1,4*}

¹ NeuroCure Clinical Research Center, Charité-Universitätsmedizin Berlin, Corporate Member of Freie Universität Berlin, Humboldt-Universität zu Berlin, and Berlin Institute of Health, Berlin, Germany, ² Experimental and Clinical Research Center, Max Delbrück Center for Molecular Medicine and Charité-Universitätsmedizin Berlin, Corporate Member of Freie Universität Berlin, Humboldt-Universität zu Berlin, and Berlin Institute of Health, Berlin, Germany, ³ Department of Neurology, Charité-Universitätsmedizin Berlin, Corporate Member of Freie Universität Berlin, Humboldt-Universität zu Berlin, and Berlin Institute of Health, Berlin, Germany, ⁴ Department of Neurology, University of California, Irvine, Irvine, CA, United States

OPEN ACCESS

Edited by:

John Jing-Wei Chen,
Mayo Clinic, United States

Reviewed by:

Jui-Kai Wang,
The University of Iowa, United States
Heather Moss,
Stanford University, United States

*Correspondence:

Alexander Ulrich Brandt
alexander.brandt@charite.de

Specialty section:

This article was submitted to
Neuro-Ophthalmology,
a section of the journal
Frontiers in Neurology

Received: 08 May 2019

Accepted: 07 October 2019

Published: 25 November 2019

Citation:

Motamedi S, Gawlik K, Ayadi N, Zimmermann HG, Asseyer S, Bereuter C, Mikolajczak J, Paul F, Kadas EM and Brandt AU (2019) Normative Data and Minimally Detectable Change for Inner Retinal Layer Thicknesses Using a Semi-automated OCT Image Segmentation Pipeline. *Front. Neurol.* 10:1117. doi: 10.3389/fneur.2019.01117

Neurodegenerative and neuroinflammatory diseases regularly cause optic nerve and retinal damage. Evaluating retinal changes using optical coherence tomography (OCT) in diseases like multiple sclerosis has thus become increasingly relevant. However, intraretinal segmentation, a necessary step for interpreting retinal changes in the context of these diseases, is not standardized and often requires manual correction. Here we present a semi-automatic intraretinal layer segmentation pipeline and establish normative values for retinal layer thicknesses at the macula, including dependencies on age, sex, and refractive error. Spectral domain OCT macular 3D volume scans were obtained from healthy participants using a Heidelberg Engineering Spectralis OCT. A semi-automated segmentation tool (SAMIRIX) based on an interchangeable third-party segmentation algorithm was developed and employed for segmentation, correction, and thickness computation of intraretinal layers. Normative data is reported from a 6 mm Early Treatment Diabetic Retinopathy Study (ETDRS) circle around the fovea. An interactive toolbox for the normative database allows surveying for additional normative data. We cross-sectionally evaluated data from 218 healthy volunteers (144 females/74 males, age 36.5 ± 12.3 years, range 18–69 years). Average macular thickness (MT) was $313.70 \pm 12.02 \mu\text{m}$, macular retinal nerve fiber layer thickness (mRNFL) $39.53 \pm 3.57 \mu\text{m}$, ganglion cell and inner plexiform layer thickness (GCIPL) $70.81 \pm 4.87 \mu\text{m}$, and inner nuclear layer thickness (INL) $35.93 \pm 2.34 \mu\text{m}$. All retinal layer thicknesses decreased with age. MT and GCIPL were associated with sex, with males showing higher thicknesses. Layer thicknesses were also positively associated with each other. Repeated-measurement reliability for the manual correction of automatic intraretinal segmentation results was

excellent, with an intra-class correlation coefficient >0.99 for all layers. The SAMIRIX toolbox can simplify intraretinal segmentation in research applications, and the normative data application may serve as an expandable reference for studies, in which normative data cannot be otherwise obtained.

Keywords: optical coherence tomography (OCT), retina, normative data, inner retinal layer, segmentation, macula, healthy population, minimally detectable change

1. INTRODUCTION

Optical coherence tomography (OCT) allows non-invasive high-resolution *in vivo* imaging of the retina (1). Spectral domain OCT (SD-OCT) provides 3D volume scans of the retina, and intraretinal segmentation of macular volume scans enables quantitative OCT applications in neurodegenerative and autoimmune neuroinflammatory disorders (2, 3). The inner retinal layers, in particular, are currently of pivotal interest for several neurologic disorders. For example, the combined macular ganglion cell and inner plexiform layer (GCIPL) thickness reflects disease severity and activity in patients with multiple sclerosis (MS) (4) and is suggested for monitoring disease activity in MS (5). GCIPL might further serve to identify neurodegeneration already very early on in the disease (6), and could thus be used as a marker for assessing the individual risk of a patient at onset for an active disease course (7). GCIPL is also suggested as a sensitive marker for attack severity in acute optic neuritis (8, 9). The inner nuclear layer (INL), on the other hand, is a marker for inflammatory disease activity in MS and might be utilized to monitor treatment response (10–12). In neuromyelitis optica spectrum disorders (NMOSD), the INL might be affected as part of an autoimmune reaction against Müller cells (13), which could lead in turn to progressive GCIPL loss (14).

Intraretinal layer segmentation is a crucial step in measuring GCIPL or INL changes. In recent years, many algorithms for intraretinal layer segmentation have been developed, and are now routinely implemented in clinical OCT devices or are available as external tools for research (15). While reliability in healthy eyes is usually good (16), many scans in diseases with macroscopic retinal changes or signal quality issues caused by more difficult OCT measurement in vision-impaired individuals require quality control and manual correction (17). Proper user interfaces for manual correction of automatic segmentation results are not always available, having led to many studies with questionable OCT data based on very small regions of interest (6) or inappropriate quality control (17).

Many studies have investigated intraretinal layer thicknesses in healthy eyes to establish normative reference values, recently e.g., Invernizzi et al. (18). Clinical features like age, sex, and axial length have been reported to physiologically affect intraretinal layer thicknesses (18, 19). But normative data studies are often only applicable in a narrow context depending on the selected samples and the methodology used, and data from studies from Asia, or as a control for different diseases, are not necessarily applicable in the context of neuroinflammatory diseases in European or North American populations.

In this study we aimed (a) to establish normative values for inner intraretinal layer thicknesses in a healthy Caucasian population and age/sex distribution suitable for typical autoimmune neuroinflammatory disorders, and (b) to evaluate layer thicknesses in association with age and sex. For this task we developed an easily usable and adaptable intraretinal segmentation pipeline based on an interchangeable third-party segmentation algorithm (20) as well as a survey tool for additional normative data, which together allow data surveys also beyond the scope of this study. Both are made available as an open source application along with this publication.

2. MATERIALS AND METHODS

2.1. Study Population

We queried our institute's research database to create a normative OCT database. The database contained healthy control data from two multimodal register studies aiming to evaluate quantitative measurements of neuro-axonal damage in MS and other neuroinflammatory disorders who were recruited from July 2010 to March 2018 at the NeuroCure Clinical Research Center at the Charité-Universitätsmedizin Berlin. Each participant underwent an examination of both eyes with Spectralis SD-OCT. Retrospective inclusion criteria for the present study were participants in a healthy condition aged between 18 and 70 years, Caucasian ethnicity, and high-quality macular OCT scans (signal strength more than 15 dB). Exclusion criteria were any neurological condition, any other disorder known to affect the retina (i.e., diabetes), any eye disease affecting the retina (i.e., glaucoma), any relevant pathological finding in the neurovisual examination performed by experienced optometrists, and a refractive error above ± 6 diopters. Twenty high quality macular OCT scans (signal strength more than 15 dB) of NMOSD patients all with the history of optic neuritis (ON) were randomly selected from our database to test the performance of the segmentation pipeline presented in this study.

The study was approved by the ethics committee of Charité-Universitätsmedizin Berlin and conducted according to the Declaration of Helsinki in its currently applicable version. All participants gave written informed consent.

2.2. Optical Coherence Tomography

All OCT measurements were carried out with a Spectralis SD-OCT and Heidelberg Eye Explorer (HEYEX) version 5.7.5.0 (Heidelberg Engineering, Heidelberg, Germany), by eight individual operators, with automatic real-time (ART) function for image averaging and an activated eye tracker in a dimly lit room. Macular 3D volumes were assessed by a custom scan

comprising 61 vertical B-scans (each with 768 A-Scans, with ART of 13 frames) with a scanning angle of $30 \times 25^\circ$ focusing on the fovea. All scans were quality controlled according to the OSCAR-IB criteria (21) and reporting adheres to APOSTEL recommendations (22). Scans not passing the quality control were excluded from analysis.

The macular scans were exported from the device and stored in HEYEX Vol file format (*.vol files), and then intraretinal segmentation was performed using the segmentation pipeline as described below. All segmentation results were quality controlled and manually corrected in case of errors by an experienced grader. In the end, the thickness data was calculated and stored in a CSV file format (.csv) for further analysis. The Early Treatment Diabetic Retinopathy Study (ETDRS) macular map, as described by the ETDRS research group (23), were used for this study. We report average macular thickness (MT), macular retinal nerve fiber layer thickness (mRNFL), combined ganglion cell and inner plexiform layer thickness (GCIPL), and inner nuclear layer thickness (INL) in the entire ETDRS macular map (the 6 mm diameter circular area around the fovea). Other layer thicknesses (e.g., outer retinal layers) and the thicknesses in different sectors of the ETDRS macular map can be studied using the provided *shiny* application and source data (**Supplementary Material**).

2.3. Intraretinal Segmentation

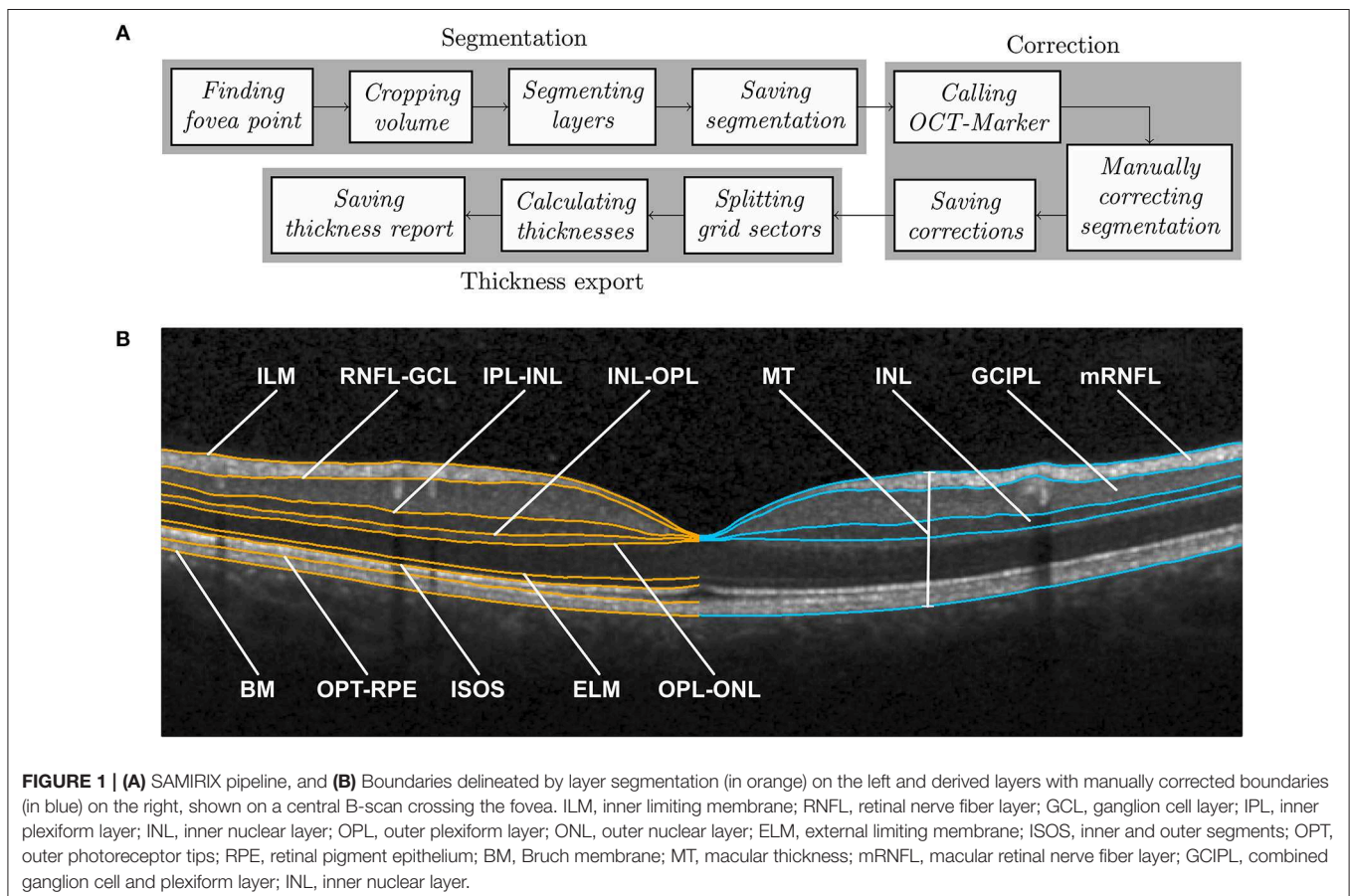
Intraretinal segmentation, manual correction, and thickness data export of all macular scans were done using a custom-developed

intraretinal segmentation pipeline (SAMIRIX). SAMIRIX modularly includes import filters for OCT data, a third-party segmentation algorithm, a user interface for controlling and correcting segmentation results, and batch-operations for processing multiple OCT images (**Figure 1A**).

SAMIRIX was developed in MATLAB (R2017a, MathWorks, Natick, MA, USA) and the user interface OCT-Marker was written in C++11, by using Qt5, Boost, and OpenCV libraries.

2.3.1. Segmentation Algorithm

As a segmentation algorithm we used OCTLayerSegmentation (20), which has been released as a package of AURA Tools on NITRC (https://www.nitrc.org/projects/aura_tools/). We chose OCTLayerSegmentation, because it showed good performance and accuracy with an overall absolute error of $3.5 \mu\text{m}$ by combining a machine learning approach for boundary classification (random forest classification) and a robust state-of-the-art graph-cut algorithm boundary refinement (optimal graph search) in a previous study (24). OCTLayerSegmentation delineates the inner limiting membrane (ILM), external limiting membrane (ELM), Bruch membrane (BM), and the boundaries between the retinal nerve fiber layer and ganglion cell layer (RNFL-GCL), inner plexiform layer and inner nuclear layer (IPL-INL), inner nuclear layer and outer plexiform layer (INL-OPL), outer plexiform layer and outer nuclear layer (OPL-ONL), inner and outer segments (ISOS), and outer photoreceptor tips and retinal pigment epithelium (OPT-RPE) (**Figure 1B**). These



boundaries then serve to calculate intraretinal layer areas with nomenclature as suggested by the APOSTEL criteria (22).

For segmentation, the first step is to automatically find the central fovea point of the macular volume scan to be segmented. Based on the segmentation of the ILM and BM by the Heidelberg Engineering Eye Explorer (HEYEX) software, the height difference between the two layers is computed. In order to detect the lowest point of the foveal surface, we look at the minimum of this difference within the 1 mm circular area around the center automatically defined by HEYEX. If several minima are detected, then the median point of them is taken as the center of the foveal pit. The next step is to crop the volume to 6–6 mm square around the fovea, aligned with the main direction of the scan. This was done because many segmentation approaches work with a priori assumption regarding the expected image. The algorithm by Lang et al. used in this version of SAMIRIX works well with this volume, which was also used by the original developers of the algorithm (20). After being cropped, the volume is segmented by the integrated 3rd-party segmentation algorithm (20). The segmentation results are then read by SAMIRIX and saved alongside the volume in a single file.

2.3.2. User Interface for Manual Correction

For quality control and manual correction, we developed a graphical user interface (OCT-Marker). In the first step, the scan to be checked and corrected if necessary, is opened in OCT-Marker. A Piecewise Cubic Hermite Interpolating Polynomial (PCHIP) based correction method with defined control points is provided to the user to ease the correction process. This enables modifications on the segmentation results while going through the volume scan, B-scan by B-scan. When the correction is done, the modified segmentation is written and saved over the previous one in the data file.

2.3.3. Data Export and Batch Processing

For thickness data export, the user selects the upper and lower boundaries of the layer, and also the grid in which the thickness is going to be calculated (e.g., ETDRS 6 mm grid). Then, each volume is split into these sectors, and the average thickness of each is computed. At the end, the calculated values are written and saved in a comma separated values (csv) file.

SAMIRIX also offers the possibility of performing batch segmentation. For this purpose, the selected volumes are taken through the steps in the segmentation module, one by one. Also, in the thickness export module, the first two steps are repeated for each volume, and then the end result consists in a single thickness report saved in a single table. SAMIRIX only works with Spectralis OCT scans in HEYEX Vol file format (*.vol files). Screenshots from SAMIRIX and OCT-Marker are provided in **Supplementary Material**.

2.4. Statistical Analysis

Statistical analysis was done in R [Version 3.4.4 (25)]. Exploratory data analysis and data visualization were performed using the ggplot2 package (26). For assessment of consistency, the intra-class correlation coefficient (ICC) and 95% confidence intervals were estimated using the ICC package (27), based

on the variance components from a one-way ANOVA. The coefficient of variation (CV), standard error of measurement (SEM), and minimum detectable change (MDC) for inter-rater and intra-rater consistency analysis were calculated based on the formulas described by Beckerman et al. (28). SEM and MDC, the latter sometimes also called smallest real difference (SRD), are statistical approaches to estimate the minimally needed difference between two measurements that a method is able to detect (28), and is used in this study as a measure to quantify the amount of noise. In this study, an ICC >0.9 was considered as high, between 0.8 and 0.9 as moderate, and <0.8 as insufficient, as suggested by Vaz et al. (29).

Analysis of OCT values against age, sex, and refractive error was performed by linear mixed effect models (LMM), including inter-eye within-patient correlations as a random effect [lme4 package (30), and lmerTest package (31)]. The conditional and marginal coefficients of determination were calculated with pseudo R-squared [MuMIn package (32)]. The correlation of OCT values was assessed using Pearson's product-moment correlation [stats package (25)] and regression analysis was carried out using LMM with the inclusion of inter-eye within-patient correlations as a random effect. For this study, *p*-values below 0.05 were considered significant.

All statistical and exploratory results of this study were established in an interactive HTML document using R Markdown (33) and Shiny (34) packages. R Markdown is a framework to run codes written in R and generates reports based on the output of the codes. By using Shiny R package, the reports can be turned into interactive web applications. The documents based on R Markdown and Shiny packages can be deployed on web servers and are therefore accessible, like web pages. A screenshot of the interactive HTML document is provided in the **Supplementary Material**.

3. RESULTS

Initially, macula scans of 438 eyes of 219 subjects were collected from our database according to the inclusion and exclusion criteria, from which the scans from 15 eyes of 14 subjects were excluded due to insufficient scan quality. Therefore, in this study, macula scans of 423 eyes of 218 subjects of Caucasian descent were included, from which 144 (66%) subjects were females and 74 (34%) were males. Age ranged between 18 and 69 years, with an average [\pm standard deviation (SD)] of 36.5 ± 12.27 years. Refractive error was available from a subset of 70 eyes (35 subjects), from which the average was -0.55 ± 1.38 SD diopter with a range between -4.75 and $+1.75$ diopter.

Table 1 provides descriptive statistics of average MT, mRNFL, GCIPL, and INL thicknesses, including the mean, SD, coefficient of variation, range, first percentile, fifth percentile, ninety-fifth percentile, and ninety-ninth percentile. **Figure 2** shows the distribution of the average layer thicknesses together with an overlaid curve representing normal distribution fitted to each graph.

Additionally, the normative (mean) thickness of the MT, mRNFL, GCIPL, and INL layers in the ETDRS macular map is

shown as heat maps in **Figure 3**, alongside the normative values of the average layer thicknesses of the eyes included in this study in the ETDRS macular map sectors. Descriptive statistics of the layer thicknesses in the ETDRS macular map sectors is provided in **Supplementary Material**.

To test inter-rater reliability, the automatic segmentation results of 44 eyes of 24 subjects from this study were manually corrected by two different experienced graders, who were masked. We then calculated the intra-class correlation coefficient (ICC) and minimum detectable change (MDC) for MT, mRNFL, GCIPL, and INL, which is detailed in **Table 2**.

TABLE 1 | Descriptive statistics of average thicknesses in the entire ETDRS macular map.

Average thickness (μm)	Mean \pm SD	CV (%)	Min-Max	1st-99th percentile	5th-95th percentile
MT	313.70 \pm 12.02	3.83	281.29–362.29	286.53–339.59	294.20–333.25
mRNFL	39.53 \pm 3.57	9.03	30.22–54.38	32.41–49.18	34.35–45.68
GCIPL	70.81 \pm 4.87	6.87	56.60–86.03	59.00–83.56	63.16–77.95
INL	35.93 \pm 2.34	6.52	28.31–41.94	31.00–40.97	32.08–39.87

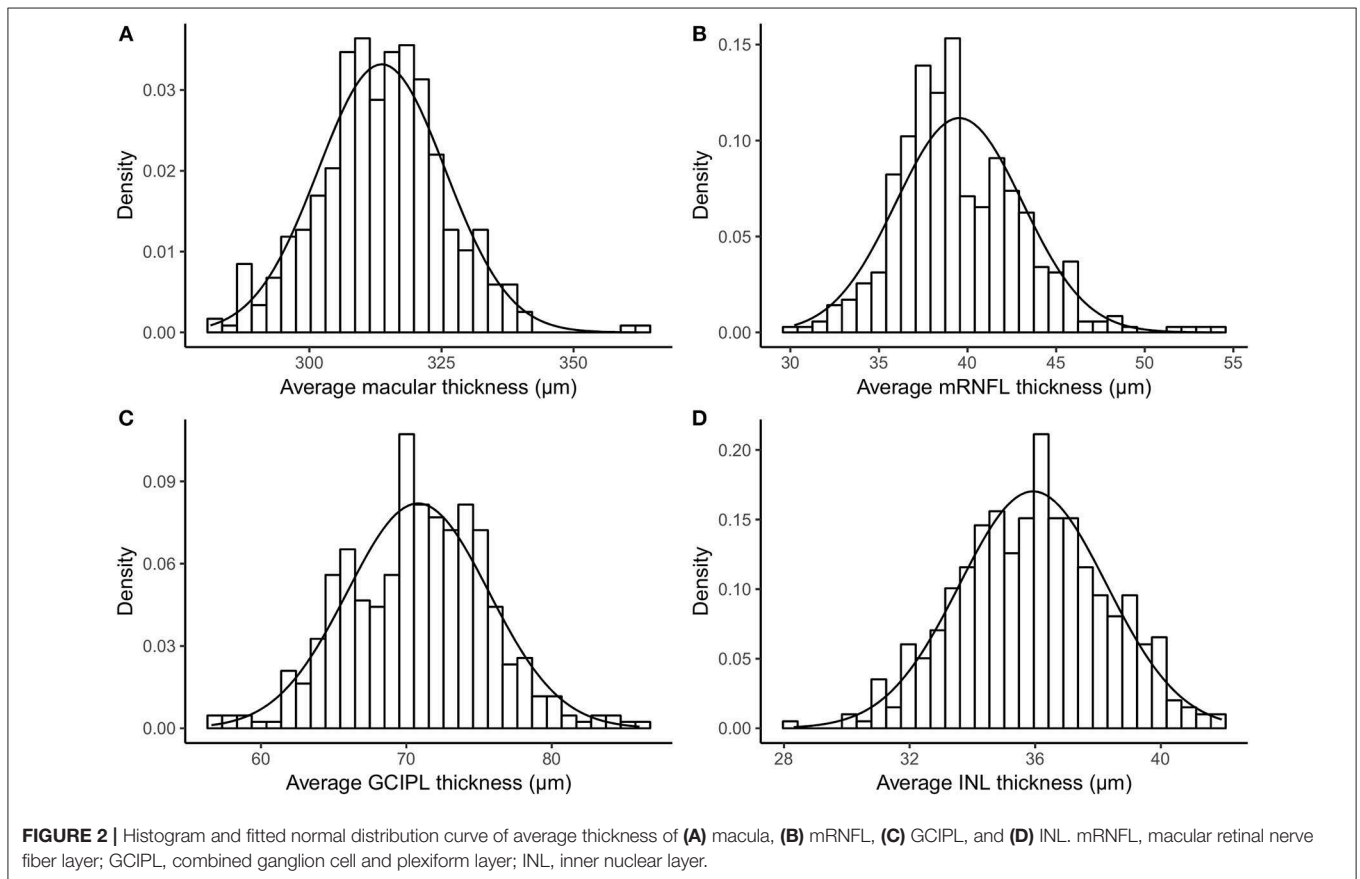
MT, macular thickness; mRNFL, macular retinal nerve fiber layer; GCIPL, combined ganglion cell and plexiform layer; INL, inner nuclear layer; CV, coefficient of variation; Min, minimum; Max, maximum.

Intra-rater reliability of the manual correction was tested by manually correcting the segmentation results of the same set of OCT scans from the previous reliability test (44 eyes of 24 subjects) twice by an experienced grader. The MDC (and ICC) was 0.24 (0.99994), 0.31 (0.99861), 0.23 (0.99947), and 0.19 micrometers (0.99890) for MT, mRNFL, GCIPL, and INL, respectively.

Regression analysis of layer thicknesses against age showed significant changes. In particular, MT showed an average decrease of 0.215 μm per year (p -value = 0.001). Likewise, GCIPL thickness decreased by on average 0.088 μm per year (p -value = 0.001). Significant changes of average thickness of mRNFL and INL by aging are also reported; **Table 3** provides detailed results.

Analysis of average layer thicknesses vs. sex revealed significant differences in MT and GCIPL between males and females. Males showed on average 4.18 μm higher MT than females (p -value = 0.015). Further, males had a 1.52 μm thicker GCIPL in comparison to females (p -value = 0.029). As reported in **Table 3**, neither mRNFL nor INL thickness showed significant sex differences.

Since GCIPL and INL are of particular interest, **Figure 4** shows the average GCIPL and INL thicknesses against age. The INL thickness was also plotted against the GCIPL thickness in **Figure 4**. The correlation coefficient between the INL and GCIPL thicknesses was 0.579 (p -value $< 2 \times 10^{-16}$) and the slope (B) of the linear regression was 0.277 [standard error (SE) = 0.022, p -value $< 2 \times 10^{-16}$].



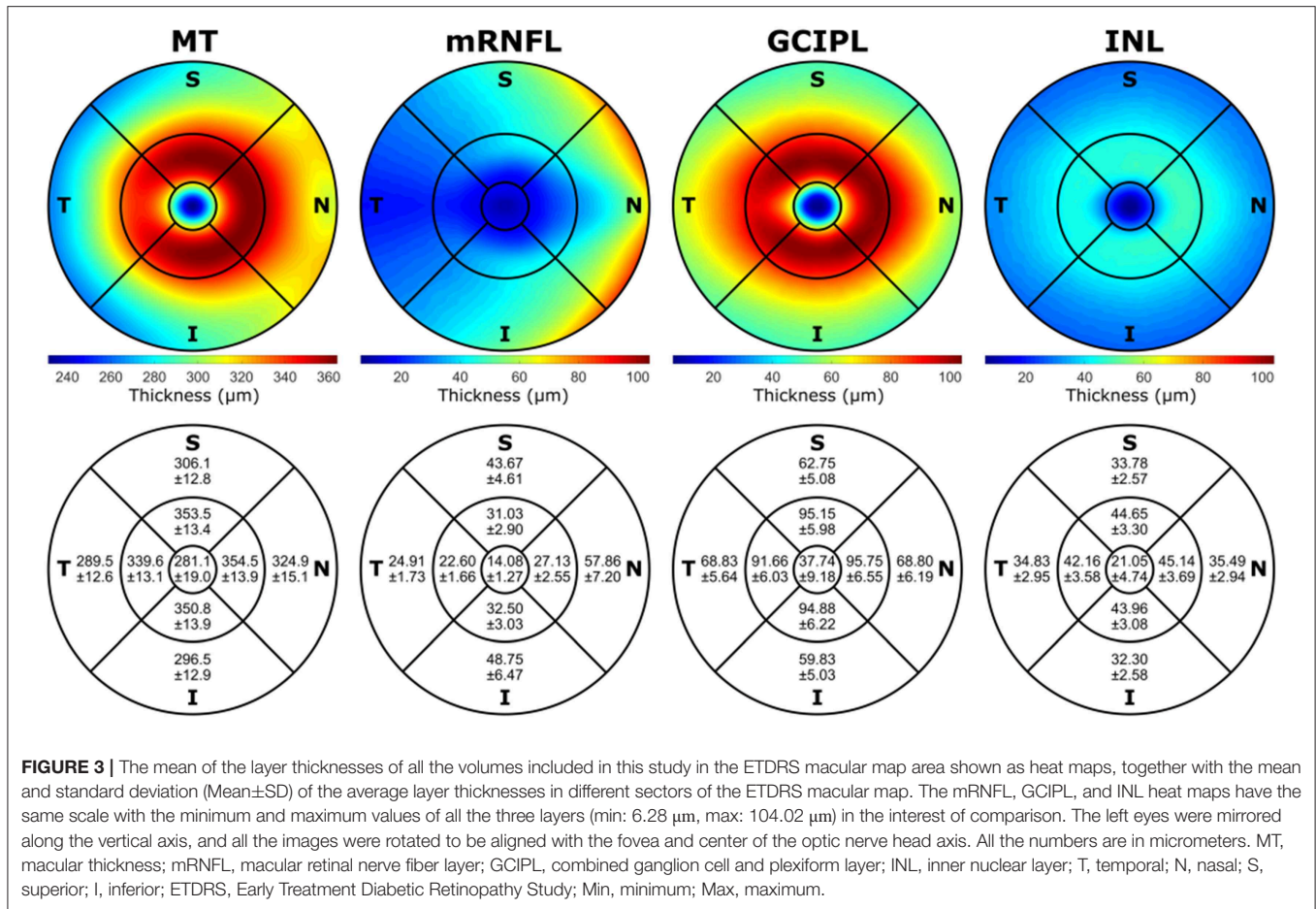


TABLE 2 | Inter-rater reliability measurements of segmentation corrections.

Average thickness (μm)	ICC	Upper CI	Lower CI	CV	SEM	MDC
MT	0.99984	0.99971	0.99991	0.04464	0.13728	0.38052
mRNFL	0.99350	0.98817	0.99644	0.57594	0.23771	0.65889
GCIPL	0.99794	0.99625	0.99887	0.21960	0.16519	0.45788
INL	0.99734	0.99515	0.99854	0.27271	0.10564	0.29281

MT, macular thickness; mRNFL, macular retinal nerve fiber layer; GCIPL, combined ganglion cell and plexiform layer; INL, inner nuclear layer; ICC, intra-class correlation coefficient; CI, confidence interval; CV, coefficient of variation; SEM, standard error of measurement; MDC, minimum detectable change.

To test the performance of SAMIRIX and to compare it with the performance of the HEYEX software, 20 OCT scans from NMOSS patients, all with a history of optic neuritis (ON) were segmented, and the segmentation results were manually corrected by a grader experienced in both SAMIRIX and HEYEX. The median correction time for SAMIRIX was 7:59 min (minimum: 5:07 min, maximum: 27:22 min), while the median correction time for HEYEX was 10:30 min (minimum: 8:01 min, maximum: 22:01 min). The mean absolute correction in the 6 mm ETDRS circle (the amount of correction for all the five

corrected boundaries ILM, RNFL-GCL, IPL-INL, INL-OPL, and BM divided by the number of A-Scans in the 6 mm ETDRS circle) was also calculated. For the mean absolute correction in SAMIRIX, the median was 0.16 μm (minimum: 0 μm, maximum: 22.45 μm), and in HEYEX, the median was 0.79 μm (minimum: 0.06 μm, maximum: 2.02 μm).

4. DISCUSSION

In this study we present normative data for inner intraretinal layer thicknesses of a large cohort of 218 healthy subjects (423 eyes) of Caucasian ethnicity aged between 18 and 69 years, using Spectralis SD-OCT 3D macular scans.

In our study the average thickness of all investigated layers was associated with age, which is consistent with other studies (35–40). Recently, Invernizzi et al. (18) investigated the association of different intraretinal layer thicknesses in the outer and middle rings and the center of the ETDRS thickness map, with age, and showed no significant association in any regions except the center of macular thickness, which is consistent with some other studies (41, 42). von Hanno et al. (43) suggested a positive association between macular thickness and age up to around 60 years and a negative association afterwards, by studying retinal OCTs of 4,508 eyes. Previous studies investigating retinal thicknesses in relation

TABLE 3 | Regression analysis of average thicknesses against age, sex, and refractive error.

Average thickness (μm)	Against	Mean (SD)	B	SE	P	$R^2_{\text{Marg.}}$	$R^2_{\text{Cond.}}$
MT	Age (years)		-0.2148	0.0648	0.0010	0.0478	0.9679
	Sex: F	312.32 (12.11)	4.1771	1.6941	0.0145	0.0268	0.9679
	vs. M	316.38 (11.41)					
	RE (diopter)		-0.3926	0.7013	0.5777	0.0030	0.9644
mRNFL	Age (years)		-0.0523	0.0192	0.0072	0.0312	0.8821
	Sex: F	39.46 (3.69)	0.3152	0.5056	0.5337	0.0017	0.8820
	vs. M	39.67 (3.33)					
	RE (diopter)		-0.6067	0.2936	0.0430	0.0729	0.8753
GCIPL	Age (years)		-0.0874	0.0263	0.0010	0.0480	0.9652
	Sex: F	70.28 (4.98)	1.5150	0.6896	0.0291	0.0214	0.9652
	vs. M	71.82 (4.48)					
	RE (diopter)		0.0049	0.2950	0.9869	0	0.9730
INL	Age (years)		-0.0453	0.0125	0.0004	0.0558	0.9331
	Sex: F	35.82 (2.40)	0.3526	0.3312	0.2883	0.0050	0.9331
	vs. M	36.15 (2.22)					
	RE (diopter)		0.2394	0.1783	0.1841	0.0209	0.9512

MT, macular thickness; mRNFL, macular retinal nerve fiber layer; GCIPL, combined ganglion cell and plexiform layer; INL, inner nuclear layer; F, female; M, male; vs., versus; RE, refractive error; SD, standard deviation; B, slope; SE, standard error of B; P, p-value; $R^2_{\text{Marg.}}$, Marginal R-squared; $R^2_{\text{Cond.}}$, Conditional R-Squared. Significant p-values marked in bold.

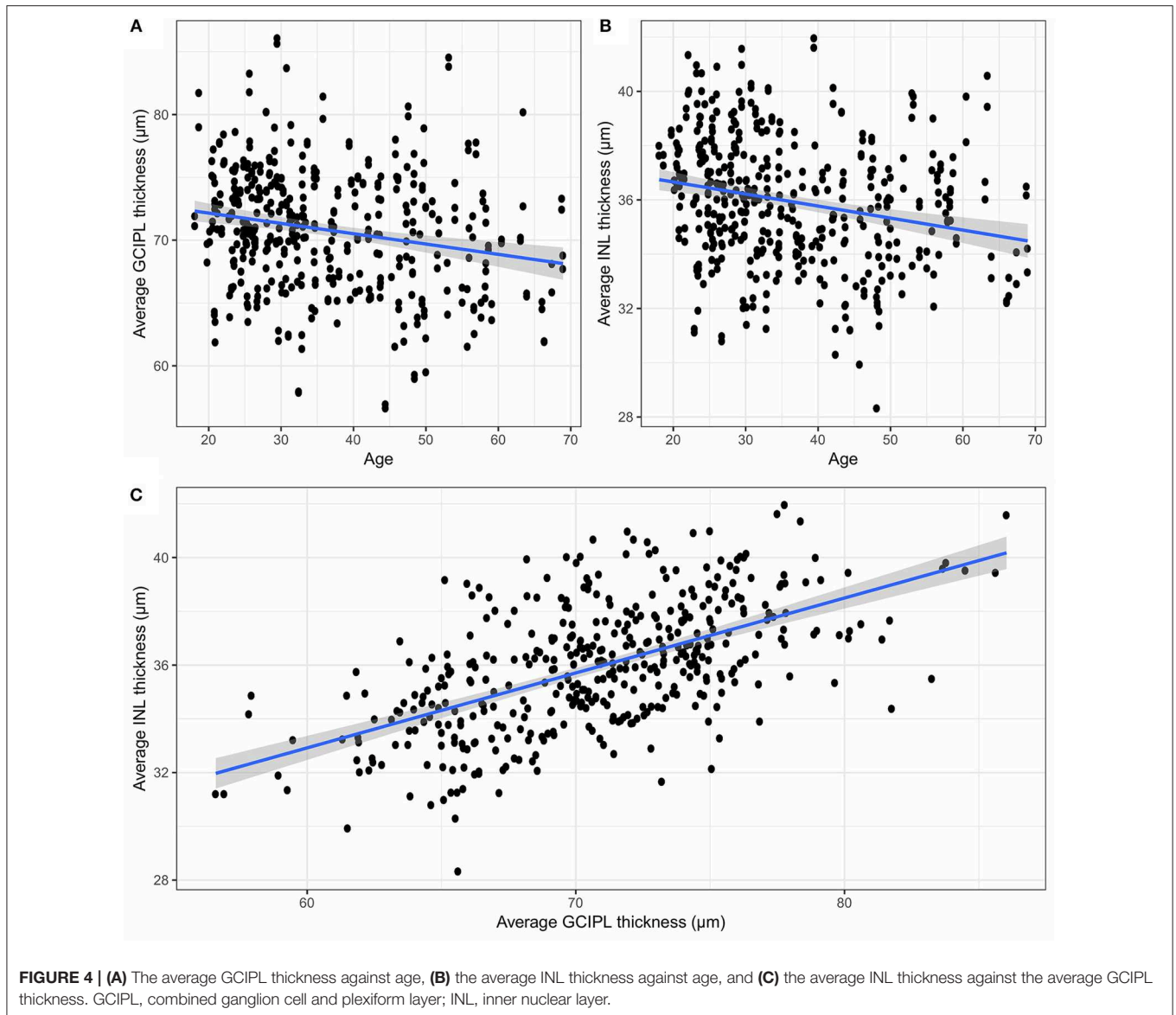
to sex in a healthy population showed that women had thinner retinal thickness measures than men (36, 40, 41, 43, 44). Our results are in accordance with this for MT and GCIPL, but not for mRNFL and INL, which were both not sex-dependent in our cohort. The analysis using OCT data from the UK Biobank study (67,321 adults) from (45) reported associations among older age, ethnicity, BMI, smoking, and macular thickness.

Inter-rater reliability of manually corrected segmentation results was excellent with ICC values above 0.99 for all layers. MDC, from the inter-rater reliability test, was 0.46 μm for GCIPL, which is higher than the projected annual loss in healthy subjects in this study (0.09 μm per year) and similar to the average annual GCIPL loss reported in patients with MS (-1.1 μm over 2 years) (46). This means that current intraretinal segmentation is not able to reliably detect annual GCIPL loss in an individual MS patient, and further technological improvements in acquisition and image analysis are required to allow this, e.g., for clinical monitoring applications. Intraretinal segmentation of the GCIPL is, however, suited to track optic neuritis associated damage, which is often magnitudes higher than the observed MDC in this study (8, 9). For INL, the inter-rater MDC in our study was 0.29 μm , which is similar to group-wise changes reported with disease activity related effects in the range of 0.35 to 0.71 μm (12). Again, this suggests that current OCT intraretinal segmentation is not able to reliably detect meaningful INL change for this application. A previous multicenter study using the device's own semi-automatic segmentation approach with manual correction produced even higher MDC (17). While previous studies, and our current study only investigated segmentation-based reliability on a single scan, the additional acquisition noise from two different scans is likely to result in even higher MDC in a real world scenario of follow-up measurements. The reported MDC

is below the resolution of the used SD-OCT technology, which suggests that imaging rather than segmentation is the limiting issue in detecting change.

To further support the opposing roles of GCIPL and INL measurements in neuroinflammatory disorders, we investigated their association in healthy controls. Both showed a moderate to strong correlation in our study, indicating that retinal thickness is reflected similarly throughout layers in an individual person. This relationship might be of relevance when interpreting GCIPL and INL in neuroinflammatory diseases, where GCIPL and INL are supposed to change in opposite directions, with GCIPL thickness reduction due to neurodegeneration (4) and INL thickening due to inflammation (12) or in response to ganglion cell loss (10).

The presented semi-automatic OCT image segmentation pipeline, SAMIRIX, provides an accessible and flexible toolbox, which can handle the entire process needed to analyze intraretinal layer thicknesses on raw SD-OCT images. SAMIRIX is not introducing a new segmentation approach, but rather implements an existing algorithm, and extends it with processing pipelines and comfortable manual correction tools. For research use, SAMIRIX was faster compared to HEYEX, and the initial segmentation more accurate. In a few cases with severely affected eyes, initial automatic segmentation produced large errors. These cases then needed more processing time than with HEYEX, suggesting a potential in improving the initial segmentation approach. Importantly, SAMIRIX offers a transparent open-source segmentation pipeline. Of note, while we compared SAMIRIX to HEYEX, there are other commercial and academic intraretinal segmentation tools available, e.g., Orion (by Voxeleron LLC, <https://www.voxeleron.com/orion/>) and Iowa Reference Algorithms (by Iowa Institute for Biomedical Imaging, <https://www.iibi.uiowa.edu/oct-reference>).



4.1. Strengths and Limitations

A general problem with reporting normative data is not only different optical properties and acquisition strategies of different devices, but also different regions of interest, which are then summarized in the respective thickness or volume measurements (47). While we report 6 mm ETDRS ring thicknesses in micrometers in this study, other regions of interest can be surveyed using the accompanying *shiny* web application. Other strengths of this study are its sample size and the similar age and sex distribution in comparison to typical cohorts of autoimmune neuroinflammatory diseases. A limitation of this study is the cross-sectional design, which impairs inferences about temporal development. The most important limitation is that we included OCT scans from only one device and one scan protocol, which limits generalizability of normative data (47). Particular caution should be taken when interpreting data

acquired with various instruments, since comparative studies revealed that measurements are not directly comparable between different OCT devices (48, 49) and results can even be influenced by simple software upgrades (50). Currently, SAMIRIX is only able to work with the HEYEX Vol file format (*.vol files), which is only available through specific collaborative arrangements with Heidelberg Engineering, which is a clear limitation.

Because this study was done on a Caucasian population, readers should keep in mind that our results are not necessarily applicable to other ethnicities. Grover et al. (42) found Black subjects to have a thinner retinal thickness compared to Caucasian subjects, while Tariq et al. (51) showed that average inner macula was significantly thicker in Caucasian than East Asian and South Asian children, with South Asian children having the thinnest values. These findings were also confirmed by Girkin et al. (35), which reported that Hispanic and Indian

participants showed higher thickness compared to Europeans and Africans.

DATA AVAILABILITY STATEMENT

All analyses of this study are combined in a single R markdown code embedding R shiny interactive applications, which is provided alongside the raw data as **Supplementary Material** as well as in a public repository, in <https://github.com/neurodial/am-HC-project-analysis-public.git>. A copy of the source code of SAMIRIX which was used in this study and described in this paper is also provided as **Supplementary Material**. An up-to-date version of SAMIRIX can be found in a public repository with the address of https://github.com/neurodial/am_SAMIRIX.git. Additionally, the markdown HTML document was deployed to a server and is ready-to-use, available under http://shiny-apps.neurodial.de/shiny/am-HC-project-analysis-public/HC_traditional_params_markdown.Rmd with the username of “guest_user” and the password of “NeuroDiaL.”

ETHICS STATEMENT

The study was approved by the ethics committee of Charité–Universitätsmedizin Berlin and conducted according to the Declaration of Helsinki in its currently applicable version. All participants gave written informed consent.

AUTHOR CONTRIBUTIONS

SM collected the data, developed SAMIRIX, manually corrected layers segmentation, performed statistical analysis, contributed to data interpretation, and wrote the manuscript. KG developed

the OCT-Marker. NA contributed to the data collection and manual correction of layer segmentation. HZ contributed to the data collection, visual examinations, and data interpretation. SA contributed to the data collection and participant recruitment. CB contributed to the data collection and visual examinations. JM contributed to the data collection and visual examinations. FP contributed to the study management. EK contributed to the data interpretation and wrote the manuscript. AB planned and coordinated the study, contributed to statistical analysis and data interpretation, and reviewed the manuscript. All authors approved the final draft of the manuscript submitted for review and publication.

FUNDING

This work was supported by the Einstein Foundation Berlin (Einstein Junior Scholarship) to SM, the German Federal Ministry of Economic Affairs and Energy (BMWi EXIST 03EFE079) to AB, and EK, German Research Foundation (DFG Exc. 257) to FP and AB; and German Federal Ministry of Education and Research (BMBF Neu² ADVISIMS) to FP and AB.

ACKNOWLEDGMENTS

We thank Robyn Cunningham for her excellent technical assistance.

SUPPLEMENTARY MATERIAL

The Supplementary Material for this article can be found online at: <https://www.frontiersin.org/articles/10.3389/fneur.2019.01117/full#supplementary-material>

REFERENCES

- Huang D, Swanson EA, Lin CP, Schuman JS, Stinson WG, Chang W, et al. Optical coherence tomography. *Science* (1991) 254:1178–81.
- Oertel FC, Zimmermann H, Paul F, Brandt AU. Optical coherence tomography in neuromyelitis optica spectrum disorders: potential advantages for individualized monitoring of progression and therapy. *EPMA J.* (2017) 9:21–33. doi: 10.1007/s13167-017-0123-5
- Oertel FC, Zimmermann HG, Brandt AU, Paul F. Novel uses of retinal imaging with optical coherence tomography in multiple sclerosis. *Expert Rev Neurother.* (2019) 19:31–43. doi: 10.1080/14737175.2019.1559051
- Petzold A, Balcer LJ, Calabresi PA, Costello F, Frohman TC, Frohman EM, et al. Retinal layer segmentation in multiple sclerosis: a systematic review and meta-analysis. *Lancet Neurol.* (2017) 16:797–812. doi: 10.1016/S1474-4422(17)30278-8
- Brandt AU, Martinez-Lapiscina EH, Nolan R, Saidha S. Monitoring the course of MS with optical coherence tomography. *Curr Treat Options Neurol.* (2017) 19:15. doi: 10.1007/s11940-017-0452-7
- Oberwahrenbrock T, Ringelstein M, Jentschke S, Deuschle K, Klumbies K, Bellmann-Strobl J, et al. Retinal ganglion cell and inner plexiform layer thinning in clinically isolated syndrome. *Mult Scler J.* (2013) 19:1887–95. doi: 10.1177/1352458513489757
- Zimmermann HG, Knier B, Oberwahrenbrock T, Behrens J, Pfuhl C, Aly L, et al. Association of retinal ganglion cell layer thickness with future disease activity in patients with clinically isolated syndrome. *JAMA Neurol.* (2018) 75:1071–9. doi: 10.1001/jamaneurol.2018.1011
- Brandt AU, Specovius S, Oberwahrenbrock T, Zimmermann HG, Paul F, Costello F. Frequent retinal ganglion cell damage after acute optic neuritis. *Mult Scler Relat Disord.* (2018) 22:141–7. doi: 10.1016/j.msard.2018.04.006
- Soelberg K, Specovius S, Zimmermann HG, Grauslund J, Mehlsen JJ, Olesen C, et al. Optical coherence tomography in acute optic neuritis: a population-based study. *Acta Neurol Scand.* (2018) 138:566–73. doi: 10.1111/ane.13004
- Brandt AU, Oberwahrenbrock T, Kadas EM, Lagreze WA, Paul F. Dynamic formation of macular microcysts independent of vitreous traction changes. *Neurology.* (2014) 83:73–7. doi: 10.1212/wnl.0000000000000545
- Kaufhold F, Zimmermann H, Schneider E, Ruprecht K, Paul F, Oberwahrenbrock T, et al. Optic neuritis is associated with inner nuclear layer thickening and microcystic macular edema independently of multiple sclerosis. *PLoS ONE.* (2013) 8:e71145. doi: 10.1371/journal.pone.0071145
- Knier B, Schmidt P, Aly L, Buck D, Berthele A, Mühlau M, et al. Retinal inner nuclear layer volume reflects response to immunotherapy in multiple sclerosis. *Brain.* (2016) 139:2855–63. doi: 10.1093/brain/aww219
- Oertel FC, Kuchling J, Zimmermann H, Chien C, Schmidt F, Knier B, et al. Microstructural visual system changes in AQP4-antibody-seropositive NMOSD. *Neurol Neuroimmunol Neuroinflamm.* (2017) 4:e334. doi: 10.1212/NXI.0000000000000334
- Oertel FC, Havla J, Roca-Fernández A, Lizak N, Zimmermann H, Motamedi S, et al. Retinal ganglion cell loss in neuromyelitis optica: a longitudinal study. *J Neurol Neurosurg Psychiatry.* (2018) 89:1259–65. doi: 10.1136/jnnp-2018-318382
- Tian J, Varga B, Tatrai E, Fanni P, Somfai GM, Smiddy WE, et al. Performance evaluation of automated segmentation software on optical coherence tomography volume data. *J Biophoton.* (2016) 9:478–89. doi: 10.1002/jbio.201500239

16. Ctori I, Huntjens B. Repeatability of foveal measurements using spectralis optical coherence tomography segmentation software. *PLoS ONE*. (2015) 10:e0129005. doi: 10.1371/journal.pone.0129005
17. Oberwahrenbrock T, Traber GL, Lukas S, Gabilondo I, Nolan R, Songster C, et al. Multicenter reliability of semiautomatic retinal layer segmentation using OCT. *Neurol Neuroimmunol Neuroinflamm*. (2018) 5:e449. doi: 10.1212/NXI.0000000000000449
18. Invernizzi A, Pellegrini M, Acquistapace A, Benatti E, Erba S, Cozzi M, et al. Normative data for retinal-layer thickness maps generated by spectral-domain OCT in a white population. *Ophthalmol Retina*. (2018) 2:808–15.e1. doi: 10.1016/j.oret.2017.12.012
19. Ooto S, Hangai M, Tomidokoro A, Saito H, Araie M, Otani T, et al. Effects of age, sex, and axial length on the three-dimensional profile of normal macular layer structures. *Investig Ophthalmol Vis Sci*. (2011) 52:8769. doi: 10.1167/iovs.11-8388
20. Lang A, Carass A, Hauser M, Sotirchos ES, Calabresi PA, Ying HS, et al. Retinal layer segmentation of macular OCT images using boundary classification. *Biomed Opt Express*. (2013) 4:1133–52. doi: 10.1364/BOE.4.001133
21. Tewarie P, Balk L, Costello F, Green A, Martin R, Schippling S, et al. The OSCAR-IB consensus criteria for retinal OCT quality assessment. *PLoS ONE*. (2012) 7:e34823. doi: 10.1371/journal.pone.0034823
22. Cruz-Herranz A, Balk LJ, Oberwahrenbrock T, Saidha S, Martinez-Lapiscina EH, Lagreze WA, et al. The APOSTEL recommendations for reporting quantitative optical coherence tomography studies. *Neurology*. (2016) 86:2303–9. doi: 10.1212/WNL.0000000000002774
23. ETDRS Research Group. Grading diabetic retinopathy from stereoscopic color fundus photographs—an extension of the modified Airlie House classification. ETDRS report number 10. Early Treatment Diabetic Retinopathy Study Research Group. *Ophthalmology*. (1991) 98:786–806.
24. Oberwahrenbrock T, Jost R, Zimmermann H, Beckers I, Paul F, Brandt AU. Signal quality dependency of intra-retinal segmentation algorithms. In: *ECTRIMS Online Library* (2016). p. 146399. Available online at: <https://onlinelibrary.ectrims-congress.eu/ectrims/2016/32nd/146399/timm.oberwahrenbrock.signal.quality.dependency.of.intra-retinal.segmentation.html>
25. R Core Team. *R: A Language and Environment for Statistical Computing*. Vienna: R Core Team (2018). Available online at: <https://www.R-project.org/>
26. Wickham H. *ggplot2: Elegant Graphics for Data Analysis*. New York, NY: Springer-Verlag (2009). Available online at: <http://ggplot2.org>
27. Wolak ME, Fairbairn DJ, Paulsen YR. Guidelines for estimating repeatability. *Methods Ecol Evol*. (2012) 3:129–37. doi: 10.1111/j.2041-210X.2011.00125.x
28. Beckerman H, Roebroek ME, Lankhorst GJ, Becher JG, Bezemer PD, Verbeek AL. Smallest real difference, a link between reproducibility and responsiveness. *Qual Life Res*. (2001) 10:571–8. doi: 10.1023/a:1013138911638
29. Vaz S, Falkmer T, Passmore AE, Parsons R, Andreou P. The case for using the repeatability coefficient when calculating test–retest reliability. *PLoS ONE*. (2013) 8:e73990. doi: 10.1371/journal.pone.0073990
30. Bates D, Mächler M, Bolker B, Walker S. Fitting linear mixed-effects models using lme4. *J Stat Softw*. (2015) 67:1–48. doi: 10.18637/jss.v067.i01
31. Kuznetsova A, Brockhoff PB, Christensen RHB. lmerTest package: tests in linear mixed effects models. *J Stat Softw*. (2017) 82:1–26. doi: 10.18637/jss.v082.i13
32. Barton K. *MuMIn: Multi-Model Inference* (2018). R package version 1.40.4. Available online at: <https://CRAN.R-project.org/package=MuMIn>
33. Allaire J, Horner J, Marti V, Porte N. *Markdown: 'Markdown' Rendering for R; 2017*. R package version 0.8. Available online at: <https://CRAN.R-project.org/package=markdown>
34. Chang W, Cheng J, Allaire J, Xie Y, McPherson J. *Shiny: Web Application Framework for R* (2017). R package version 1.0.5. Available online at: <https://CRAN.R-project.org/package=shiny>
35. Girkin CA, McGwin G, Sinai MJ, Sekhar GC, Fingeret M, Wollstein G, et al. Variation in optic nerve and macular structure with age and race with spectral-domain optical coherence tomography. *Ophthalmology*. (2011) 118:2403–8. doi: 10.1016/j.ophtha.2011.06.013
36. Gupta P, Sidhartha E, Tham YC, Chua DKP, Liao J, Cheng CY, et al. Determinants of macular thickness using spectral domain optical coherence tomography in healthy eyes: the Singapore Chinese eye study. *Investig Ophthalmol Vis Sci*. (2013) 54:7968. doi: 10.1167/iovs.13-12436
37. Mítkova-Hristova VT, Konareva-Kostyanova MI. Macular thickness measurements in healthy eyes using spectral optical coherence tomography. *Folia Med*. (2011) 53:28–33. doi: 10.2478/v10153-011-0064-z
38. Myers CE, Klein BEK, Meuer SM, Swift MK, Chandler CS, Huang Y, et al. Retinal thickness measured by spectral-domain optical coherence tomography in eyes without retinal abnormalities: the Beaver dam eye study. *Am J Ophthalmol*. (2015) 159:445–56.e1. doi: 10.1016/j.ajo.2014.11.025
39. Nieves-Moreno M, de-la Casa JMM, Morales-Fernández L, Sánchez-Jean R, Sáenz-Francés F, García-Feijóo J. Impacts of age and sex on retinal layer thicknesses measured by spectral domain optical coherence tomography with spectralis. *PLoS ONE*. (2018) 13:e0194169. doi: 10.1371/journal.pone.0194169
40. Song WK, Lee SC, Lee ES, Kim CY, Kim SS. Macular thickness variations with sex, age, and axial length in healthy subjects: a spectral domain–optical coherence tomography study. *Investig Ophthalmol Vis Sci*. (2010) 51:3913. doi: 10.1167/iovs.09-4189
41. Adhi M, Aziz S, Muhammad K, Adhi MI. Macular thickness by age and gender in healthy eyes using spectral domain optical coherence tomography. *PLoS ONE*. (2012) 7:e37638. doi: 10.1371/journal.pone.0037638
42. Grover S, Murthy RK, Brar VS, Chalam KV. Normative data for macular thickness by high-definition spectral-domain optical coherence tomography (spectralis). *Am J Ophthalmol*. (2009) 148:266–71. doi: 10.1016/j.ajo.2009.03.006
43. von Hanno T, Lade AC, Mathiesen EB, Peto T, Njølstad I, Bertelsen G. Macular thickness in healthy eyes of adults (N = 4508) and relation to sex, age and refraction: the Tromsø Eye Study (2007–2008). *Acta Ophthalmol*. (2016) 95:262–9. doi: 10.1111/aos.13337
44. Duan XR, Liang YB, Friedman DS, Sun LP, Wong TY, Tao QS, et al. Normal macular thickness measurements using optical coherence tomography in healthy eyes of adult Chinese persons: the Handan eye study. *Ophthalmology*. (2010) 117:1585–94. doi: 10.1016/j.ophtha.2009.12.036
45. Patel PJ, Foster PJ, Grossi CM, Keane PA, Ko F, Lotery A, et al. Spectral-domain optical coherence tomography imaging in 67,321 adults. *Ophthalmology*. (2016) 123:829–40. doi: 10.1016/j.ophtha.2015.11.009
46. Balk LJ, Cruz-Herranz A, Albrecht P, Arnow S, Gelfand JM, Tewarie P, et al. Timing of retinal neuronal and axonal loss in MS: a longitudinal OCT study. *J Neurol*. (2016) 263:1323–31. doi: 10.1007/s00415-016-8127-y
47. Oberwahrenbrock T, Weinhold M, Mikolajczak J, Zimmermann H, Paul F, Beckers I, et al. Reliability of intra-retinal layer thickness estimates. *PLoS ONE*. (2015) 10:e0137316. doi: 10.1371/journal.pone.0137316
48. Pierro L, Giatsidis SM, Mantovani E, Gagliardi M. Macular thickness interoperator and intraoperator reproducibility in healthy eyes using 7 optical coherence tomography instruments. *Am J Ophthalmol*. (2010) 150:199–204.e1. doi: 10.1016/j.ajo.2010.03.015
49. Seigo MA, Sotirchos ES, Newsome S, Babiarez A, Eckstein C, Ford E, et al. *In vivo* assessment of retinal neuronal layers in multiple sclerosis with manual and automated optical coherence tomography segmentation techniques. *J Neurol*. (2012) 259:2119–30. doi: 10.1007/s00415-012-6466-x
50. Coric D, Petzold A, Uitdehaag BMJ, Balk LJ. Software updates of OCT segmentation algorithms influence longitudinal assessment of retinal atrophy. *J Neurol Sci*. (2018) 387:16–20. doi: 10.1016/j.jns.2018.01.020
51. Tariq YM, Li H, Burlutsky G, Mitchell P. Ethnic differences in macular thickness. *Clin Exp Ophthalmol*. (2011) 39:893–8. doi: 10.1111/j.1442-9071.2011.02593.x

Conflict of Interest: EK, FP, and AB are co-founders and hold shares in technology start-up Nocturne GmbH, which has commercial interest in OCT applications in neurology. EK is now an employee of Nocturne.

The remaining authors declare that the research was conducted in the absence of any commercial or financial relationships that could be construed as a potential conflict of interest.

Copyright © 2019 Motamedi, Gawlik, Ayadi, Zimmermann, Asseyer, Bereuter, Mikolajczak, Paul, Kadas and Brandt. This is an open-access article distributed under the terms of the Creative Commons Attribution License (CC BY). The use, distribution or reproduction in other forums is permitted, provided the original author(s) and the copyright owner(s) are credited and that the original publication in this journal is cited, in accordance with accepted academic practice. No use, distribution or reproduction is permitted which does not comply with these terms.

Mein Lebenslauf wird aus datenschutzrechtlichen Gründen in der elektronischen Version meiner Arbeit nicht veröffentlicht.

Publikationsliste

Artikel in Fachzeitschriften

Noah Ayadi, Jan Dörr, Seyedamirhosein Motamedi, Kay Gawlik, Judith Bellmann-Strobl, Janine Mikolajczak, Alexander U. Brandt, Hanna Zimmermann, Friedemann Paul, Temporal visual resolution and disease severity in MS, *Neurol Neuroimmunol Neuroinflamm*, 2018.

Journal Impact Factor 2018: 7.353

Noah Ayadi, Frederike C Oertel, Susanna Asseyer, Rebecca Rust, Ankelien Duchow, Joseph Kuchling, Judith Bellmann-Strobl, Klemens Ruprecht, Alexander Klistorner, Alexander U Brandt, Friedemann Paul, Hanna G Zimmermann, Impaired motion perception is associated with functional and structural visual pathway damage in multiple sclerosis and neuromyelitis optica spectrum disorders, *Mult Scler.*, 2021.

Journal Impact Factor 2019: 5.412

Seyedamirhosein Motamedi, Kay Gawlik, **Noah Ayadi**, Hanna G. Zimmermann, Susanna Asseyer, Charlotte Bereuter, Janine Mikolajczak, Friedemann Paul, Ella Maria Kadas, Alexander Ulrich Brandt, Normative Data and Minimally Detectable Change for Inner Retinal Layer Thicknesses Using a Semi-automated OCT Image Segmentation Pipeline, *Front Neurol*, 2019.

Journal Impact Factor 2017: 3.508

Noah Ayadi, Martin Marziniak, COVID-19 und MS - Einfluss auf die Therapieentscheidung?, *DNP*, 2021 (kein Journal Impact Factor)

Noah Ayadi, Martin Marziniak, Die Retina - Fenster zum Gehirn und prognostischer Biomarker der MS. *DNP*, 2021 (kein Journal Impact Factor)

Kongressbeiträge

Ayadi, N.; Zimmermann, H.; Mikolajczak, J.; Dörr, J-M; Brandt, A. U.; Paul, F. Critical flicker frequency is reduced in multiple sclerosis patients independently of retinal axonal damage. Poster auf dem ECTRIMS Kongress, Paris, Frankreich, 2017.

Ayadi, N.; Zimmermann, H.; Oertel, F.C.; Borisow, N.; Giess, R.M.; Bellmann-Strobl, J.; Ruprecht, K.; Brandt, A.U.; Paul, F. Motion perception is associated with functional and structural visual pathway damage in multiple sclerosis and neuromyelitis optica spectrum disorders, Poster auf dem ECTRIMS Kongress, Berlin, Deutschland, 2018.

Vitkova, V.; Zimmermann, H.; **Ayadi, N.**; Martorell Serra, I.; Koduah, P.; Chien, C.; Kuchling, J.; Gieß, R.; Motamedi, S.; Gawlik, K.; Bellmann-Strobl, J.; Ruprecht, K.; Scheel, M.; Paul, F.; Brandt, A. Quantitative OCT and MRI in MS as surrogates for clinical activity based on annual follow-ups, Poster auf dem ECTRIMS Kongress, Berlin, 2018.

Zimmermann, H.G.; Vitkova, V.; **Ayadi, N.**; Martorell Serra, I.; Bereuter, C.; Motamedi, S.; Kuchling, J.; Asseyer, S.; Scheel, M.; Ruprecht, K.; Bellmann-Strobl, J.; Paul, F.; Brandt, A.U. Individual reflection of brain atrophy on intraretinal thickness changes in multiple sclerosis, Poster auf dem ECTRIMS Kongress, Stockholm, Schweden, 2019.

Danksagung

Ohne die Unterstützung, Ermutigung und Geduld zahlreicher Menschen hätte meine Promotion nicht glücken können. An dieser Stelle möchte ich allen Personen herzlich danken, die mich dabei unterstützt haben.

An erster Stelle ist mein Doktorvater Friedemann Paul zu nennen, der mir diese Promotion ermöglicht hat und mich darin stets unterstützt hat.

Ebenso herzlich möchte ich meinem Erstbetreuer Alexander Brandt für die Unterstützung danken.

Mein besonderer Dank gilt meiner Betreuerin Hanna Zimmermann für ihre wertvolle Unterstützung und Begleitung, ihre hilfreichen Anmerkungen und ihr immer offenes Ohr für meine Fragen. Vielen Dank!

Herzlichen Dank schulde ich auch meinen Mitautor*innen und Kolleg*innen am NeuroCure Research Center der Charité Berlin für die hervorragende Zusammenarbeit.

Weiter möchte ich allen Patient*innen und Proband*innen für die Teilnahme an den Studien danken. Durch sie wurde meine Promotion erst möglich.

Ein besonderer Dank gebührt meinen Eltern und insbesondere meiner Freundin Lena, die mich während meiner Promotion stets unterstützt hat.

Zuallerletzt möchte ich meinen Patient*innen im klinisch-neurologischen Alltag als Assistenzarzt danken, durch sie wird jeder Tag zu einer neuen spannenden Herausforderung, welche mein Interesse an der Neurologie stets anfeuert.